

DISSERTATION

THE KINETOCHORE PROTEIN KNL1 LINKS KINETOCHORE-MICROTUBULE
ATTACHMENT AND CHECKPOINT SIGNALING DURING MITOSIS

Submitted by

Gina V. Caldas

Department of Biochemistry and Molecular Biology

In partial fulfillment of the requirements

For the Degree of Doctor of Philosophy

Colorado State University

Fort Collins, Colorado

Summer 2014

Doctoral committee:

Advisor: Jennifer DeLuca

Christopher Allen
Santiago Dipietro
Olve Peersen
Jessica Prenni

Copyright by Gina V. Caldas 2014

All Rights Reserved

ABSTRACT

THE KINETOCHORE PROTEIN KNL1 LINKS KINETOCHORE-MICROTUBULE ATTACHMENT AND CHECKPOINT SIGNALING DURING MITOSIS

Mitosis is the phase of the cell cycle in which replicated chromosomes physically separate, resulting in the formation of two genetically identical daughter cells. This process is not only essential for the development of a single fertilized cell into a multicellular organism, but also for replacement of damaged and dying cells during the span life of an organism.

The distribution of chromosomes during mitotic cell division requires accurate yet dynamic attachment between the plus-ends of spindle microtubules (MTs) and kinetochores, which are protein structures assembled at the centromeric region of replicated chromatids. The tightly regulated connection between kinetochores and MTs allows for chromosome congression to the metaphase plate and subsequent separation of the replicated chromosomes during anaphase. Not surprisingly, the inability of cells to resolve erroneous kinetochore-MT attachments results in missegregation of chromosomes, which is linked to uncontrolled cell proliferation and cancer. Thus, proper kinetochore-MT attachment during cell division is essential for the maintenance of genetic integrity.

Despite a growing understanding of the identity of proteins that compose the kinetochore and the processes for which they are required, the precise functions of many kinetochore proteins are still unknown. KNL1, a large kinetochore scaffolding protein, contributes to several signaling pathways coordinated by the kinetochore. Yet, how KNL1 recruits its various binding partners to the kinetochore, and whether KNL1 directly or indirectly modulates protein function during

mitosis are unresolved questions. In this dissertation, I examine the function of KNL1 in the regulation of kinetochore-MT attachment and determine the regions of KNL1 required for the accumulation of an array of kinetochore proteins. By loss of function analyses using a set of KNL1 mutants, combined with functional assays in cells, I demonstrate that the KNL1 N-terminus is essential for Aurora B kinase activity at kinetochores and for correct kinetochore-MT dynamics. Aurora B kinase phosphorylates kinetochore proteins during early mitosis, increasing kinetochore-microtubule (MT) turnover and preventing premature stabilization of kinetochore-MT attachments. Therefore, KNL1 is required for correct Aurora B-mediated kinetochore-MT attachment regulation during mitosis. I provide evidence that the KNL1 N-terminus influences Aurora B activity by mediating the activity of Bub1 kinase, a kinetochore protein required for the spindle assembly checkpoint (SAC). The SAC mediates amplification of an inhibitory signal to prevent mitotic exit until all chromosomes are correctly attached to MTs. Although the SAC is known to be tightly coupled to kinetochore-MT attachment, how such coupling occurs at the kinetochore is a major unanswered question. The finding that KNL1 mediates Aurora B activity through Bub1 establishes KNL1 as a key integrator of multiple signaling pathways at the kinetochore. Finally, I determine the regions of KNL1 required for the accumulation of several kinetochore proteins, providing a broad view and better understanding of kinetochore organization inside the cell. Overall, results from these studies establish KNL1 as a central organizer of kinetochore architecture and function, and demonstrate the direct influence of this scaffolding protein on kinetochore-mediated regulatory processes during mitosis.

ACKNOWLEDGMENTS

It is a pleasure to acknowledge all the people that made this journey possible and enjoyable. Since my arrival here, I found fantastic people around, always willing to help. Although adapting to a new culture, language, and sitting in a classroom for the first time in a long time, was not easy, I had the support from people in this department and in my daily life, to successfully accomplish my goals. First and foremost, I want to express my sincere gratitude and appreciation to my advisor, Jake DeLuca. I thank Jake for her unconditional support in every aspect of my career, and for her unique and wonderful guidance, always an inspiration. Jake introduced me to cell biology and since then, my continuous interest and enthusiasm for this science has not stopped, to the point that today I could not be more fascinated with this field. For that, and for encouraging independence and creativity during my time in her lab, I will always be thankful. I am sure I could not have chosen a better mentor.

I also want to thank my fellows and DeLuca labmates for their friendship, kindness and support over these years. I would have not enjoyed this time so much without the company of Eric Tauchman, Geoff Guimaraes, Jacob Herman, Jeanne Mick, Keith DeLuca, Lysie Sundin, and O'Neil Wiggan. Also, I would have never learn all the inappropriate English slang without them, and that would have been catastrophic for my future. For that, and for much more, I will always have them in my heart.

I specially want to thank Tina Lynch and Chase Wesley. I had the pleasure of training them in the lab, and I really enjoyed the process. Their hard work and commitment has been impressive, and I feel very proud of them. I know they both will have a brilliant future in science.

I want to thank my colleague and amazing classmate Ada Ndoja. More than my classmate, Ada has been my unconditional friend, and my grad school experience would not have been the same without her company. I also thank Lindsey Long, Francesco Scavone, Andrea Ambrosio, Elena Ruggeri, and Daniel Feliciano, for their priceless friendship. I was very lucky to have them around during this time.

I am very thankful with my grad school committee. The participation of Santiago, Olve, Jessica, and Chris in my development as a scientist was very valuable. I really appreciate their willingness to help me and guide me every time I needed it. I also thank other professors in the Biochemistry and Molecular Biology department, in particular, Jim Bamburg and Shing Ho, for their kindness and support throughout my career.

Finally, and most importantly, I thank my family, and my husband Dimas, for their amazing support over all these years, and for their unrestricted love. They have been and will always be my motivation.

This work is dedicated to my father, who from my early years, always tried to find logical answers to both my most trivial, and my most significant questions.

TABLE OF CONTENTS

Abstract	ii
Acknowledgments	iv
Table of Contents	vi
List of Figures	viii
Chapter 1: Introduction	1
1.1 The kinetochore and its role during mitosis	1
1.2 KNL1: the unknown structure	2
1.3 KNL1 and the KMN network	4
1.4 KNL1 in kinetochore assembly	5
1.5 KNL1 in SAC activation	6
1.6 KNL1 in SAC silencing	8
1.7 Thesis Rationale	9
1.8 Figures	11
Chapter 2: KNL1 Facilitates Phosphorylation of Outer Kinetochore Proteins by Promoting Aurora B Kinase Activity	18
2.1 Introduction	18
2.2 Results	20
2.3 Discussion	29
2.4 Methods	31
2.5 Figures	38
Chapter 3: KNL1 as a Tool to Investigate Kinetochore Architecture and Kinetochore Proteins Dependencies	55
3.1 Introduction	55
3.2 Results	57
3.3 Discussion	63
3.4 Methods	67
3.5 Future Experiments	71
3.5 Figures	73
References	83
Appendix 1: The KNL1 N-terminus does not Rescue Alignment Defects in KNL1-depleted Cells	90
A1.1 Introduction	90
A1.2 Results and Discussion	90
A1.3 Methods	92

A1.4 Figures	94
Appendix 2: Implementation of the CRISPR System for editing endogenous kinetochore genes	95
A2.1 Introduction	95
A2.2 Overview of the CRISPR system	97
A2.3 Experimental design	98
A2.4 Experimental procedure	99
A2.5 Future experiments	103
A2.6 Figures	105
List of Abbreviations	114

LIST OF FIGURES

Figure 1.1	11
Figure 1.2	12
Figure 1.3	13
Figure 1.4	14
Figure 1.5	15
Figure 1.6	16
Figure 1.7	17
Figure 2.1	38
Figure 2.2	40
Figure 2.3	41
Figure 2.4	42
Figure 2.5	43
Figure 2.6	44
Figure 2.7	45
Figure 2.8	46
Figure 2.9	47
Figure 2.10	48
Figure 2.11	49
Figure 2.12	51
Figure 2.13	52
Figure 2.14	53
Figure 2.15	54
Figure 3.1	73
Figure 3.2	74
Figure 3.3	75
Figure 3.4	76
Figure 3.5	77
Figure 3.6	78
Figure 3.7	79
Figure 3.8	80
Figure 3.9	82
Figure A1.1	94
Figure A2.1	105
Figure A2.2	106
Figure A2.3	108

Figure A2.4	109
Figure A2.5	110
Figure A2.6	111
Figure A2.7	112
Figure A2.8	113

CHAPTER 1

INTRODUCTION

1.1 The kinetochore and its role during mitosis

During mitosis, replicated chromosomes attach to spindle microtubules (MTs) in order to congress to the spindle equator and correctly segregate to opposite spindle poles during anaphase. Attachment between replicated chromosomes and MTs is mediated by the kinetochore, a complex network of proteins assembled on centromeric DNA of each mitotic sister chromatid. The kinetochore also orchestrates a sophisticated signaling network called the spindle assembly checkpoint (SAC), a fail-safe mechanism that prevents mitotic exit until all chromosomes are attached to spindle MTs. Kinetochores are comprised of over 100 proteins, many of which are evolutionarily conserved and exhibit high interdependency and functionally diverse roles [1-3]. Despite this complexity, we are beginning to understand the molecular basis for kinetochore assembly [1,3], chromosome congression [4-6], and SAC signaling [7-9].

This chapter, presented as an introduction to my doctoral work, was published as a review article in 2013 under the title “KNL1: bringing order to the kinetochore”; the full reference appears below. Modifications to the published version have been made and, for simplicity, some sections contained in the published manuscript are not presented here. Some figures shown in this chapter are not included in the published review article.

J.G.D and I conceived the content of this review. I wrote the manuscript with input from J.G.D.

Caldas, G.V. and DeLuca, J.G. (2013) KNL1: Bringing order to the kinetochore. *Chromosoma*, Dec 6, Epub ahead of print.

The scaffold protein KNL1, a relatively recently described kinetochore protein, plays an important role in these critical mitotic processes, however, its specific contributions to each are just beginning to be appreciated. Here, I provide an overview of the current state of understanding of KNL1, a protein that is emerging as a key integrator of multiple kinetochore activities.

1.2 KNL1: the unknown structure

KNL1 is an evolutionarily conserved kinetochore-associated protein essential for accurate chromosome segregation in eukaryotic cells. In human cells, KNL1 was first recognized as a kinetochore protein in 2004, and its conserved role in kinetochore assembly was later demonstrated [10-13]. Since its discovery, KNL1 has been known as a critical platform for kinetochore protein recruitment and as a linker between centromeric DNA and the plus-ends of spindle MTs, not only in human cells but also in yeast, chicken, and flies [11, 14-17].

Despite being evolutionarily conserved, KNL1 displays low overall sequence similarity between species, and according to folding prediction algorithms, it is mostly intrinsically disordered (FoldIndex, Phyre) (Figure 1.2). In human KNL1 for example, with over 2300 amino acids, less than half of the protein is predicted to fold into an ordered structure. Most of this ordered structure resides at the far C-terminus of the protein, and it is composed of a globular domain containing tandem RWD motifs [18] and a coiled-coil domain [19]. The RWD motifs mediate direct interaction with the Mis12 complex, while the coiled-coil domain mediates interaction with Zwint-1. Both Mis12 and Zwint-1 are proteins important for proper kinetochore assembly (Figure 1.3). Within the remaining “unstructured” region of the protein, several motifs

have been identified. The RVSF (RVXF) and SILK ([SG]ILK) motifs, both of which reside at the far N-terminus of KNL1, mediate binding of the phosphatase PP1 [20]. Two KI motifs, KI1 and KI2 (KI[DN]XXXF[LI]XXLK), also localized in the N-terminus of KNL1, interact with the essential SAC proteins Bub1 and BubR1, respectively [13, 21, 22] (Figure 1.3). More recently, MELT motifs (M[ED][ILVM][ST]) in the N-terminal and central regions of KNL1 have been identified and demonstrated as mediators for recruitment of Bub1 and Bub3, another essential SAC component [23-26] (Figure 1.3). A search for KNL1 orthologs across eukaryotes recently identified KNL1 in three out of all six eukaryotic supergroups [27]. Although KNL1 primary sequence similarity across species is poor and the predicted protein size is quite variable, the C-terminal region, SILK, RVSF, and MELT motifs are well conserved. The number of MELT motifs across species, however, is widely variable [27] (Figure 1.4).

Full-length *C. elegans* KNL1 and fragments of yeast and human KNL1 have been successfully reconstituted *in vitro* [21, 22, 25, 26, 28, 29]. However, there is a dearth of structural information for KNL1, as only small fragments of the human N-terminal region containing the KI motifs [21, 22], and small fragments of yeast KNL1 (Spc105) containing MELT motifs have been crystallized [24] (Figure 1.5). In these atomic structures only a handful of residues (~15) showed significant electron density, presumably due to the disordered nature of KNL1. The residues identified with confidence in the structures of both KNL1 KI motifs fold into short alpha-helices when bound to Bub1 or BubR1 [21, 22]. Circular dichroism experiments indicate that these regions of KNL1 by themselves lack secondary structure [21], thus it appears that KNL1 transitions from a disordered configuration to an ordered one upon binding to other proteins.

1.3 KNL1 and the KMN network

KNL1 is a component of the “KMN network,” a complex of proteins that makes up the primary MT binding interface at the kinetochore. The KMN network is comprised of the KNL1 protein, the Mis12 complex (Mis12, Dsn1, Nsl1, and Nnf1) and the Ndc80 complex (Hec1, Nuf2, Spc24, and Spc25) [30-32] (Figure 1.6). The high binding affinity measured *in vitro* between several KMN components (K_d -nM range) [19], their apparent cooperative binding to MTs [28] and their substantial co-dependency for kinetochore recruitment *in vivo* [32] (Figure 1.7), suggest that these proteins function together during mitosis. The most recognized function of the KMN network at kinetochores is linkage of the inner kinetochore (chromatin-proximal region) to plus-ends of spindle MTs. Association with the inner kinetochore region requires binding between the Mis12 complex and the CCAN (Constitutive Centromere Associated Network), a large group of centromere-associated proteins responsible for establishing and maintaining centromere identity [33] (Figure 1.1). The KMN-MT interaction on the other hand, is primarily mediated by Hec1, a component of the Ndc80 complex [28, 34-37]. KNL1 also directly binds MTs *in vitro*, however, a significant role for this MT-binding activity in the formation of end-on, force-generating kinetochore-MT attachments has not been demonstrated. Although the KMN network is considered a functional unit [28], it is important to note that depletion of individual KMN components results in different phenotypes. For instance, Mis12 and KNL1 depletion from human cells leads to a partial chromosome alignment phenotype [11, 38, 39], while depletion of any of the Ndc80 complex subunits leads to severe kinetochore-MT attachment defects and completely unaligned chromosomes [31]. To what extent the components of the KMN network rely on each other to carry out their functions, independent of their role in network connectivity, is an interesting question for further study.

1.4 KNL1 in kinetochore assembly

In *C. elegans*, depletion of KNL1 by RNAi results in loss of kinetochore-localized Hec1 (CeNdc80), Nuf2 (HIM10), Spc25 (KBP3), Bub1, CENP-F (HCP-1), CLASP2, and reduced kinetochore localization of Dsn1 (KNL3) and Mis12 [10, 40]. Of those tested, total protein levels were maintained in KNL1-depleted embryos, indicating that KNL1 is required for their recruitment and/or maintenance at kinetochores but not for their stability [10, 40]. In addition, Zwilch (ZWL-1, a component of the RZZ complex which additionally contains ZW10 and Rod), Spindly (SPDL-1), and PP1 kinetochore localization is also dependent on KNL1 in *C. elegans* [29, 41].

Depletion of KNL1 from human cells results in a similar loss of kinetochore proteins as observed in *C. elegans*, with some variations (Figure 1.7). Bub1, Zwint-1 and RZZ components are lost from kinetochores in KNL1-depleted cells [11, 12, 42]. BubR1, Cenp-E, Cenp-F, Mad1, and Mad2 kinetochore localization rely on Bub1 [43]. Therefore, logic dictates that depletion of KNL1 correspondingly results in kinetochore delocalization of Bub1 downstream targets. Not surprisingly, BubR1, Cenp-F and Mad2 kinetochore localization is decreased in KNL1-depleted cells [11, 12, 39], and we observe a reduction of kinetochore-associated Cenp-E upon KNL1 depletion from human cells (G.C. and J.D., unpublished data). Presumably, although untested, kinetochore recruitment of the dynein-dynactin complex, which depends on the RZZ complex, is also perturbed after KNL1 depletion.

Kinetochore levels of the Mis12 complex component Dsn1 are reduced after KNL1 depletion from human cells [11]. An early study reported that depletion of KNL1 from DT40 chicken cells resulted in a 45% reduction of Hec1 at kinetochores, but in human cells Hec1 localization was not affected [11]. In contrast, a recent study found that Hec1 levels decreased

by ~40% after KNL1 depletion in HeLa cells [44]. Despite the disparity, it is evident that the Ndc80 complex retains some ability to localize to kinetochores in KNL1-depleted human cells. This is not surprising, as it has been demonstrated that the CCAN component CENP-T also contributes to kinetochore recruitment of the Ndc80 complex in human cells [45]. Such KNL1-independent Hec1 kinetochore localization does not follow a pattern through evolution, since as in *C. elegans*, Hec1 relies on KNL1 for localization in *Drosophila* [17, 40], but this dependency is not observed in fission yeast [46].

1.5 KNL1 in SAC activation

KNL1 serves as a binding platform, both directly and indirectly, for proteins involved in the SAC (Spindle Assembly Checkpoint), the safety mechanism that prevents mitotic exit until all kinetochores are correctly attached to spindle MTs (Figure 1.6). The SAC delays anaphase by promoting and sustaining inhibition of the anaphase promoting complex/cyclosome (APC/C), an E3 ubiquitin ligase that, upon activation by Cdc20, targets securin and cyclin B for degradation, which ultimately drives mitotic exit [7, 8, 47] (Figure 1.6). The core components of the SAC are the evolutionarily conserved proteins Bub1, BubR1/Mad3, Bub3, Mad1, Mad2, and Mps1. All of these SAC components, except for Mps1, have been shown to rely on KNL1 for kinetochore localization (Figure 1.7). Bub1, Bub3, and BubR1 directly interact with KNL1 [21, 22, 24-26, 48] (Figure 1.3). Mad1 and Mad2 kinetochore localization depends on Bub1 [49-51] and the RZZ complex [52] (Figure 1.7); therefore, it is expected that KNL1 depletion compromises Mad1 and Mad2 kinetochore localization [39].

KNL1 was first found to associate with Bub1 and BubR1 through yeast two-hybrid experiments [12, 13]. Later experiments demonstrated that the two closely related but distinct KI

motifs in KNL1, KI1 and KI2, directly bind the TPR (tetra-ricopeptide repeat) domains of Bub1 and BubR1, respectively [13, 21, 22]. Interestingly, the KI/TPR interactions are dispensable for both Bub1 and BubR1 kinetochore targeting in human cells [22]. However, that is not the case in fission yeast, where a Δ TPR Bub1 mutant does not efficiently target to kinetochores [53]. It is possible that in human cells, the KI/TPR interaction enhances, but is not essential for SAC protein recruitment and/or function. Recent studies in yeast and human cells established that Mps1-mediated phosphorylation of the KNL1 MELT repeats is required for Bub1/Bub3 kinetochore targeting [23-26]. Although Bub1 and Bub3 require each other for KNL1-mediated kinetochore localization, the inter-dependency of BubR1 with Bub1 and/or Bub3 for kinetochore localization and function remains unresolved. In addition, whether all MELT repeats, specific repeats, or a threshold number of repeats are critical for recruiting Bub1 and Bub3 and if MELT phosphorylation also mediates direct BubR1 recruitment are outstanding, unanswered questions.

KNL1 also plays a role in recruiting the essential SAC proteins Mad1 and Mad2 to kinetochores, likely through indirect pathways. Mad1, the kinetochore receptor for Mad2, requires both Bub1 and the RZZ complex for kinetochore localization [54]. Unattached kinetochores accumulate complexes of Mad1–Mad2 that catalyze the conversion of inactive, cytoplasmic Mad2 (“open” Mad2) to a form of Mad2 that binds Cdc20 (“closed” Mad2) and inhibits APC/C activity [9]. Cdc20-bound Mad2, at the kinetochore or in the cytoplasm, also potentially mediates Mad2 catalytic conversion, resulting in further inhibition of APC/CCdc20. Mad2-based amplification of the APC/CCdc20 inhibitor is thought to be critical for delaying mitotic exit in the presence of unattached kinetochores [55-59]. Although it is clear that Mad1 and Mad2 are indispensable for SAC function, whether their kinetochore localization is explicitly required is not yet resolved [2, 47].

While we are closer to understanding how the checkpoint proteins interact with KNL1, how these interactions impact their function in SAC signaling is a fundamental issue that remains to be addressed.

1.6 KNL1 in SAC silencing

The RVSF and SILK motifs in the KNL1 N-terminus mediate direct binding to PP1 (Figure 1.3), a phosphatase that counteracts Aurora B kinase activity [60]. Aurora B kinase itself regulates the interaction between KNL1 and PP1 as binding is disrupted by Aurora B-mediated phosphorylation of the RVSF motif [20]. In human cells, PP1 binding to KNL1, together with KNL1-BubR1-mediated PP2A kinetochore recruitment, is proposed as a mechanism by which outer kinetochore substrates are dephosphorylated during late mitosis, allowing stabilization of kinetochore–MT attachments [20, 61, 62]. Interestingly, in both budding and fission yeast and in *C. elegans*, KNL1-mediated PP1 binding contributes to checkpoint silencing [29, 63-66], the mechanism that allows APC/Cdc20-mediated mitotic exit.

The MT binding region of KNL1 is also necessary for SAC silencing in *C. elegans* (Figure 1.3) [29]. Embryos containing mutations in the MT binding domain of KNL1 that disrupted MT interaction *in vitro* were able to congress chromosomes to the metaphase plate without obvious kinetochore–MT attachment defects but exhibited delayed anaphase onset [29]. It remains to be tested if PP1 binding and/or MT binding activities are crucial for SAC silencing in human cells. Experimental manipulation of KNL1, which acts as both a platform for SAC-activating and SAC-silencing proteins, will help elucidate how checkpoint activation and amplification are coupled with checkpoint silencing and how MT attachment modulates this complex kinetochore machinery.

1.7 Thesis rationale

The success of mitosis relies on the (1) formation of kinetochore–MT attachments able to facilitate both correct congression and segregation of all replicated chromosomes and (2) production of a temporally controlled, SAC-generated APC/CCdc20 inhibitor that prevents mitotic exit until all chromosomes are properly attached to spindle MTs. Despite considerable progress in the understanding of key proteins and molecular mechanisms involved in these two processes, there is no unified view of how they are linked. KNL1 is necessary for the establishment of a reliable kinetochore–MT interface that attaches dynamic spindle MT plus-ends to mitotic chromosomes. KNL1 also ensures that SAC proteins required to inhibit APC/CCdc20 accumulate at unattached kinetochores to amplify the inhibitory signal and delay mitotic exit when appropriate. Moreover, KNL1 is required to quench APC/CCdc20 inhibition and silence the SAC to promote mitotic exit when the cell is ready to divide. How KNL1 contributes to the organization of kinetochore proteins and their interactivity, and how this large and mostly “unstructured” protein mediates the coupling of these fundamental mitotic processes is the focus of my thesis work.

In Chapter 2 I demonstrate that the N-terminal region of KNL1 is required for Aurora B and Bub1 kinase activities at kinetochores. Aurora B phosphorylates kinetochore proteins during early mitosis, increasing kinetochore–MT turnover and preventing premature stabilization of kinetochore–MT attachments, which can be detrimental to mitotic progression. Bub1 on the other hand, is necessary for the recruitment of checkpoint proteins to kinetochores to ensure amplification of the signal that delays mitosis exit when MT attachment is incorrect. Although Bub1 has been implicated in the pathway that drives accumulation of Aurora B at the inner centromere region, and accumulation of Aurora B at this location is thought to be a requirement

for full Aurora B activity, I provide evidence that Aurora B accumulation is not sufficient to reach full levels of kinase activity in the absence of KNL1. Based on these findings, I propose a mechanism to explain how Aurora B activity is modulated during mitotic progression through Bub1/KNL1 and how Aurora B-mediated correction of erroneous kinetochore-MT attachments is linked to checkpoint signaling. Importantly, these results raise the possibility that KNL1, functioning beyond a kinetochore scaffolding molecule, may play a more direct role, not only in the regulation, but also in the coupling of essential mitotic processes. Accordingly, several questions come to light. Which proteins are spatially organized by KNL1? What regions or motifs on KNL1 are necessary for the localization of these kinetochore proteins? Do these proteins compete for the same binding sites on KNL1? Is there interdependency between them? How does KNL1 influence the activities of kinetochore proteins? Is KNL1-dependent kinetochore organization temporally regulated during mitosis? In Chapter 3, I attempt to address some of these questions by systematically mapping kinetochore proteins on different regions of KNL1. Although further experiments are required for publication of this work, results from these analyses highlight key aspects regarding dependencies and organization of the kinetochore network with KNL1 as a central player, and they exemplify the use of KNL1 as a tool to dissect kinetochore signaling pathways and kinetochore architecture.

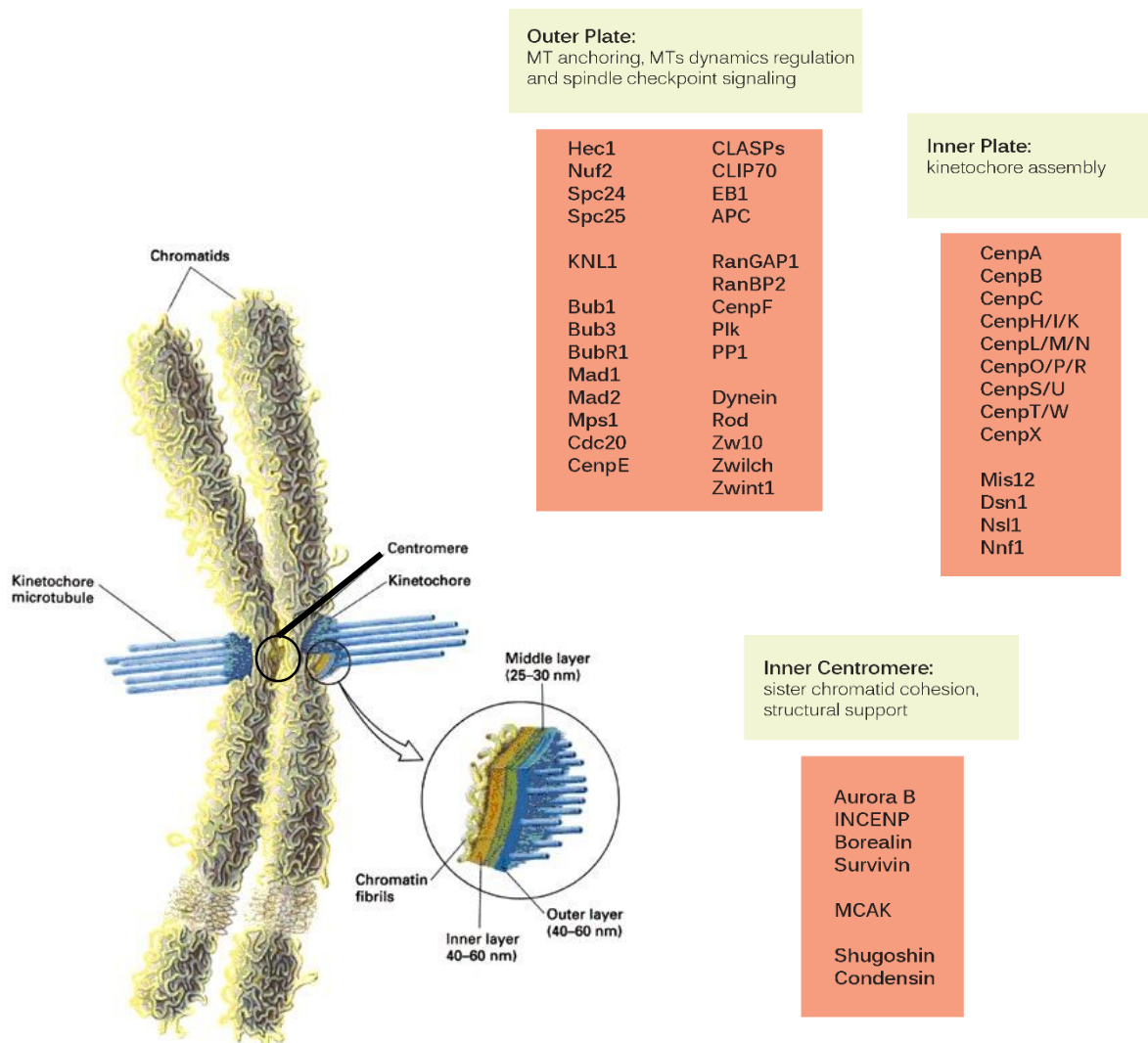
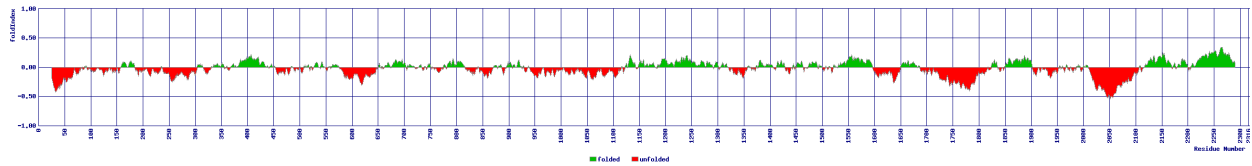


Figure 1.1. The kinetochore-MT interface. The inner and outer layers/plates of the kinetochore and the inner centromere region are depicted. Some of the most representative proteins of each layer are listed. Figure adapted from Molecular Cell Biology, 3rd ed. [67] and Maiato et al. 2004 [68].



1	MDGVSSEANE	ENDNIERPVR	RRHSSILKPP	RSPLQDLRGG	NERVQESNAL	1201	FPKDNSCVQE	IAEKQALAVG	NKIVLHTEQK	QQLFAATNRT	TNEIKFHS
51	RNKGNSRRVS	FADTIKVFQT	ESHMKIVRKS	EMEETETGEN	LLLIQNKKLE	1251	AMDEKVIQKV	VDQACTLEKA	QVESQQLNRR	DRRNVDFTSS	HATAVCGSSD
101	DNYCEITGMN	TLLSAPIHTQ	MQOKEFSIIE	HTRERKHAND	QTVLFSDENO	1301	NYSCLPNVIS	CTDNLEGSAM	LLCDKDEEKA	NYCPVQNDLA	YANDFASEYY
151	MDLTSSTVM	ITKGLLDNPI	SEKSTKIDTT	SFLANLKLHT	EDSRMGEVNV	1351	LESECGPLSA	PCPLLEKEEV	IQTSTKQQLD	CVITLHKQDD	LIKDPRNLLA
201	FSDVQNTSSE	NKIDFNDFIK	RLKTGKCSAF	PDVPDKENFE	IPIYSKEPNS	1401	NQTLVYSQDL	GEMTKLNSKR	VSFKLPKQDM	KVYVDDIYVI	POPHFSTQDP
251	ASSTHQMHSV	LKEDENNSNI	TRLFREKODD	MNFTQCHTAN	IQTLIPTSSSE	1451	PLPKKGQSSI	NKEEVLKSKA	GNKSLNLIEN	SSAPICENKP	KILNSEEWA
301	TNSRESKGNL	ITIIYGNDFMD	LTFNHTLQIL	PATGNFSEIE	NQTNAMQVMT	1501	AACKGELKEN	IQTNYNTAL	DFHSNSDVTK	QVIQTHVNAG	EAPDPVITSN
351	TCYGVKASGN	KTVFKSKQNT	AFQDLSINSA	DKIHITRSHI	MGAETHIVSQ	1551	VPCFHSIKPN	LNNLNGKTCG	FLAFQTVHLP	PLPQLLELG	NKAHNDMHIV
401	TCNQDARILA	MTPESIYNSP	SIQGCCTVFY	SSCNDAMEMT	KCLSNMREEK	1601	QATEIHNINI	ISSNAKDSRD	EENKGSNGA	ETTSLPPKTV	FKDKVRRCSL
451	NLLKHDSNYA	KMYCNPDAMS	SLTEKTIYSG	EENMDITKSH	TVAIDNQIFK	1651	GIFLPRLPNK	RNCNVTGIDD	LEQIPADTTD	INHLETQVPS	SKDSGIGSVA
501	QQQSNVQIAA	APTPEKEMML	QNLMTTSEDG	KMNVCNSVVP	HVSKERIQQS	1701	GKLNLSPSQY	INEENLPVYP	DEINSSDSIN	IETEEKALIE	TYQKEISPYE
551	LSNPLSISLT	DRKTELLSCE	NMDLTSHTS	NLGSQVPLAA	YNLAPESTSE	1751	NMGKTCNSQ	KRTWQEEED	IHKKIKIRKV	EIKFSDTTQD	REIFDHHTEE
601	SHSQSKSSSD	ECEEITKSRN	EPFQRSDIIA	KNSLTDTWNK	DKDOWLKILP	1801	DIDKANSVL	IKNLSRTPSS	CSSSLDSIKA	DGTSLDFSTY	RSSQMESQFL
651	YLDKDS PQSA	DCNQEIATSH	NIVYCGGVL	KQITNRNTVS	WEQSLFSTTK	1851	RDVICEESLR	EKLQDGRITI	REFFILLQVH	ILIQKPRQSN	LPGNFTVNTF
701	PLFSSQFQSM	KNHDTAISSH	TVKSVLQONS	KLAEP LRKSL	SNPTPDYCHD	1901	PTPEDLMLSQ	YVVRPKIQIY	REDCEARRQK	IEELKLSASN	QDKLLVDINK
751	KMIICSEEQ	NMDLTKSHTV	VIGFGPSELQ	ELGKTNLEHT	TGQLTMMNRQ	1951	NLWEKMRHCS	DKELKAFGIY	LNKIKSCFTK	MTKVFTHQCK	VALYKLVQS
801	IAVKVEKCGK	SPIEKSGVLK	SNCIMDVLED	ESVQKPKFPK	EKQNVKIWR	2001	AQNEREKLOI	KIDEMDKILK	KIDNCLTEME	TETKNLEDEE	KNNPVEEWS
851	KSVGGPKIDK	TIVFSEDDKN	DMDITKSYTI	EINHRP LLEK	RDCHLVPLAG	2051	EMRAAEKELE	QLKTEEEELQ	RNLLELEVQK	EQTLAQIDFM	QKQRNRTEEL
901	TSETILYTCG	QDDMEITRSH	TTALECKTVS	PDEITTRPMD	KTVVFDNVH	2101	LDQLSLSEWD	VVEWSDQAV	FTFVYDTIQL	TITFEESVVG	FPFLDKRYRK
951	ELEMTESHTV	FIDYQEKERT	DRPNFELSQR	KSLGTPVIC	TPTEESVFFP	2151	IVDVNFQSL	DEDQAPPSSL	LVHKLIFQYV	EKESWIKKTC	TTQHQLPKML
1001	NGCESDRLVA	NDSQLTPLEE	WSNRRGPVEV	ADNMELSKSA	TCNKIKDVQS	2201	EEFSLVWHHC	RLLGEEIEYL	KRWGPNYNLM	NIDINNNELR	LLFSSAAFA
1051	PGFLNEPLSS	KSQRKGLKL	KNDKTI VFS	NHKNDMDITQ	SCMVEIDNES	2251	KFEITLFLSA	YYPVPLPST	IQNHVGNVTSQ	DDIATILSKV	PLENNYLRKV
1101	ALEDKEDFHL	AGASKTILYS	CQDDMEITR	SHTTALECKT	LLPNEIAIRP	2301	VKQIYQDLFQ	DCHFVH			
1151	MDKTVLFTDN	YSDLEVTDH	TVFIDCQATE	KILEENPKFG	IGKGNLGV						

Figure 1.2. Human KNL1 Fold Index prediction (<http://bip.weizmann.ac.il/flddb/in/findex>). The predicted unfolded segments of the protein are shown in red. The sequence is shown below.

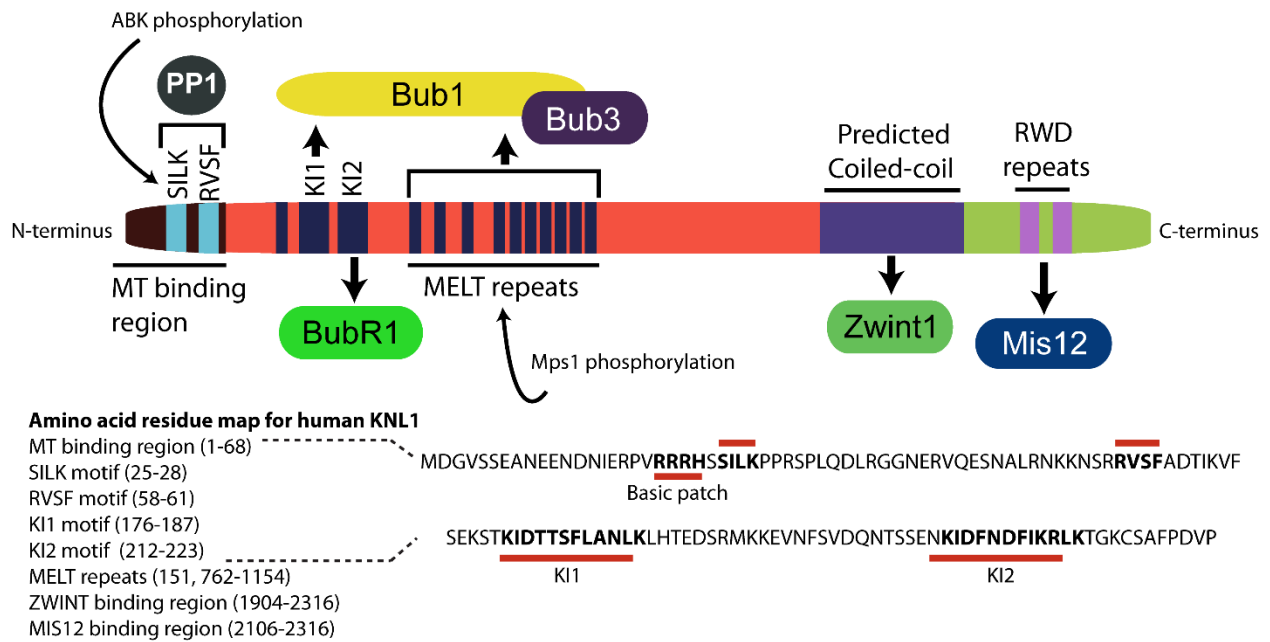


Figure 1.3. Domain architecture of human KNL1. Key regions involved in KNL1 function are indicated schematically (top), and the corresponding amino acid sequences for each region in human KNL1 are listed (bottom). Aurora B kinase phosphorylates the N-terminus of KNL1 to inhibit association with PP1 (Liu et al. 2010) [20]. Mps1 phosphorylates the KNL1 MELT repeats to promote association with Bub1 and Bub3 (London et al. 2012; Primorac et al. 2013; Shepperd et al. 2012; Yamagishi et al. 2012) [23-26]. Amino acid residues 1-68 indicate the MT binding domain (Welburn et al. 2010) [69], and underlined is a basic patch of residues (RRRH), whose analogous residues in *C. elegans* have been implicated in direct MT interaction (Espeut et al. 2012) [29]. Figure adapted from Caldas and DeLuca 2013 [44].

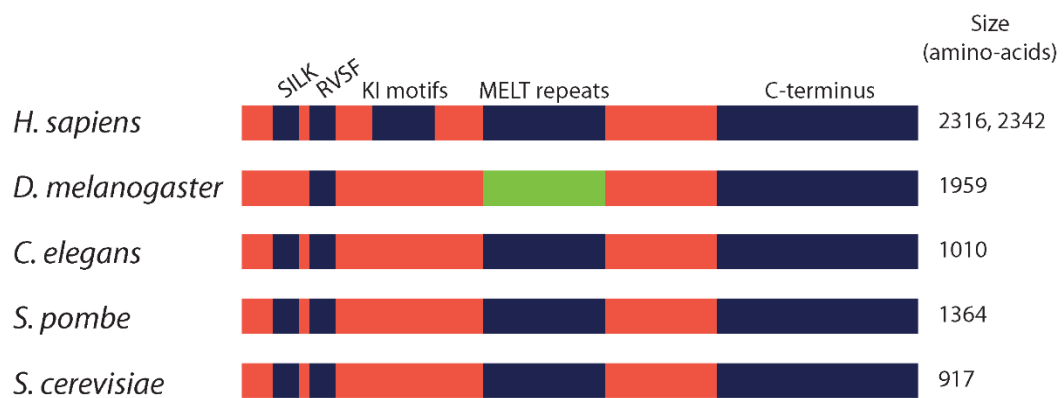


Figure 1.4. Evolutionary conservation of KNL1 domain architecture. Key KNL1 functional regions are shown for several organisms. The number of amino acids in KNL1 for the various organisms are shown (right). Two values in this column indicate multiple isoforms (*H. sapiens*). The green region in *D. melanogaster* indicates the presence of repetitive motifs that differ from the MELT consensus motif observed in other organisms (Schittenhelm et al. 2009) [17]. Figure adapted from Caldas and DeLuca 2013 [44].

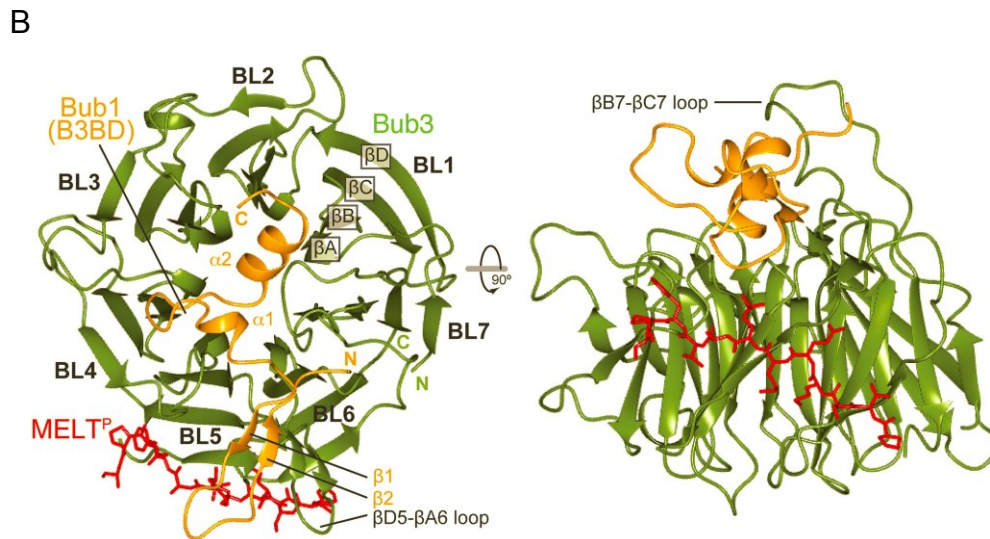
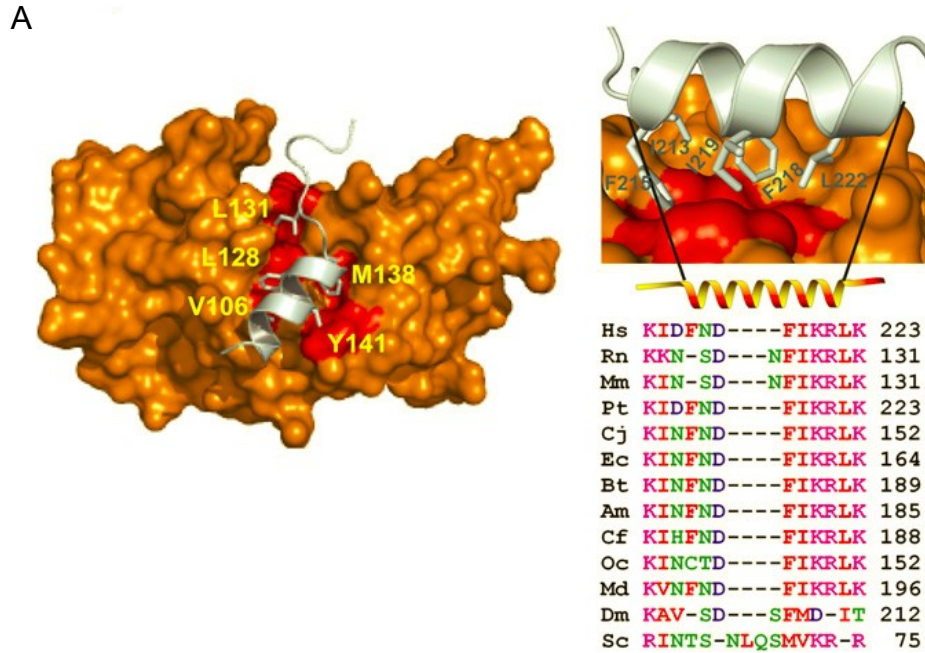


Figure 1.5. KNL1 crystal structures. (A) Crystal structure of the TPR domain of hBUBR1 (orange) in complex with the KI2 motif of hKNL1 (white) (adapted from Bolanos-Garcia et al. 2011) [21]. Hydrophobic residues key for this interaction are depicted in red. A close up image shows that residues I213, F215, F218 and I219 of KNL1-KI2 bind a shallow hydrophobic groove on BubR1-TPR. The amino acid sequence of KNL1-KI2 in different species is also shown. (B) Crystal structure of ScBub1 (amino acids 289–359) (yellow), in complex with ScBub3 (green), and a phosphorylated MELT motif from ScSpc105 (KNL1) (red) (adapted from Primorac et al. 2013) [24]. Side view of the ternary complex is shown to the left.

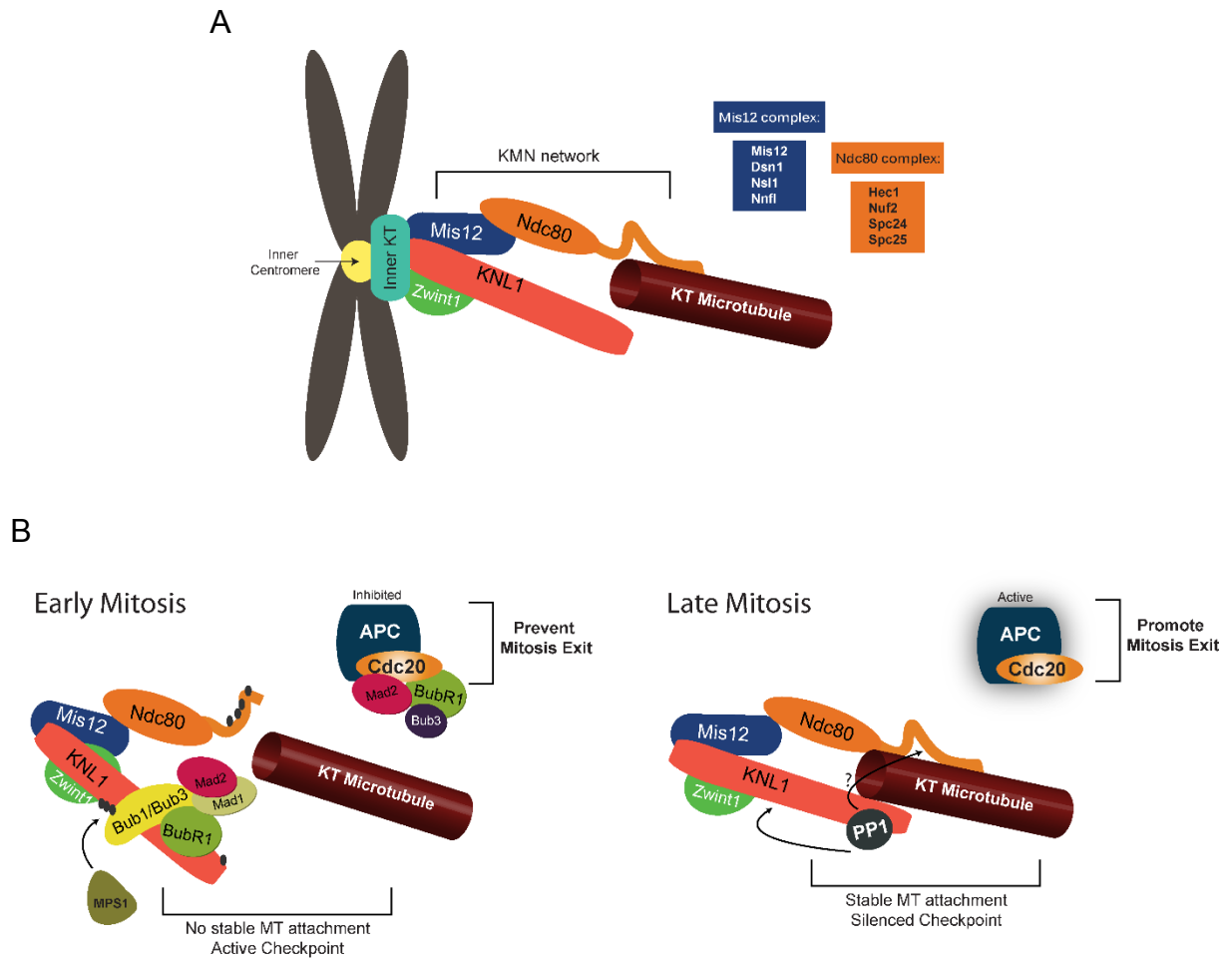


Figure 1.6. Representation of the principal kinetochore components involved in kinetochore-MT attachment and checkpoint signaling . (A). The KMN network, required for correct kinetochore-MT attachment and formed by KNL1, the Mis12 complex, and the Ndc80 complex, is depicted. The subunits that compose the Mis12 complex and the Ndc80 complex are listed. (B) Current model for checkpoint signaling. In early mitosis, when unstable kinetochore-MT attachments are present, the proteins BubR1, Bub3, and Mad2 inhibit Cdc20, the APC activator. Mad2 accumulation at kinetochores is required for Cdc20 inhibition. In late mitosis, upon stabilization of kinetochore-MT attachments, the checkpoint is silenced, presumably by the phosphatase PP1 which releases checkpoint proteins from the kinetochore, and Cdc20 is able to activate the APC. KNL1 is required for the kinetochore recruitment of the SAC proteins Bub1, BubR1, Bub3, Mad1, and Mad2, and for recruitment of PP1. Figure adapted from Caldas and DeLuca 2013 [44].

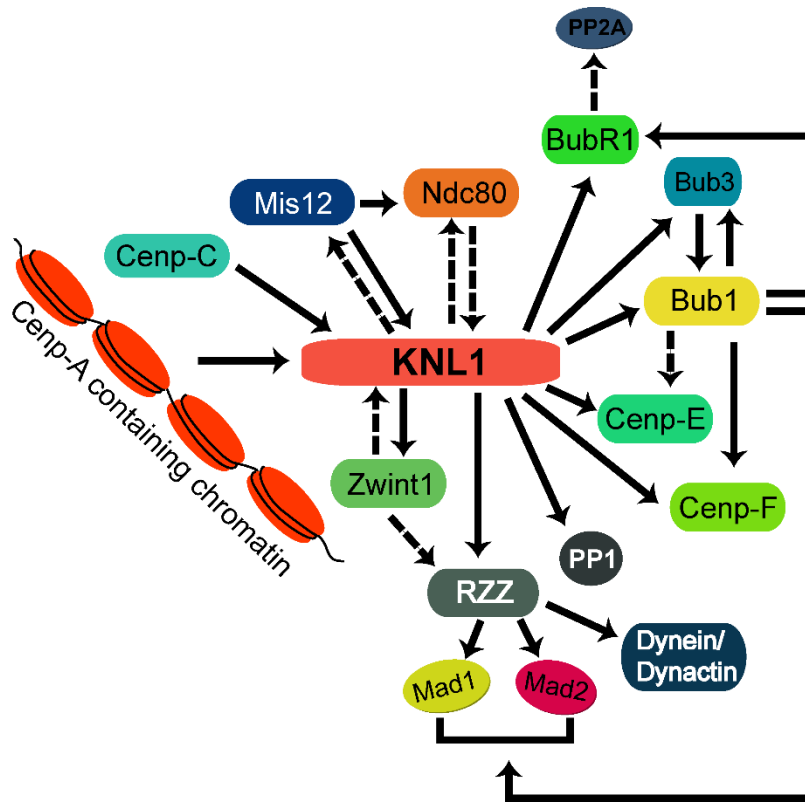


Figure 1.7. KNL1-dependency of kinetochore protein localization. Solid arrows indicate a high level of dependence for localization and dashed arrows indicate a partial dependence. Arrows do not indicate direct interaction. Figure adapted from Caldas and DeLuca 2013 [44].

CHAPTER 2

KNL1 FACILITATES PHOSPHORYLATION OF OUTER KINETOCHORE PROTEINS BY PROMOTING AURORA B KINASE ACTIVITY

2.1 Introduction

Congression and proper segregation of mitotic chromosomes is critically dependent on the interaction between spindle microtubules (MTs) and kinetochores. The strength of kinetochore–MT attachments must be precisely regulated to prevent the accumulation of attachment errors and to facilitate proper activation and silencing of the spindle assembly checkpoint (SAC). Aurora B kinase influences the binding affinity between kinetochores and MTs [70-72], in part through phosphorylation of the NDC80 complex component Hec1 [28, 36]. During early mitosis, Hec1 is highly phosphorylated by Aurora B, reducing its MT binding activity and preventing premature stabilization of kinetochore–MT attachments. Conversely, during late mitosis, Hec1 phosphorylation levels are low, increasing kinetochore–MT binding affinity and promoting stable

The work presented here was published as a research article in 2013 under the same title; the full reference appears below. Figures presented in the original manuscript as supplementary figures, because of length constraints, are shown in this chapter as main figures.

J.G.D and I conceived the paper, designed the experiments, and interpreted the data. I performed the research. K.F.D carried out the phenotypic analysis displayed in Figure 2.4 B-D and made the original observation that Hec1 phosphorylation was decreased upon KNL1 depletion. I wrote the original paper with input from J.G.D.

Caldas, G.V., DeLuca, K.F., DeLuca, J.G. (2013) KNL1 Facilitates Phosphorylation of Outer Kinetochore Proteins by Promoting Aurora B Kinase Activity. *The Journal of Cell Biology*, 203:957-969.

attachments and SAC silencing [73]. A current model to explain the marked change in Aurora B kinase-mediated phosphorylation posits that phosphorylation efficiency depends on the distance between kinetochore substrates and the permanently activated kinase that emanates as a gradient from the inner centromere, such that increased inter-kinetochore distance results in decreased levels of substrate phosphorylation [69, 74, 75]. Although protein gradients exist and can be sustained in the cytoplasm [76], the mechanism by how a steep, nanometer-scale gradient of active Aurora B arises and regulates the interaction between kinetochores and MTs is not well understood. Alternatively, Aurora B activity at the kinetochore may be modulated during mitotic progression as a result of biochemical and physical changes occurring at the kinetochore. Indeed, several kinetochore proteins have been demonstrated to influence Aurora B activity. However, little is known about the interplay between Aurora B regulators and the mechanisms by which they modulate Aurora B activity.

The kinetochore-associated phosphatases PP1 and PP2A have been implicated in counteracting Aurora B activity to facilitate kinetochore–MT stabilization [20, 61, 62, 77]. The kinetochore protein KNL1 mediates recruitment of PP1 (directly) and PP2A (indirectly through BubR1) to kinetochores, as well as recruitment of the SAC proteins BubR1 and Bub1, which are known to down-regulate Aurora B kinase activity and promote Aurora B localization, respectively [12, 20, 62, 77, 78]. Although KNL1 is a scaffold for both positive and negative regulators of Aurora B activity, the consequences of KNL1 depletion in mammalian cells and its effect on Aurora B–mediated regulation of kinetochore–MT attachment have not been studied. Here we find that depletion of KNL1 or perturbation of the KNL1 N terminus abolishes Aurora B–mediated phosphorylation of outer kinetochore proteins, including Hec1 and Dsn1, and prevents cells from properly regulating kinetochore–MT attachments. This lack of phosphorylation is correlated to a

significant decrease in Aurora B activity at kinetochores. We show that the N terminus of KNL1 also facilitates kinase activity of Bub1, a SAC protein known to promote Aurora B recruitment by phosphorylating histone H2A. However, bypassing the requirements of Bub1-mediated Aurora B recruitment in KNL1-depleted cells by direct targeting of Aurora B does not rescue wild-type levels of Aurora B activity or substrate phosphorylation, suggesting that Bub1 and KNL1 may act in an alternative pathway to regulate Aurora B activity. Together, our results demonstrate that KNL1 is essential for Aurora B kinase activity at kinetochores and for proper regulation of kinetochore–MT attachments.

2.2 Results

KNL1 facilitates phosphorylation of the outer kinetochore protein Hec1

The kinetochore protein KNL1 has been described as a scaffold for both SAC proteins and phosphatase activities. PP1 is recruited to kinetochores by an N-terminal RVSF motif, and PP2A is recruited by BubR1, a well-known KNL1 interacting partner [20, 62, 77]. Both PP1 and PP2A are proposed to counteract Aurora B activity. In support of this, depletion of BubR1 (which recruits PP2A to kinetochores) or Sds22 (a PP1 regulatory subunit) results in hyperactivation of Aurora B [78, 79]. Based on these findings, we predicted that loss of KNL1, a hub for kinetochore Aurora B antagonists, would result in high levels of Hec1 phosphorylation. To test this, we depleted KNL1 from HeLa and RPE-1 cells and quantified Hec1 phosphorylation at kinetochores (Figure 2.1A-F). Quantification was performed in early mitotic cells, when Hec1 phosphorylation levels at kinetochores are highest [73]. Surprisingly, KNL1 depletion caused a significant decrease in Hec1 phosphorylation (>80%; Figure 2.1C-F). We measured a 42% decrease in total Hec1 levels at kinetochores after KNL1 depletion, but measured no change in total Hec1 protein levels (Figure

2.1G). The reduction in Hec1 phosphorylation after KNL1 depletion was significant after accounting for the 42% loss of total Hec1 at kinetochores Figure 2.1H). Thus, KNL1 is required for Hec1 phosphorylation in early mitosis.

KNL1 is required for Aurora B activation

To determine if the observed defects in Hec1 phosphorylation upon KNL1 depletion were due to perturbation of Aurora B kinase activity, we evaluated levels of active Aurora B kinase in KNL1-depleted cells. Active Aurora B has been detected using antibodies to either auto-phosphorylated Thr232 (pT232) [80] or phosphorylated Ser331 (pS331) [81]. Compared with control cells, kinetochores of KNL1-depleted cells exhibited a marked reduction of Aurora B pT232 and pS331 localization (Figure 2.2A-D), suggesting that KNL1 is involved in the regulation of Hec1 phosphorylation by facilitating recruitment and/or activation of Aurora B. Contrary to the bulk of centromeric Aurora B (between sister kinetochores) observed with pan-Aurora B antibodies, pT232 and pS331 Aurora B antibodies localize at the kinetochore region in early mitosis. Despite the different localization patterns, the Aurora B phosphospecific antibodies are not detected in cells when Aurora B is chemically inhibited [73, 81], and Western blotting with the pT232 antibody suggests that it primarily recognizes Aurora B (Figure 2.2C). Whether phosphorylated Aurora B is recruited to specific sites at the kinetochore or whether Aurora B localizes to multiple sites between sister kinetochores and only those molecules near the kinetochore are phosphorylated at T232 (and S331) is unclear. Regardless, auto-phosphorylation of Aurora B (a requirement for kinase activity) [80] and phosphorylation of Aurora B substrates significantly decrease after KNL1 depletion. Thus, we conclude that KNL1 is essential for proper Aurora B activity at the kinetochore.

Using a non-phosphospecific Aurora B antibody (AIM1), we determined if KNL1 depletion had an effect on centromeric Aurora B localization. We found only a modest reduction of inner centromeric Aurora B (40%) in cells depleted of KNL1 (Figure 2.3A) compared with the more severe reduction of Aurora B pT232 (>80%). Strikingly, depletion of KNL1 resulted in a significant decrease in phosphorylation of the Aurora B substrate and chromosomal passenger complex (CPC) component INCENP (Figure 2.3B), indicating that activity of Aurora B at the inner centromere is also compromised upon KNL1 depletion. In contrast, global Aurora B activity, determined by phosphorylation of Ser10 histone H3 [82], did not significantly change upon depletion of KNL1 (Figure 2.3C). Together, our data demonstrate that KNL1 promotes activity of Aurora B at the centromere and kinetochore region and acts as a mediator of outer kinetochore protein phosphorylation.

KNL1 is required for proper regulation of kinetochore–MT dynamics

Given its role in promoting Aurora B kinase activity at kinetochores, we next probed the phenotypic consequences of KNL1 depletion. Lack of Aurora B kinase activity in early mitosis results in premature stabilization of kinetochore–MT fibers, which persist after exposing cells to cold-induced MT depolymerization [74, 83]. Both KNL1-depleted cells and cells treated with ZM447439, an Aurora B kinase inhibitor, exhibited higher spindle fluorescence intensity in early mitosis than control cells after cold-induced MT depolymerization (Figure 2.4A). This indicates that depletion of KNL1 results in premature stabilization of kinetochore–MT attachments and further supports the idea that KNL1 promotes Aurora B kinase activity. KNL1 depletion leads to a phenotype in which a population of chromosomes aligns at the spindle equator, while another population of chromosomes remains trapped near one or both poles (Figure 2.1A and 2.1E) [11].

Interestingly, chromosomes trapped at the poles in KNL1-depleted cells generally did not exhibit stable, end-on kinetochore–MT attachments after cold treatment (unpublished data). Although this may appear inconsistent with reduced Aurora B activity at kinetochores, the result is possibly due to kinetochore delocalization of proteins required to mediate attachment of chromosomes stranded in regions of low MT density (e.g., Cenp-E) that occurs upon KNL1 depletion. Similar to previous observations in cells with decreased Aurora B activity or impaired Hec1 phosphorylation [36, 72, 73], aligned chromosomes in KNL1-depleted HeLa cells exhibited abnormal chromosome oscillations (Figure 2.4B-D). Specifically, oscillatory movements of kinetochores in KNL1-depleted cells were significantly dampened compared with those in control cells (Figure 2.4B–D). These results indicate that despite its MT-binding activity [28], KNL1 is not absolutely essential for the formation of end-on kinetochore–MT attachments in human cells, but is instead required for their proper regulation. Consistent with this idea, KNL1 MT-binding activity does not contribute to chromosome biorientation in *Caenorhabditis elegans* [29]. Together, these results demonstrate that KNL1 contributes to the regulation of kinetochore–MT plus-end attachment dynamics likely through activation of Aurora B.

The N-terminal region of KNL1 is sufficient to promote Aurora B activity and phosphorylation of outer kinetochore proteins

To define the domain in KNL1 required to promote Aurora B activity at kinetochores we generated isogenic doxycycline-inducible HeLa stable cell lines containing KNL1 fragments fused to GFP for use in silence and rescue experiments (Figure 2.5A). All fragments contained a small C-terminal region required to target KNL1 to kinetochores (aa 2056–2316, “250C”), which on its own was not sufficient to rescue Aurora B pT232 localization (Figure 2.5D). KNL1 fragments

containing portions of the N terminus (300N, 300–800N, 1500C) significantly restored Aurora B pT232, whereas the fragments containing only the C terminus (1200C, 800C) did not (Figure 2.5B and 2.5C). Similar results were obtained by transient transfection with KNL1 fragments (Figure 2.6A-C). In all cases, GFP fluorescence intensity levels of the mutant constructs at kinetochores were comparable, as well as the penetrance of KNL1 depletion (Figure 2.6D-F). As expected, the KNL1 N terminus coordinately rescued phosphorylation of Hec1 and phosphorylation of the Aurora B kinetochore substrate Dsn1, whose phosphorylation was also inhibited after KNL1 depletion (Figure 2.7A and 2.7B). KNL1 fragments lacking the N-terminal half of the protein were not able to significantly restore Hec1 phosphorylation, while all KNL1 fragments, including the short 250C fragment, facilitated wild-type levels of Hec1 recruitment to kinetochores as detected by a non-phosphospecific Hec1 antibody (Figure 2.7C). These results reveal a previously undescribed role for the KNL1 N-terminal region in promoting activity of Aurora B and phosphorylation of Aurora B substrates.

We next examined the requirements of the different KNL1 regions on the localization of inner centromeric Aurora B. Similar to the results observed upon KNL1 depletion, cells lacking the N-terminal half of KNL1 (1200C, 800C) exhibited a moderate reduction in centromeric Aurora B accumulation (~30–40%; Figure 2.8A). Conversely, fragments containing KNL1 N-terminal regions (300N, 300–800N, 1500C) almost completely reestablished centromeric Aurora B targeting (~90%; Figure 2.8A), indicating that the N terminus of KNL1 is also sufficient for wild-type levels of centromeric Aurora B enrichment. Importantly, the KNL1 300N region recovered high levels of centromeric Aurora B (~90%) but only partial levels of Aurora B pT232 (~60%). Thus, although the KNL1 N terminus promotes both enrichment of centromeric Aurora B and Aurora B auto-phosphorylation (pT232) at kinetochores, we did not observe a close quantitative

correlation between the levels of these two populations (Figure 2.8B). Instead, levels of phosphorylated INCENP (phospho-Ser893/Ser894) [75], a substrate and enhancer of Aurora B activity that also localizes to the inner centromere [94], correlated well with levels of Aurora B pT232 in all KNL1 mutant stable cell lines (Figure 2.8C). Thus, it is possible that KNL1 differentially influences centromeric Aurora B recruitment and Aurora B activity.

The N-terminal region of KNL1 rescues phenotypic defects observed upon KNL1 depletion

In agreement with our results demonstrating different contributions of the KNL1 N terminus to Aurora B activity at the kinetochore, 300–800N KNL1 significantly restored kinetochore oscillations of aligned chromosomes, whereas cells expressing 300N only partially restored oscillatory movements (Figure 2.9A-C). Additionally, we measured the effect of KNL1 depletion on the generation of tension across sister kinetochores. Contrary to a previous report [20], we found that inter-kinetochore distances of bi-oriented chromosomes were significantly increased in KNL1-depleted cells (Figure 2.9D), indicating either hyper-stabilized kinetochore–MT connections or weakened centromere cohesion [36, 84]. Consistently, 300N and 300–800N KNL1 significantly restored inter-kinetochore distances of aligned chromosomes to control values (Figure 2.9D). Thus, the KNL1 N terminus is critical for Aurora B activity at the kinetochore and for normal kinetochore–MT dynamics in cells.

KNL1 N terminus facilitates Bub1 kinase activity at kinetochores

The N terminus of KNL1 serves to recruit multiple outer kinetochore proteins implicated in the modulation of Aurora B activity [12, 20, 62]. We therefore examined if KNL1 promotes Aurora B activity by mediating the recruitment of these regulatory factors. Silence and rescue with

a KNL1 construct in which the PP1-binding motif (RVSF) was disrupted [20] did not affect kinetochore levels of Aurora B pT232, nor did depletion of BubR1 (Figure 2.10A-B). Bub1 depletion, in contrast, led to reduced Aurora B pT232 levels, and this resulted in decreased Hec1 phosphorylation (Figure 2.11A). These data are in agreement with recent findings suggesting that Bub1 kinase promotes Aurora B activation [85, 86]. Thus, the ability of KNL1 to promote Aurora B recruitment and activation could depend on its function as a kinetochore scaffold for Bub1. The KNL1 N terminus, which we find indispensable for Aurora B activity at the kinetochore, contains multiple MELT motifs that upon Mps1-mediated phosphorylation allow for direct recruitment of Bub1 [23, 25, 26]. Interestingly, although all KNL1 constructs capable of recovering significant levels of Aurora B pT232 localization contain at least 1 MELT repeat (Figure 2.6A), not all are able to mediate Bub1 kinetochore accumulation (Figure 2.11B and 2.11C). Fragments 300–800N (4 MELT repeats) and 1500C (5 MELT repeats) highly restored Bub1 localization to kinetochores (Figure 2.11B; unpublished data). In contrast, 300N (1 MELT repeat) was unable to mediate Bub1 kinetochore localization, even upon nocodazole treatment (Figure 2.11B-D). Thus, our data suggest that Bub1 accumulation at kinetochores enhances Aurora B activation and inner centromere Aurora B targeting, but it is not a requisite for these processes to occur.

Because the 300 N-terminal amino acids of KNL1 are not necessary or sufficient for accumulation of Bub1 at kinetochores, but mediate centromeric Aurora B accumulation and partial Aurora B activity, we asked if this region on KNL1 could facilitate Bub1 kinase activity. By analyzing the levels of histone H2A phosphorylation (T120), a well-described Bub1 kinetochore substrate [87], we found evidence of significant Bub1 kinase activity at kinetochores in cells expressing 300N KNL1 or 300–800N KNL1 but negligible activity when KNL1 was depleted or replaced with C-terminal fragments. Specifically, cells expressing the 300–800N fragment rescued

pH2A-T120 to 70%, and those expressing the 300N fragment to 55% (Figure 2.12A). Thus, the N-terminal region of KNL1 facilitates both Aurora B and Bub1 kinase activities at the kinetochore. Importantly, the 300–800N fragment recruits significantly higher levels of Bub1 to kinetochores than the 300N fragment, and this corresponds to a high level of both Aurora B and Bub1 kinase activities. These results suggest that Bub1 accumulation at kinetochores is required for wild-type levels of Aurora B–mediated phospho-regulation of kinetochore–MTs in cells.

Previous studies mapped the binding of the Bub1 tetratricopeptide repeats (TPRs) domain to aa 200–250 in the N-terminal region of KNL1 (referred to as the KI motif) [13]. Recently, however, and in agreement with our results, it was demonstrated that the Bub1 TPR domain is not sufficient for Bub1 localization to kinetochores [22, 26]. Furthermore, the catalytic activity of Bub1 measured *in vitro* was not affected by expression of a Bub1 mutant unable to interact with the KI motif of KNL1 [22]. Similarly, silence and rescue experiments in mammalian cells using a mutant of KNL1 lacking the KI motif confirmed that the TPR–KI interaction is dispensable for Bub1 localization to kinetochores [26]. Therefore, we hypothesized that a 300N KNL1 fragment containing mutations in the KI motif predicted to disrupt the KNL1–TPR interaction [22], would not impair Bub1 kinase activity in cells. Indeed, silence and rescue experiments using a GFP-tagged 300N KNL1-KI mutant (Figure 2.12B) confirmed that the ability of the KNL1 300N fragment to mediate Bub1 kinase activity does not rely on its KI motif (Figure 2.12C). We next examined if disruption of the MELT motif contained in the 300N KNL1 region disrupted Bub1-mediated histone H2A phosphorylation. Surprisingly, a 300N KNL1 mutant containing an alanine substitution in the single MELT motif (MELA) was able to mediate histone H2A phosphorylation in cells (Figure 2.12C). Therefore, neither the KI nor the MELT motif in the 300N region of KNL1 are essential for Bub1 kinase activity at kinetochores. How the 300N-terminal region of KNL1 is

able to mediate Bub1 and Aurora B kinase activities remains to be addressed. One possibility, however, is that Bub1 interaction with 300N KNL1, even transiently, results in close positioning of the kinase to its substrate (H2A). Alternatively, a transient interaction with KNL1 could promote allosteric changes in Bub1 that enhance its activation.

KNL1 is required for full Aurora B activity independent of Aurora B accumulation

Bub1 promotes Aurora B recruitment to the inner centromere through phosphorylation of histone H2A, which results in targeting of Borealin, a CPC component [88]. It is proposed that accumulation at this inner centromeric site results in Aurora B activation and a gradient of active kinase emanating toward the kinetochore to regulate kinetochore–MT interactions [75]. Therefore, it is possible that KNL1 contributes to Aurora B activity entirely by facilitating Bub1-mediated Aurora B recruitment. Our data, however, suggest distinct contributions of KNL1 to Aurora B localization and Aurora B activity (Figures 2.2, 2.3, 2.5, 2.8). We therefore hypothesized that KNL1 not only contributes to Aurora B activity by promoting its recruitment but also through an alternative pathway. To directly test this, we targeted Aurora B to the kinetochore through a Cenp-B (CB)–INCENP chimera [74] and to the inner centromere through an HP1-Survivin chimera (Figure 2.13A). Endogenous Aurora B, detected using pan-antibodies and antibodies to its phosphorylated form (pT232), was redistributed to kinetochores or to the inner centromere in cells expressing CB-INCENP or HP1-Survivin, respectively (Figure 2.13B). We quantified the levels of both Aurora B and Aurora B pT232 colocalizing with these fusion proteins in control and KNL1-depleted cells (Figure 2.13C-E and 2.14A-D). Although control and KNL1-depleted cells were able to recruit similar levels of Aurora B in the presence of the targeting chimeras (Figure 2.13E), Aurora B pT232 and substrate phosphorylation were not fully restored in KNL1-depleted

cells (Figure 2.13C, 2.13D, 2.13F). Although ectopic targeting of Aurora B to these regions may not reflect endogenous kinase activity, these results argue that kinase accumulation is not sufficient to achieve control levels of kinase activity in the absence of KNL1. Therefore, it is likely that the influence of KNL1 on Aurora B activity at kinetochores is not exclusively dependent on Bub1-mediated recruitment of the kinase.

2.3 Discussion

KNL1 is widely recognized as a kinetochore scaffolding protein that contributes to the formation of kinetochore–MT attachments and is required for accurate chromosome segregation during mitosis [40]. Studies in *C. elegans* and mammalian cells have demonstrated its involvement in the recruitment of SAC proteins (Bub1, BubR1) [12] and phosphatases (PP1 and PP2A via BubR1) to kinetochores [20, 62,77] as well as its ability to bind MTs [29, 69]. KNL1 is proposed to be required for initial activation of the SAC [12], and for checkpoint silencing [29, 63, 65], yet how this large kinetochore protein of unknown structure contributes to different signaling pathways temporally throughout mitosis is not well understood. Adding more complexity, Bub1, BubR1, and the phosphatases PP1 and PP2A are regulators of Aurora B [12, 20, 62, 77, 78], the kinase considered the “master regulator” of kinetochore–MT attachments during mitosis. Based on its role in recruiting proteins that impact Aurora B function, we reasoned that KNL1 might be critical for the proper regulation of Aurora B activity. We found that KNL1 is required for Aurora B activity and for Aurora B–mediated phosphorylation of outer kinetochore proteins including Hec1, the primary kinetochore–MT attachment protein, and Dsn1, a member of the kinetochore-associated Mis12 complex, which also contributes to the formation of stable kinetochore–MT attachments [38]. We identified the N-terminal half of KNL1 (aa 1–1200N) as sufficient to mediate

such activities. In addition, the N-terminal region of KNL1 sufficient to promote Aurora B activity and substrate phosphorylation is also required for Bub1-mediated histone H2A phosphorylation, a known contributor to Aurora B centromeric localization [89]. Previously, it was unclear if Bub1 accumulation to kinetochores was required for Bub1 to perform its functions. Here we found that KNL1-mediated Bub1 accumulation to kinetochores is not a requirement for its activity at kinetochores. However, the N-terminal region of KNL1 is necessary and sufficient to facilitate Bub1 kinase activity. The levels of Bub1 kinase activity, measured by the levels of phosphorylation of its substrate, histone H2A, correlate with the levels of Aurora B activity. Thus, we propose that KNL1 promotes Aurora B activation and Aurora B-mediated phosphorylation by facilitating Bub1 kinase activity during early mitosis (Figure 2.15). Importantly, although Bub1 functions upstream of Aurora B targeting, localization of Aurora B by ectopic targeting in the absence of KNL1 did not result in full Aurora B activity. Therefore, KNL1 and Bub1 may influence Aurora B activity in a manner that is distinct from their roles in targeting the kinase to centromeres. The interplay between Bub1 and Aurora B kinase activities at kinetochores and how Bub1 interaction with KNL1 could modulate Bub1 function during mitotic progression are issues that remain to be addressed.

The current model describing the regulation of kinetochore-MT attachment strength during mitosis proposes that Aurora B, emanating as a gradient from the inner centromere, selectively reaches kinetochore proteins by diffusion, depending on their distance from the origin of the gradient [74, 75]. However, it has been demonstrated both in chicken cells and in budding yeast that mitotic chromosomes are able to accurately bi-orient and segregate in absence of centromeric Aurora B [90, 91]. In agreement with these studies, we find that in the absence of KNL1, significant levels of centromeric Aurora B or ectopic targeting of Aurora B do not result in control

levels of Aurora B activity as the previously described model proposes. We find that maintenance of Aurora B activity, promoted by the N terminus of KNL1, correlates with Bub1 activity at kinetochores (which is low during late mitosis, when checkpoint proteins no longer accumulate at kinetochores). Thus, an alternative model for the regulation of kinetochore–MT attachment suggests that levels of active Aurora B at kinetochores are modulated during mitotic progression as a result of changes in Bub1 kinase activity (Figure 2.15). Specifically, it is possible that changes at the kinetochore during late mitosis result in decreased KNL1-mediated Bub1 kinase activity and Aurora B-mediated phosphorylation of kinetochore substrates. Our results demonstrating Bub1’s contribution to Aurora B activity at the kinetochore support the notion that a single sensory mechanism may be used for both MT turnover/error correction and checkpoint signaling (Figure 2.15) [9]. A previously demonstrated role for Bub1 in chromosome congression [49] is likely to be linked to the maintenance of Aurora B activity at the kinetochore. Conversely, a role for Aurora B in checkpoint signaling may be to not only prevent premature checkpoint silencing (by stalling PP1 recruitment) but also to maintain high levels of Bub1 kinetochore activity through the Mps1–KNL1 pathway.

2.4 Methods

Cell culture and transfection

HeLa (ATCC) and RPE1 cells (hTERT-RPE1; ATCC) were cultured in DMEM and DMEM/F12 (Invitrogen), respectively, supplemented with 10% FBS and 1% penicillin/streptomycin at 37°C in 5% CO₂. For immunostaining experiments after KNL1 depletion, cells were synchronized in early mitosis using a double thymidine block and release. Cells were treated with 2.5 mM thymidine for 16 h, washed with PBS, replaced with fresh medium,

transfected with siRNA, and incubated for 8 h. For the second block, cells were transfected with siRNA and treated with 2.5 mM thymidine for 16 h. Cells were then washed with PBS, replaced with fresh medium, and fixed after 10 h for immunostaining. For all experiments, cells were plated at 50% confluency 24 h before transfection or thymidine treatment on acid-washed glass coverslips for immunofluorescence or on glass-bottomed dishes for live-cell imaging (MatTek Corporation). For experiments with ZM447439, cells were treated with 2 μ M ZM447439 for 2 h before fixing or harvesting. For cold-induced depolymerization assays, cells were incubated in ice-cold DMEM for 10 min, fixed with paraformaldehyde, and prepared for immunofluorescence as described below. siRNA transfections were performed using Oligofectamine (Invitrogen), according to the manufacturer's instructions, and cells were analyzed 48 h after transfection. For KNL1 silence and rescue experiments, cells were transfected with siRNA, 8 h later with plasmid DNA using Effectene (QIAGEN), and analyzed 48 h after DNA transfection. siRNAs targeting KNL1 were purchased from Invitrogen. The sequences for "stealth" siRNAs were 5'-GAACACAUGCUUUCUGCUCCCAUU-3', 5'-GGGCAGGAUGACAUGGAGAUCACUA-3', and 5'-AAGAUCUGAUUAAGGAUCCACGAAA-3'. The siRNA used for KNL1 silence and rescue experiments for wild-type and RVSF/AAAA plasmids [20] was synthesized by QIAGEN (5'-AAGGAAUCCAAUGCUUUGAGA-3'). Bub1 siRNA was 5'-CAGCUUGUGAUAAAGAGUCAAA-3' and BubR1 siRNA was 5'-ACGAGAAUACC UAAUAUGUGA-3', both purchased from QIAGEN. Luciferase siRNA (QIAGEN) was used as control in all experiments displayed in Figures 2.1 and 2.2.

The FlpIn T-REx HeLa host cell line was a gift from S. Taylor (University of Manchester, Manchester, England, UK). To generate FlpIn T-REx HeLa cells containing KNL1 fragments fused to GFP at the N terminus, Flp-In T-REx HeLa host cells were cotransfected with a ratio of

9:1 (wt/wt) pOG44:pcDNA5/FRT/TO expression plasmid using Fugene HD (Promega). 48 h after transfection, cell lines were placed under selection with 100 µg/ml hygromycin (EMD Millipore) for 2 wk. Hygromycin-resistant foci were chosen, expanded, and tested for GFP expression. Gene expression was induced with 1 µg/ml doxycycline (Sigma-Aldrich) for 24 h. For silence and rescue experiments, stable cell lines were doubly blocked with thymidine and depleted of endogenous KNL1 using the corresponding siRNAs described above.

Plasmids

The siRNA-resistant KNL1 wild-type and RVSFAAAA mutant plasmids were a gift from M. Lampson (University of Pennsylvania, Philadelphia, PA). The GFP-tagged KNL1 fragments were as follows: amino acids 1–300 (300N), 300–818 (300–800N), 819–1518 (800–1500N), 1174–2316 (1200C), 1519–2316 (800C), 819–2316 (1500C), 2056–2316 (250C), and 1834–2316 (400C), and were generated by PCR using KNL1 wild-type as the template [74] and cloned into the pEGF-C2 vector and pcDNA5/FRT/TO vector using In-Fusion cloning (Takara Bio Inc.). The KNL1 fragments KNL1 300N, 300–800N, and 800–1500N were cloned into pEGFP-C2 and/or pcDNA5/FRT/TO containing the KNL1 kinetochore-binding region (aa 2056–2316). Constructs 800–1500N and 1500C differ from the sequence published in Bolanos-Garcia et al. (2011) [21], in that aa 910–1120 are not contained. The GFP-tagged CB-INCENP plasmid containing hCenp-B aa 1–158 and hINCENP aa 47–920 was a gift from S. Lens (University Medical Center, Utrecht, Netherlands). The GFP-HP1-Survivin construct was generated as follows: full-length Survivin and HP1 were obtained by RT-PCR from HeLa cells. Survivin was cloned into pEGFP-C2 to generate GFP-Survivin, and HP1 was cloned into GFP-Survivin to generate GFP-HP1-Survivin. All plasmid DNAs were purified using an Endo-free Maxi kit (QIAGEN) before transfection.

Immunofluorescence

Fixation and immunostaining of HeLa and RPE-1 cells were performed as described previously [73]. In brief, cells were rinsed in 37°C PHEM buffer (60 mM Pipes, 25 mM Hepes, 10 mM EGTA, and 4 mM MgSO₄, pH 6.9), fixed in in 4% paraformaldehyde for 20 min, and extracted in PHEM buffer + 0.5% Triton X-100 for 5 min. Staining of phospho-Ser331 Aurora B was performed as described in Petsalaki et al. (2011) [81]. In brief, cells were rinsed in PHEM buffer, extracted in PHEM buffer + 0.5% CHAPS for 5 min, and fixed with cold methanol for 5 min at 20°C. Immunostaining was performed using the following antibodies: rabbit polyclonal anti-phosphorylated Ser44-Hec1 (pSer44 against antigen PTFGKL(pS)INKPTSE) and anti-phosphorylated Ser55-Hec1 (pSer55 against antigen KPTSERKV(pS)LFGKR) were used at 1:2,000; mouse anti-Hec1 9G3 at 1:2,000 (GeneTex); rabbit anti-Dsn1 at 1:500 (GeneTex); human anti-centromere antibody at 1:500 (ACA; Antibodies, Inc.); mouse anti-tubulin at 1:200 (Sigma-Aldrich); sheep anti-tubulin at 1:300 (Cytoskeleton, Inc.); rabbit anti-phosphorylated Aurora B (pThr232) at 1:2,000 (Rockland); rabbit anti-phosphorylated Aurora-B (pSer331, against peptide CPWVRAN(pS)RRVLPPS); a gift from G. Zachos [University of Crete, Heraklion, Greece]) at 1:100; mouse anti-BubR1 at 1:500 (EMD Millipore); rabbit anti-phosphorylated INCENP (Ser893/Ser894, against peptide RYHKRT(pS)(pS)AVWNNSPC); a gift from M. Lampson) at 1:1,000; rabbit anti-phosphorylated Dsn1 (Ser109 against peptide TNRRK(pS)LHPIH); a gift from I. Cheeseman [Whitehead Institute, Cambridge, MA]) at 1:1,000; rabbit anti-phosphorylated histone H2A (Thr120) at 1:1,000 (Active Motif); mouse anti-Bub1 at 1:200 (Abcam); mouse anti-Aurora B monoclonal (AIM1) at 1:300 (BD); and mouse anti-phosphorylated histone H3 (Ser10; Cell Signaling Technology) at 1:1,000. Affinity-purified antibodies against KNL1 were generated at 21st Century Biochemicals; rabbits were immunized with the following KNL1 peptide:

MDGVSSEANEENDNIERPVRRR, and serum was double affinity purified. Secondary antibodies conjugated to either Alexa 647, Alexa 488, or Rhodamine Red-X (Jackson ImmunoResearch Laboratories, Inc.) were used at 1:300.

Image acquisition and analysis

Image acquisition was performed on an imaging system (DeltaVision Personal DV; Applied Precision) equipped with a camera (CoolSNAP HQ2; Photometrics/Roper Scientific), a 60×/1.42 NA PlanApochromat objective (Olympus), and SoftWoRx acquisition software (Applied Precision). For fixed cell experiments, images were acquired at room temperature as Z-stacks at 0.2- μm intervals and kinetochore fluorescence intensity measurements were performed using MetaMorph software (Molecular Devices). The integrated fluorescence intensity minus the calculated background was determined for each kinetochore in control and treated samples and normalized to the average value obtained from control cells [92]. Inter-kinetochore distances were determined using SoftWorx software. For live-cell imaging of kinetochore oscillations, HeLa cells in 35-mm glass-bottomed dishes (MatTek Corporation) were transfected with KNL1 siRNA and 24 h later with 0.2 μg of GFP-CENP-B (a gift from K. Sullivan, NUI Galway, Galway, Ireland) and GFP-centrin (a gift from M. Bornens, Institut Curie, Paris, France) as described above. Cells were imaged 24 h after DNA transfection in Leibovitz's L-15 media (Invitrogen) supplemented with 10% FBS, 7 mM Hepes, pH 7.0, and 4.5 g/L glucose. Stage temperature was maintained at 37°C with an environmental chamber (Precision Control). Fluorescence images of GFP-CENP-B/GFP-centrin-expressing cells were acquired every 3 s for 10 min. At each time point, 5 images were collected in a Z-series, using a 0.5- μm step size. Cells chosen for analysis expressed both GFP-CENP-B and centrin-GFP proteins and were in late prometaphase or metaphase with

primarily bi-oriented chromosomes. Sister kinetochore pairs chosen for analysis were located within the middle of the spindle. Kinetochore and spindle pole movements were tracked using CENP-B-GFP fluorescence and centrin-GFP fluorescence, respectively, on maximum projection time-lapse sequences using MetaMorph software. The spindle pole marker centrin was used to correct for cell movement during the time-lapse imaging sequence. Kinetochore movements were tracked on maximum projection time-lapse sequences using the “track points” function in MetaMorph software. Tracking data were analyzed in Microsoft Excel. A “pause” event was recorded when a kinetochore did not move for two sequential time frames. Velocity was calculated by linear regression analysis of kinetochore distance versus time plots, and deviation from average position (DAP) was determined by subtracting the position of the kinetochore in the regression line from the original kinetochore position [73, 93]. Kinetochore oscillation analysis in HeLa TRex FlpIn stable cell lines was performed as described above, with the exception that cells were expressing mCherry tagged CenpB. For live-cell imaging with mCherry-Bub1, 300N KNL1 HeLa stable cells were transfected with 0.3 μg mCherry-Bub1 and imaged 48 h after DNA transfection in filming medium containing 330 nM nocodazole. All presented data were analyzed in SigmaPlot software v.11.0 (Systat Software) and the statistical tests performed are specified in figure legends.

Immunoprecipitation and immunoblotting

Cells were lysed in lysis buffer (75 mM Hepes, pH 7.5, 150 mM KCl, 1.5 mM EGTA, 1.5 mM MgCl₂, 0.1% NP-40, Complete protease inhibitor cocktail [Roche], and PhosSTOP phosphatase inhibitors [Roche]). Western blotting was performed using the following antibodies: anti-Hec1 9G3 at 1:1,000 (GeneTex); rabbit anti-phosphorylated Aurora B (pThr232) at 1:100 (Rockland); rabbit anti-Aurora B at 1:1,000 (Abcam); rabbit anti-KNL1 at 1:500; mouse anti- β -

actin at 1:500 (Abcam); and mouse anti-tubulin at 1:2,000 (Sigma-Aldrich). For immunoprecipitation assays, lysates were incubated with mouse anti-Aurora B (mouse AIM1; BD) for 2 h at 4°C, and with a mix of Sepharose protein A/G (Bio-Rad Laboratories) for an additional 2 h at 4°C. The unbound fraction was recovered and beads were washed with lysis buffer (3×). Beads were treated with 2× SDS sample buffer and boiled at 95°C for 5 min for elution.

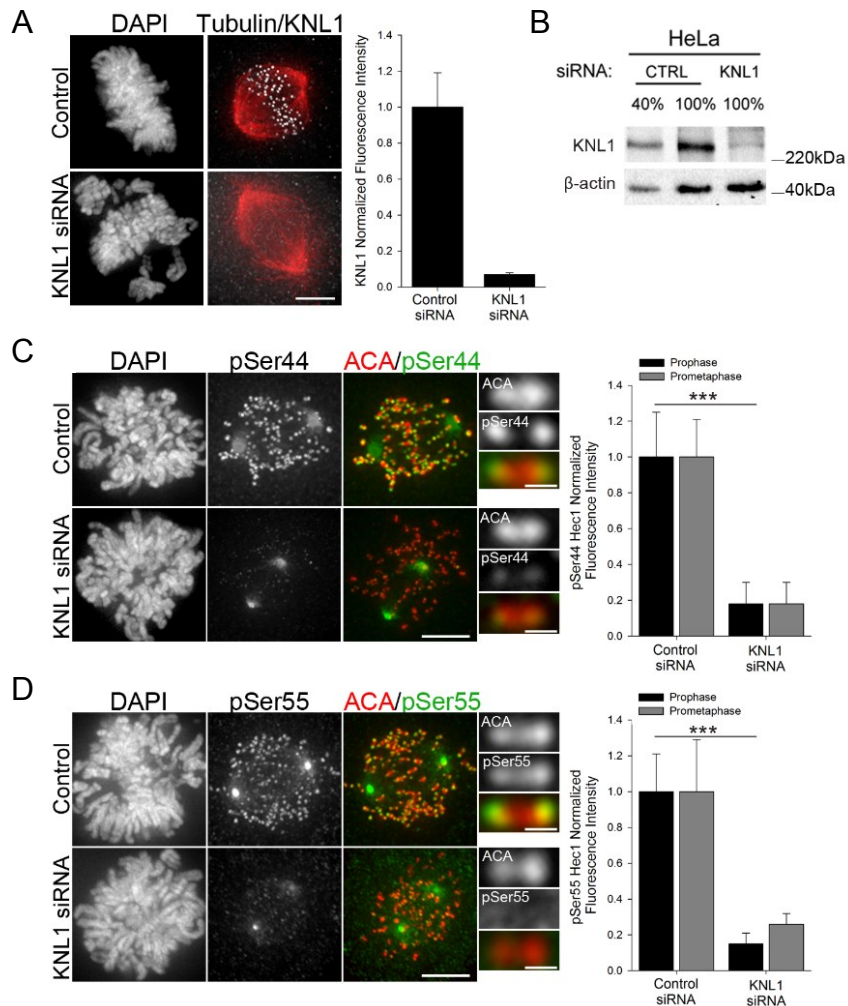


Figure 2.1. KNL1 is required for Aurora B kinase-mediated Hec1 phosphorylation at the kinetochore. (A) Control and KNL1-depleted HeLa cells immunostained with KNL1 and tubulin antibodies. Kinetochore fluorescence intensities were measured after KNL1 depletion using a KNL1 antibody. Error bars represent s.d. from independent experiments (n=3). For each experiment n≥100 kinetochores were measured from at least 10 cells. (B) Western blot of HeLa cell extracts from control and KNL1 siRNA-treated cells immunostained with KNL1 and β-actin antibodies. Percentage lysate loaded in the gel is indicated. Quantification of band intensities indicates that KNL1 levels were decreased by 96%. (C-D) Control and KNL1-depleted HeLa cells were immunostained with Hec1 phospho-specific antibodies and kinetochore fluorescence intensities were quantified. Error bars in graphs represent s.d. from independent experiments (n=3 for Hec1 pSer44; n=2 for Hec1 pSer55). For each experiment n≥100 kinetochores were measured from at least 10 cells. ***p<0.001 (Mann-Whitney rank sum test). Error bars in all controls represent s.d. between cells. Scale bars, 5 μm (cell panels) or 0.5 μm (kinetochore pair insets).

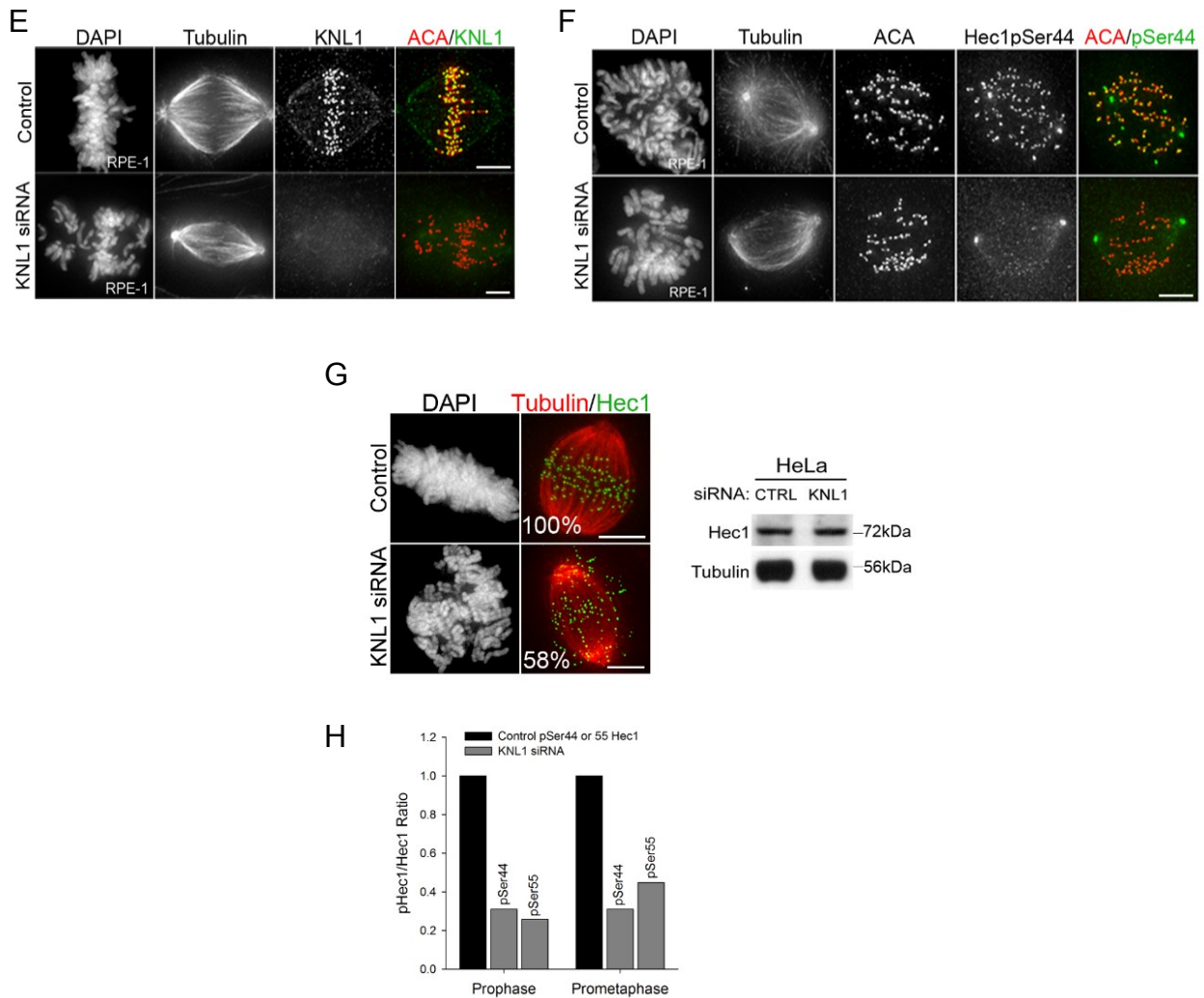


Figure 2.1. KNL1 is required for Aurora B kinase-mediated Hec1 phosphorylation at the kinetochore. (E) RPE-1 cells demonstrating the characteristic phenotype of KNL1 depletion. (F) Control and KNL1-depleted RPE-1 cells were immunostained with a Hec1 phospho-specific antibody, pSer44. (G) Control and KNL1-depleted HeLa cells were immunostained with a non-phospho-specific Hec1 antibody (9G3) and kinetochore fluorescence intensities were quantified. Fluorescence intensities are indicated as percentages in (G, left). (G) (right) Western blot of control and KNL1-depleted HeLa extracts. Blots were probed with antibodies to Hec1 and tubulin as a loading control. (H) Levels of phospho-Hec1 remaining at kinetochores calculated as a ratio of phospho-Hec1 fluorescence intensities from (C) and (D) to total Hec1 remaining at kinetochores after KNL1 depletion (58%) in (G). See (C) and (D) above for n values and statistics. (A-G) Scale bars, 5 μ m (cell panels).

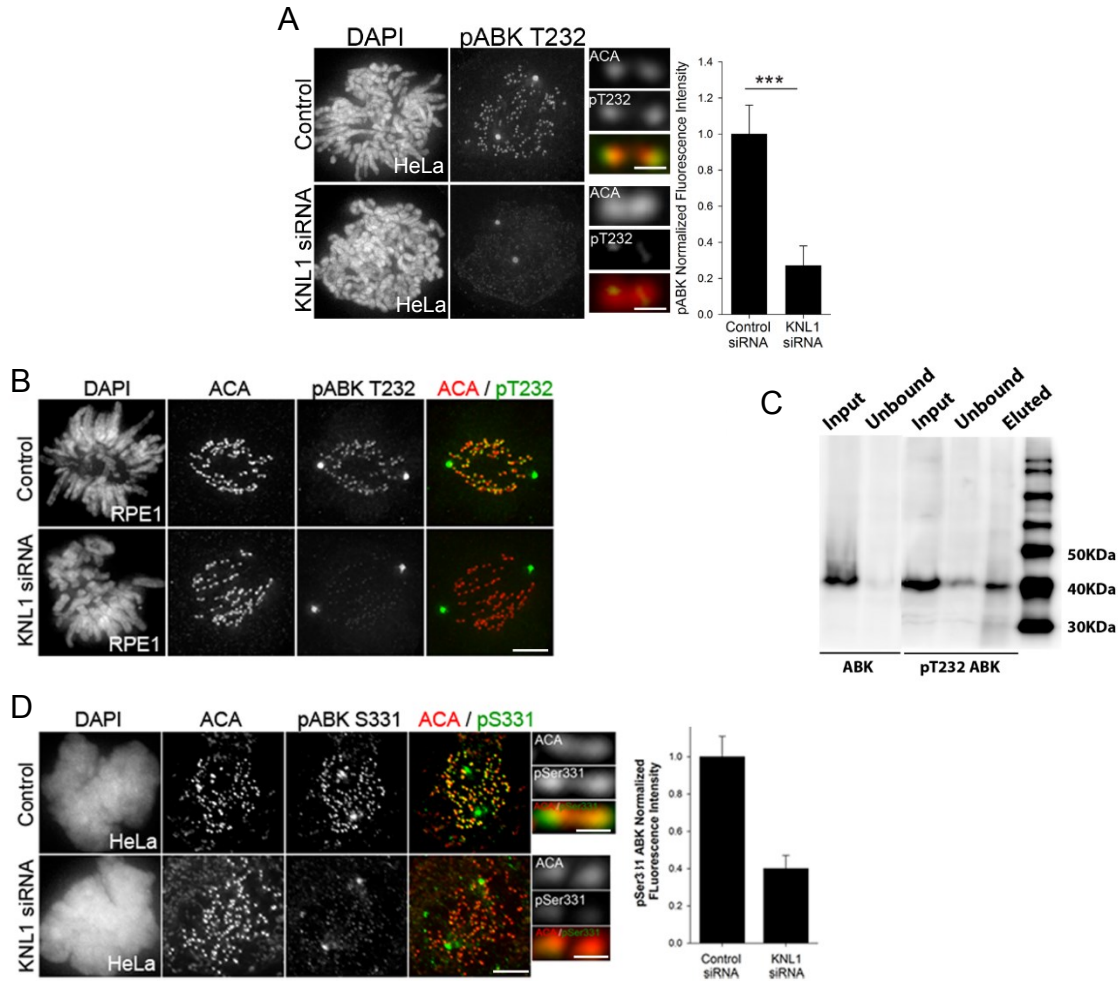


Figure 2.2. KNL1 is required for Aurora B activity at the kinetochore. (A) Control and KNL1-depleted HeLa cells were immunostained with a phospho-specific Aurora B antibody (pT232) and kinetochore fluorescence intensities were quantified. Error bars in graphs represent s.d. from independent experiments ($n=3$ for Aurora B pT232). For each experiment $n \geq 100$ kinetochores were measured from at least 10 cells. $***p < 0.001$ (Mann-Whitney rank sum test). (B) Control and KNL1-depleted RPE-1 cells were immunostained with an Aurora B phospho-specific antibody, pT232. As shown in HeLa cells, localization of pT232 is also reduced in RPE-1 cells upon KNL1 depletion. (C) Western blot of HeLa cell lysates probed with the Aurora B pT232 antibody. Input represents 5% of total protein used for immunoprecipitation assay. Input lane shows that the pT232 antibody primarily recognizes a band at 40 kDa (right), the same size at which Aurora B is recognized by a pan-Aurora B antibody (left). The unbound lane represents cell lysate after Aurora B immunodepletion using a pan-Aurora B antibody (same amount of total protein as input lane, left). The intensity of the pT232 band is significantly decreased when lysates were immunodepleted of Aurora B (right). (D) Control and KNL1-depleted HeLa cells were fixed and immunostained with a phospho-specific antibody to Aurora B kinase, p-Ser331 [81]. This antibody recognizes phosphorylated Aurora B kinase at the kinetochore in control cells (top panel), however this localization is reduced in cells depleted of KNL1 (lower panel). Quantification is shown to the right; $n \geq 100$ kinetochores from at least 9 cells. Scale bars, 5 μm (cell panels) or 0.5 μm (kinetochore pair insets).

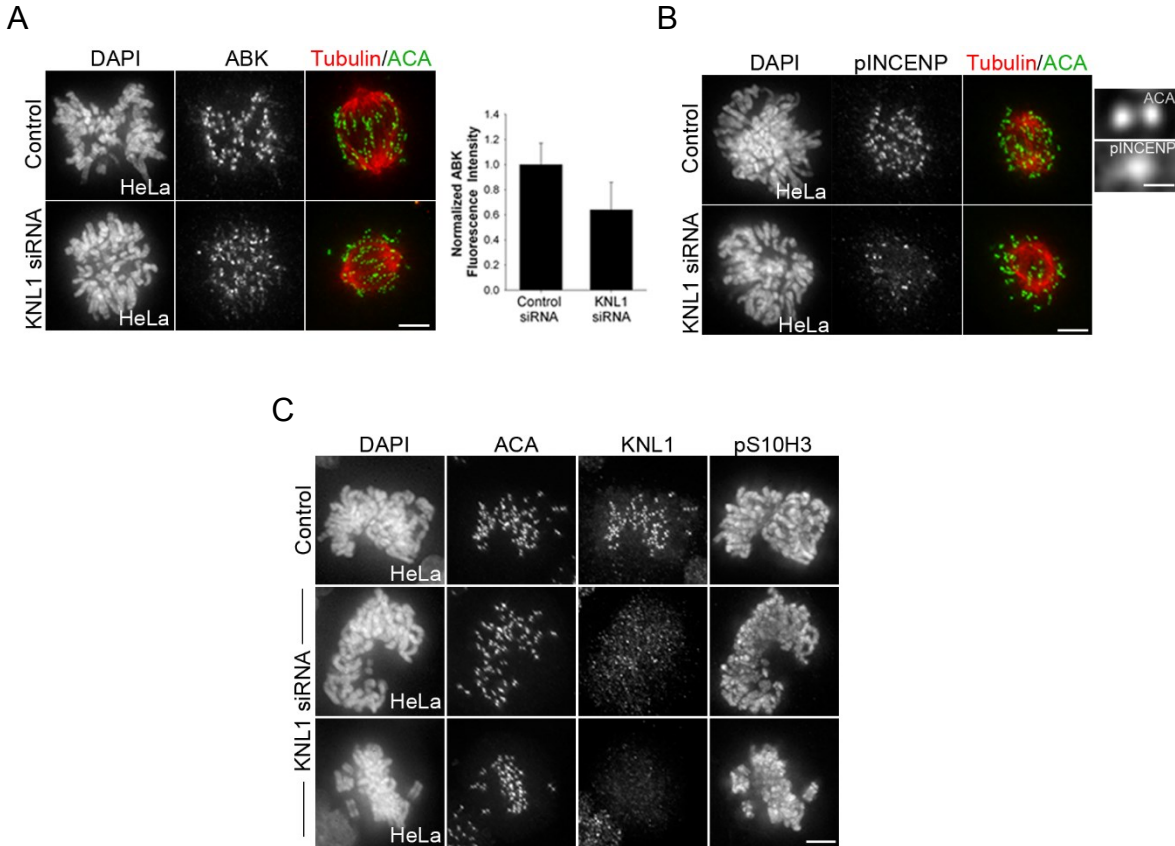


Figure 2.3. KNL1 is required for full Aurora B activity at the inner centromere. (A-C) Control and KNL1-depleted HeLa cells were immunostained with a pan antibody to Aurora B kinase (AIM1) (A), a phospho-specific antibody to INCENP (pSer893/pSer894) [75] (B), or a phospho-specific antibody to histone H3 (pSer10) (C). Kinetochores fluorescence intensities are shown in (A). Error bars represent s.d. from independent experiments (n=3). For each experiment $n \geq 100$ kinetochores were measured from at least 10 cells. Scale bars, 5 μm (cell panels) or 0.5 μm (kinetochores pair insets).

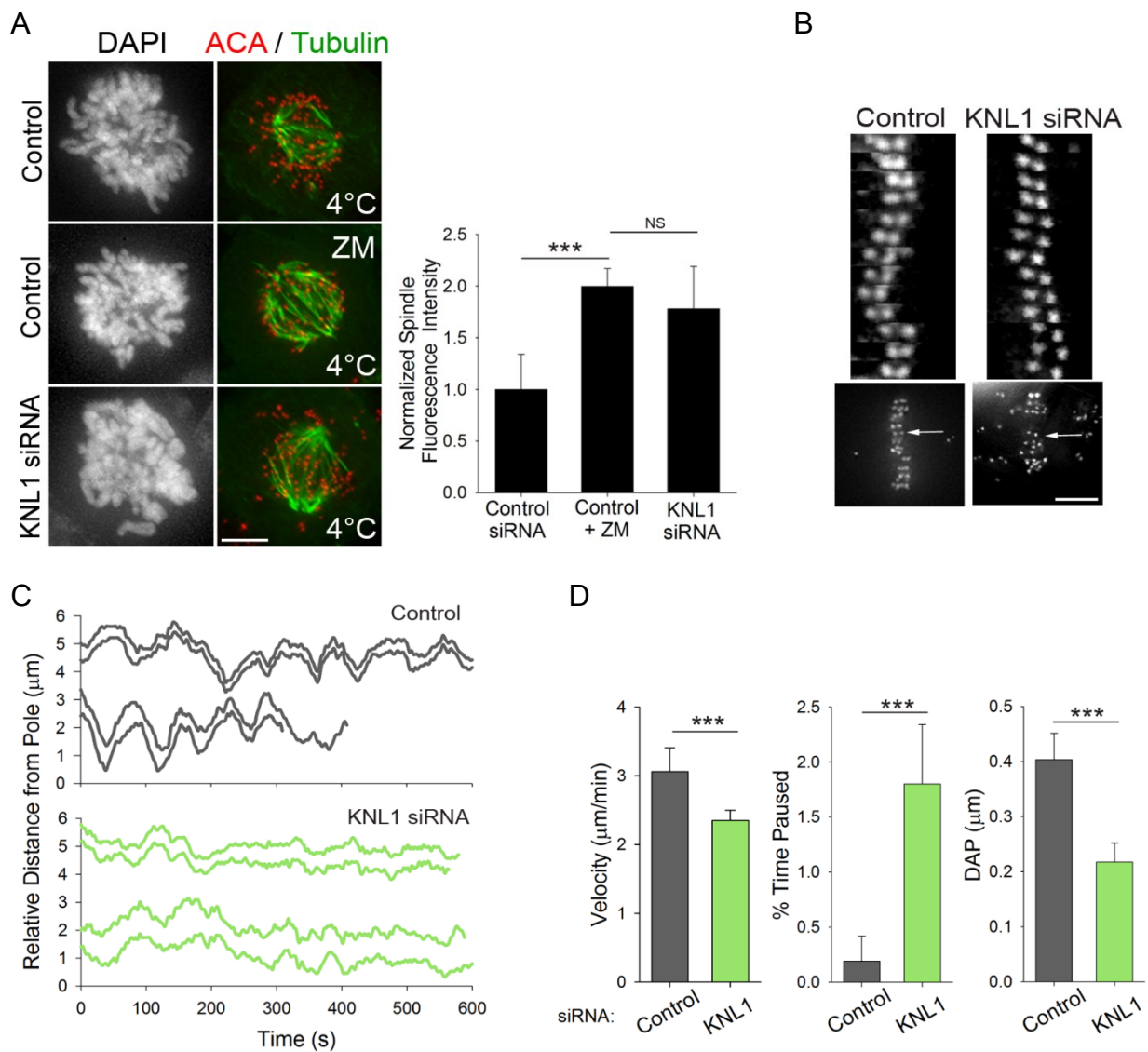


Figure 2.4. KNL1 is required for wild-type kinetochore-MT dynamics. (A) Representative images of control, ZM-treated and KNL1-depleted early mitotic HeLa cells subjected to a cold-induced MT depolymerization assay and immunostained for tubulin and a kinetochore marker (ACA). Total spindle fluorescence intensities are shown for each condition. Error bars in graph represent s.d. from independent experiments ($n=2$). For each experiment $n \geq 8$ cells per condition. *** $p < 0.001$ (Mann-Whitney rank sum test), NS= not statistically significantly different. (B) Kymographs of sister kinetochores from live-cell time-lapse imaging sequences in control and KNL1-depleted HeLa cells. Kymographs were generated from the kinetochores pairs indicated in the panels below (arrows). (C) Plots of kinetochore tracks over time in control and KNL1-depleted HeLa cells. For each condition, two representative sister kinetochores pairs are shown. (D) Quantification of kinetochore oscillations in control and KNL1-depleted cells. DAP indicates deviation from average position, a measure of oscillation amplitude [93]. Error bars represent s.d. from independent experiments ($n=3$). For each experiment $n \geq 32$ kinetochores were tracked from at least 5 cells. *** $p < 0.001$ (t-test). Scale bars, 5 μm .

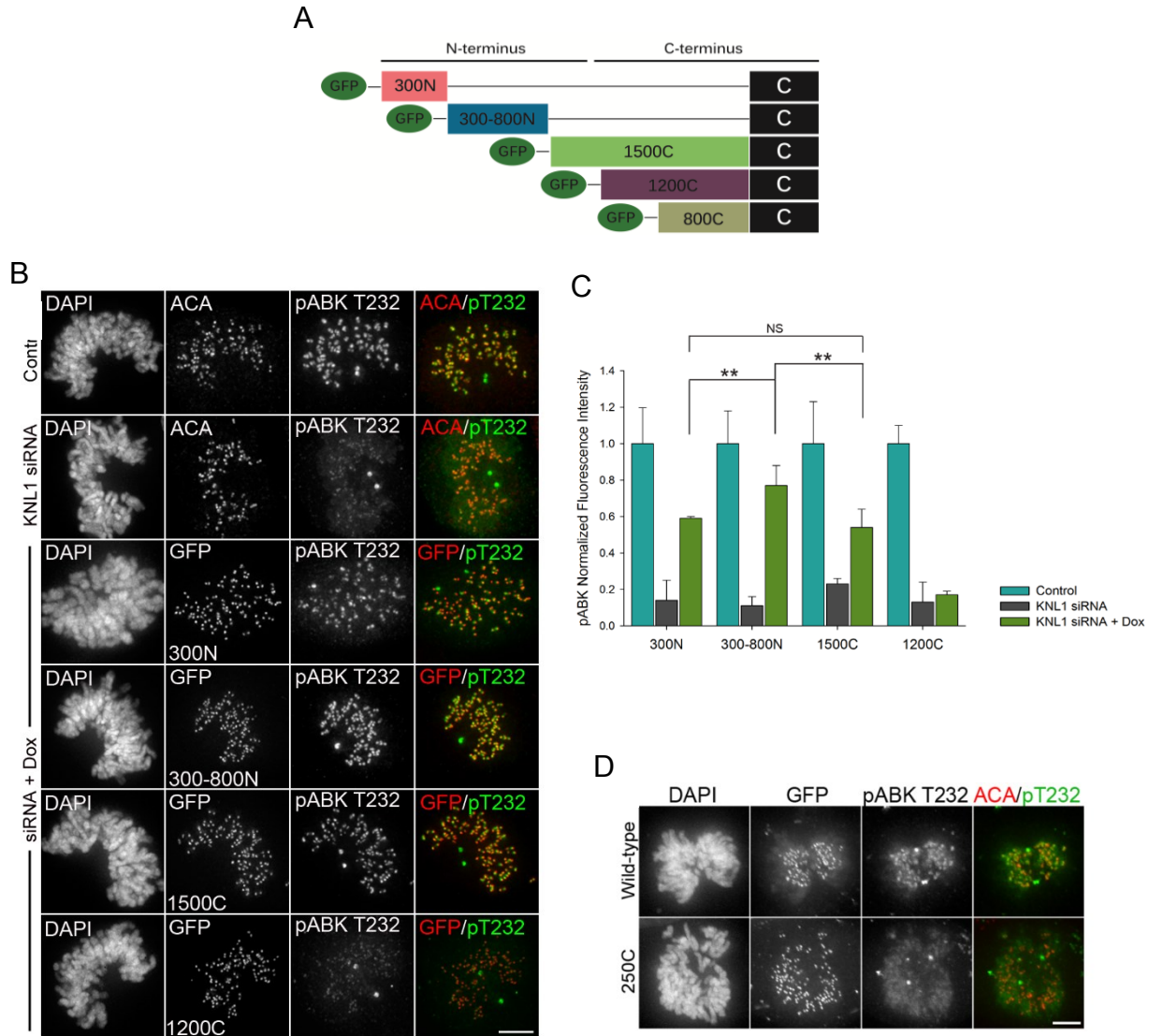


Figure 2.5. The N-terminus of KNL1 promotes Aurora B activity. (A) Schematic of GFP-KNL1 constructs stably incorporated into Flp-In T-REx HeLa cell lines; the exact amino acids of all KNL1 constructs shown are as follows: amino acids 1-300 (300N), 300-818 (300-800N), 1174-2316 (1200C), 1519-2316 (800C), 819-2316 (1500C), 2056-2316 (C). (B-C) Flp-In T-REx HeLa cells were depleted of endogenous KNL1, rescued with the indicated GFP-KNL1 fragment upon doxycycline addition and immunostained with a phospho-specific Aurora B antibody (pT232). Kinetochores fluorescence intensities were quantified as indicated in (C). Error bars represent s.d. from independent experiments ($n=3$). For each experiment $n \geq 100$ kinetochores were measured from at least 8 cells. *** $p < 0.001$, ** $p < 0.05$, NS= not statistically significantly different (Mann-Whitney rank sum test). Scale bars, 5 μm . (D) KNL1-depleted HeLa cells were depleted of endogenous KNL1, rescued with the indicated GFP-KNL1 fragment by overexpression, and immunostained with a phospho-specific Aurora B antibody (pT232). Scale bars, 5 μm .

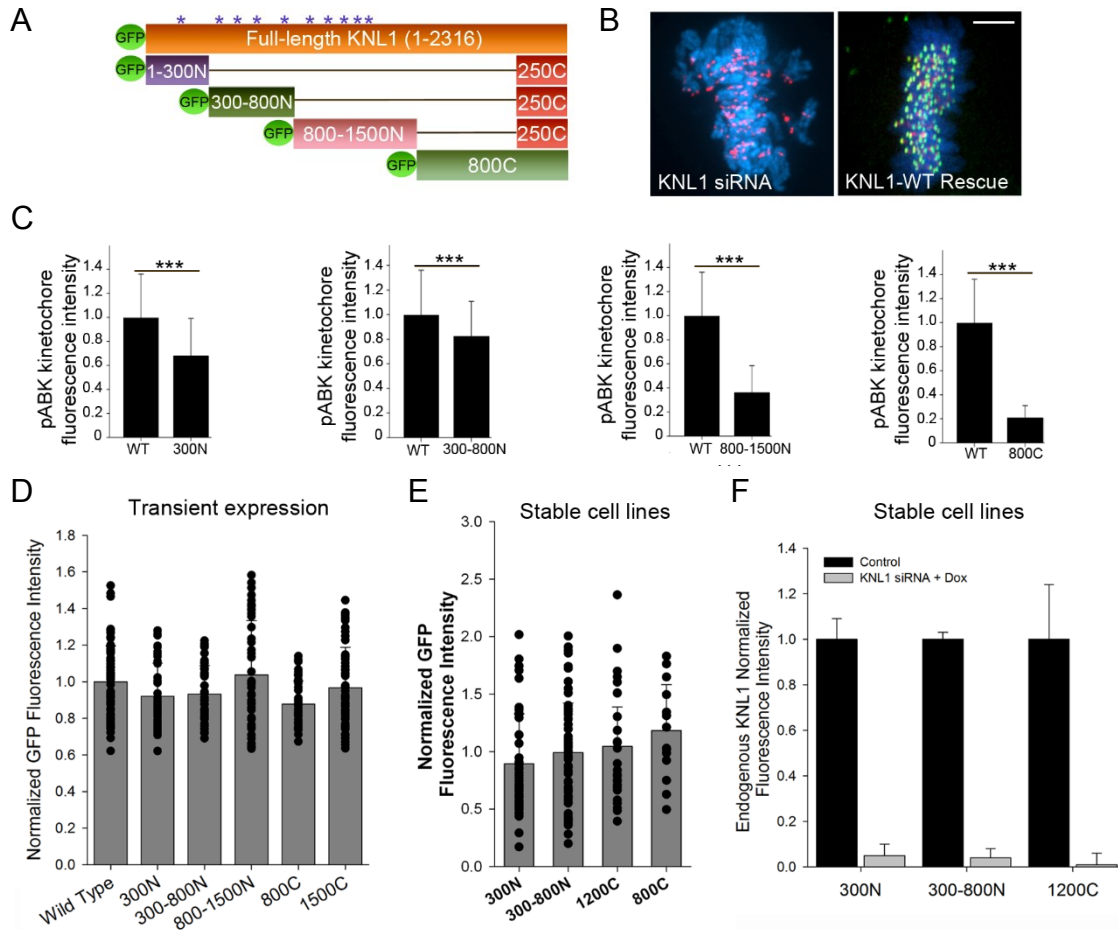


Figure 2.6. The N-terminus of KNL1 is sufficient to facilitate Aurora B activity. (A) Schematic of constructs used in silence/rescue transient expression experiments. “N” refers to amino acids from the N-terminus of the protein. “C” refers to amino acids from the C-terminus of the protein. Asterisks mark the MELT repeats present in the KNL1 constructs used in the study [23, 26]. The full-length KNL1 sequence is similar to the KNL1 sequence published in Liu et al 2010 [12]. The exact amino acids included in each construct are listed in Experimental Procedures. (B) Full-length KNL1 (KNL-WT) rescues the KNL1 depletion phenotype in HeLa cells. (C-D) HeLa cells were depleted of endogenous KNL1, rescued with the indicated GFP-KNL1 construct and immunostained with antibodies to Aurora B pT232 (pABK). Kinetochore fluorescence intensities of pABK (C) and KNL1-GFP fusion proteins (D) in silence/rescue experiments were quantified. Error bars represent s.d. from independent experiments (n=2). For each experiment n \geq 60 kinetochores were measured from at least 5 cells. ***p<0.001 (Mann-Whitney rank sum test). (E) Quantification of KNL1-GFP fusion protein levels at kinetochores in doxycycline-induced stable cell lines. Data represent at least 12 kinetochores from at least 3 cells, n=3 independent experiments. (F) Quantification of endogenous KNL1 fluorescence intensity in the indicated HeLa inducible cell lines. Levels of endogenous KNL1 in cells rescued with the 300N fragment were examined with a KNL1 antibody targeted to amino acids 1413-1624 [11]. Levels of endogenous KNL1 in cells rescued with the 300-800N or the 1200C fragment were examined with a KNL1 antibody targeted to amino acids 1-22 (Experimental Procedures). For each experiment n \geq 60 kinetochores were measured from at least 5 cells. ***p<0.001 (Mann-Whitney rank sum test). Error bars represent s.d. from 2 independent experiments. For each experiment at least 12 kinetochores were measured from at least 5 cells. Scale bars, 5 μ m.

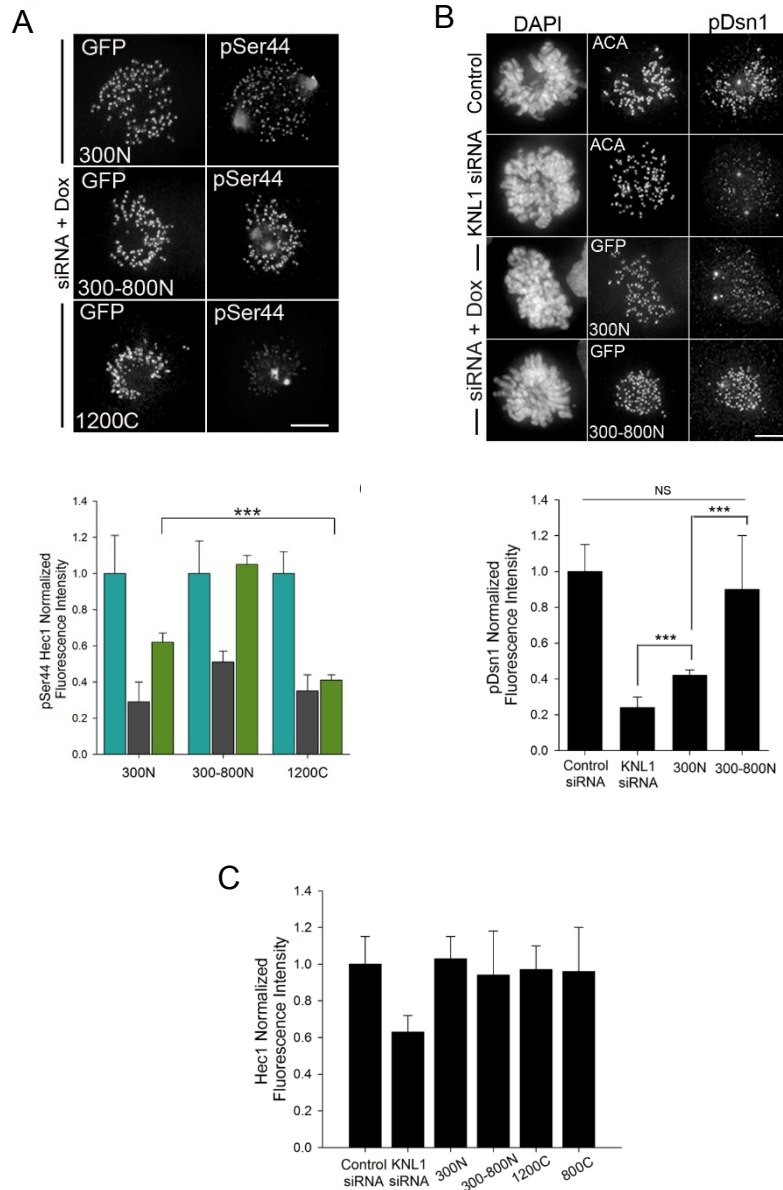


Figure 2.7. The N-terminus of KNL1 promotes Aurora B-mediated phosphorylation. (A-C) Flp-In T-Rex HeLa cells were depleted of endogenous KNL1, rescued with the indicated GFP-KNL1 fragment upon doxycycline addition and immunostained with the indicated antibodies. Kinetochores fluorescence intensities were quantified as indicated in the graphs. (A-B) Error bars represent s.d. from independent experiments, (A) Hec1 pSer44 (n=2), (B) pDsn1 (n=3). For each experiment $n \geq 100$ kinetochores were measured from at least 5 cells. *** $p < 0.001$, ** $p < 0.05$, NS= not statistically significantly different (Mann-Whitney rank sum test). (B) The 300N cell line is shown in the panel for control and KNL1 siRNA. (C) Quantification of kinetochores fluorescence intensities measured using the Hec1 9G3 antibody in stable HeLa FlpIn T-Rex cell lines expressing KNL1 fragments. Error bars represent s.d. between cells; $n \geq 100$ kinetochores and $n \geq 5$ cells. No statistical differences were found between control and HeLa stable cell lines expressing KNL1 fragments. Scale bars, 5 μm .

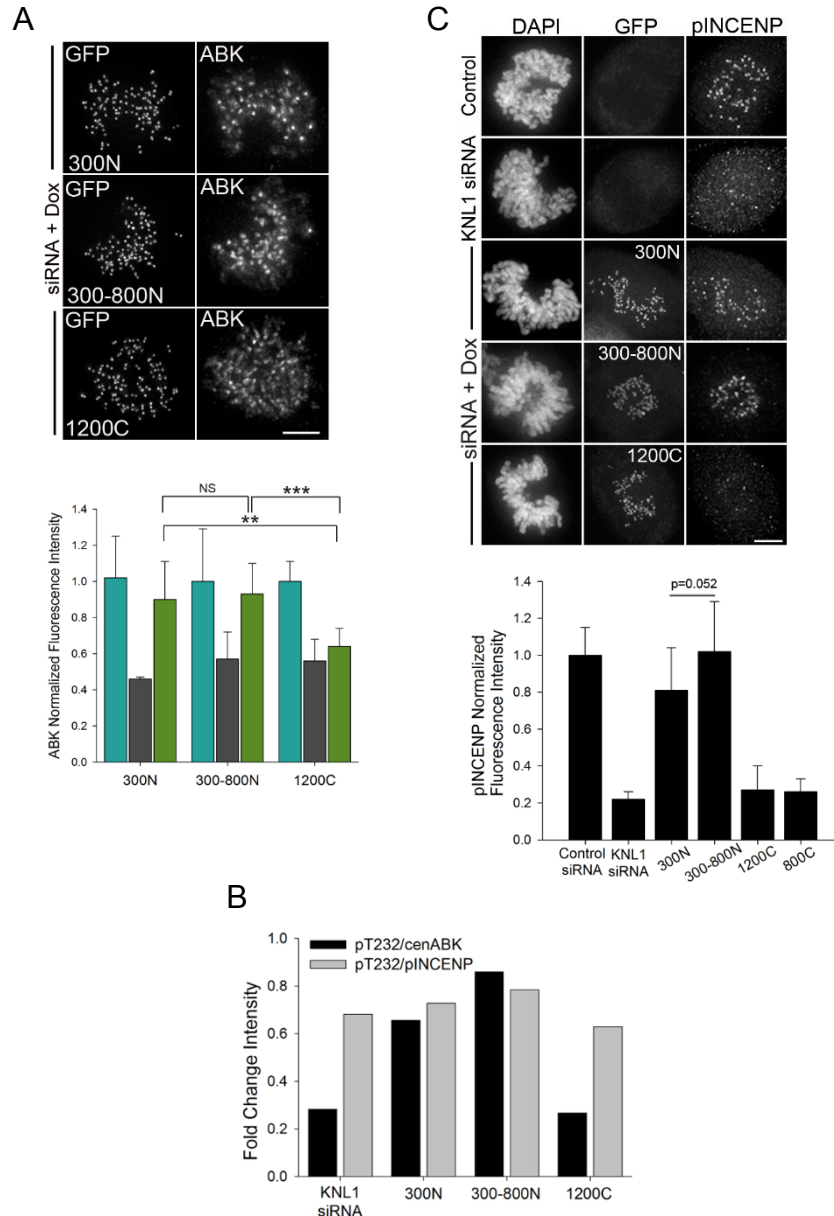


Figure 2.8. The N-terminus of KNL1 promotes centromeric Aurora B activity. (A,C) Flp-In T-REx HeLa cells were depleted of endogenous KNL1, rescued with the indicated GFP-KNL1 fragment upon doxycycline addition and immunostained with the indicated antibodies. Kinetochores fluorescence intensities were quantified as indicated in the graphs. (A) Error bars represent s.d. from independent experiments ($n=3$). For each experiment $n \geq 100$ kinetochores were measured from at least 8 cells. (C) The data shown are from a single representative experiment out of two repeats. For the experiment shown, $n \geq 100$ kinetochores and $n \geq 5$ cells. The 300N cell line is shown in the panel for control and KNL1 siRNA. Error bars represent s.d. between cells (Mann-Whitney rank sum test). (A,C) $***p < 0.001$, $**p < 0.05$, NS= not statistically significantly different (Mann-Whitney rank sum test). (D) Ratios between the average Aurora B pT232 and pINCENP fluorescence intensities and between Aurora B pT232 and AIM1 fluorescence intensities for each KNL1-mutant cell line are shown as bar graphs. The pT232/pINCENP ratio suggests that pT232 and pINCENP levels are highly correlated between cell lines. The pT232/cenABK(AIM1) ratio suggests that pT232 and cenABK are not highly correlated. Scale bars, 5 μm .

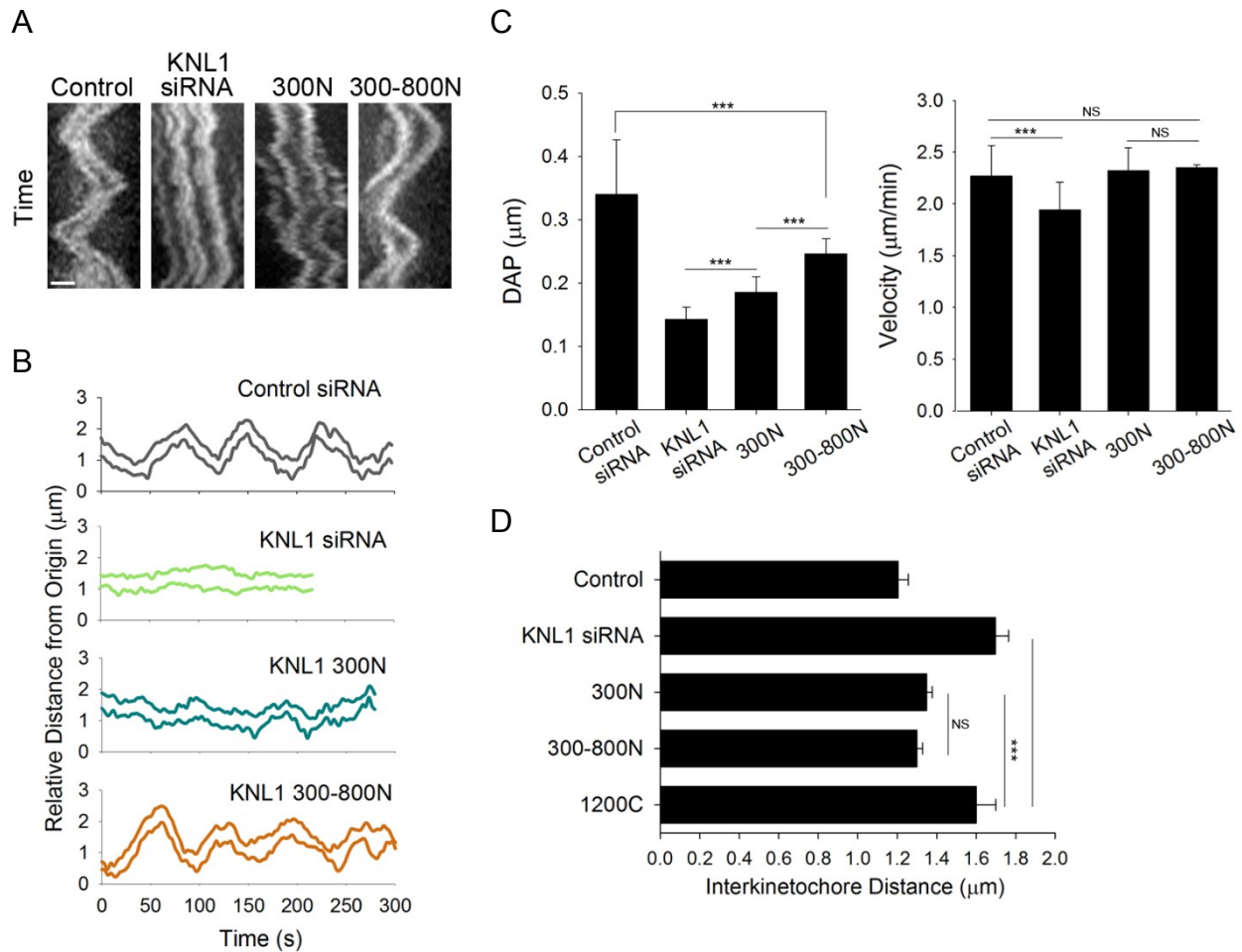


Figure 2.9. The KNL1 N-terminus partially rescues wild-type MT dynamics and kinetochore-MT attachment regulation. (A-D) Flp-In T-Rex HeLa cells were depleted of endogenous KNL1, rescued with the indicated GFP-KNL1 fragment upon doxycycline addition and analyzed for oscillatory kinetochore movements and inter-kinetochore distances in metaphase. (A) Kymographs of sister kinetochore pairs from live-cell time-lapse imaging sequences. Scale bar, 1 μm . (B) Plots of kinetochore tracks over time in cells expressing the indicated fragments. (C) Quantification of kinetochore oscillations. DAP indicates deviation from average position; $n \geq 12$ kinetochores per cell line. Error bars represent s.d. between cells. *** $p < 0.001$ (t-test). (D) Inter-kinetochore distances were measured on bi-oriented sister kinetochore pairs using ACA as a kinetochore marker. Error bars represent s.d. from independent experiments ($n=3$). For each experiment $n \geq 100$ kinetochores were measured from at least 5 cells. *** $p < 0.001$ (t-test). NS= not statistically significantly different (Mann-Whitney rank sum test).

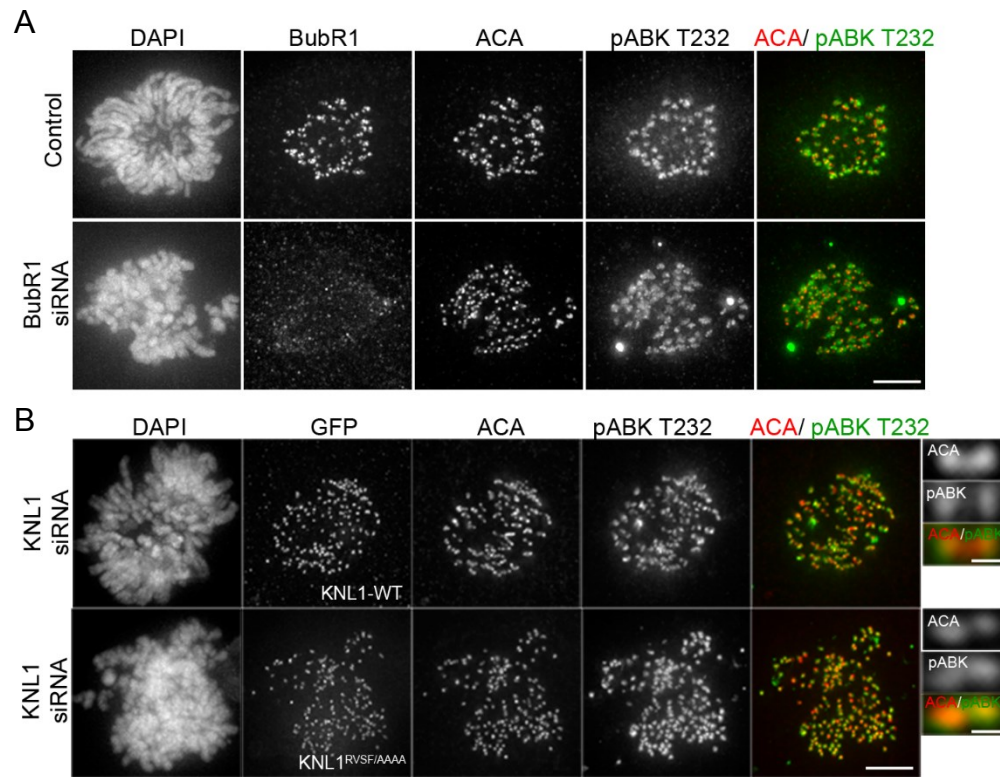


Figure 2.10. KNL1 mediates Aurora B activity in a BubR1 and PP1 recruitment independent manner. (A) Control and BubR1-depleted HeLa cells were fixed and stained with pT232 phospho-specific Aurora B kinase and BubR1 antibodies. (B) HeLa cells were depleted of KNL1, rescued with the indicated GFP-KNL1 mutant (RVSF/AAAA), and stained with the pT232 antibody. Scale bars, 5 μ m (cell panels) or 0.5 μ m (kinetochore pair insets).

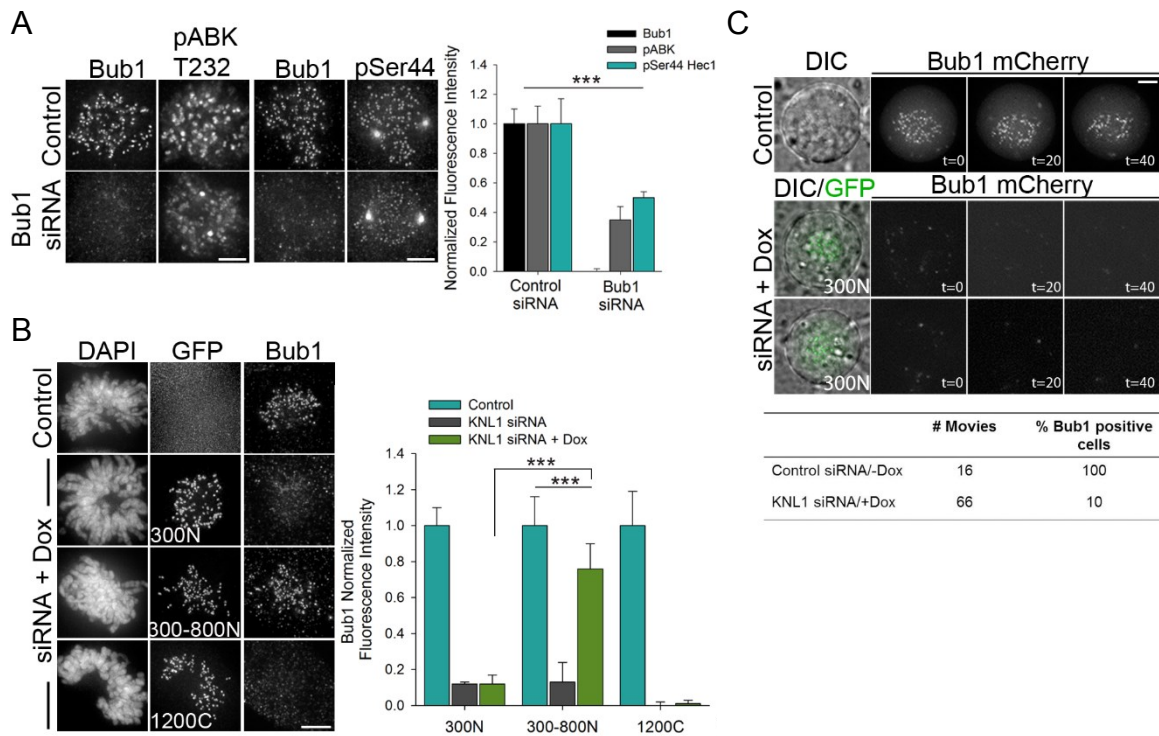


Figure 2.11. KNL1 mediates Aurora B activity in a Bub1-accumulation independent manner.

(A) Control and Bub1-depleted HeLa cells were immunostained with antibodies to Aurora B pT232 (left panels) or Hec1 pSer44 (right panels). Kinetochores fluorescence intensities are shown. Error bars represent s.d. from independent experiments ($n=2$). For each experiment $n \geq 50$ kinetochores were measured from at least 6 cells. (B-C) Flp-In T-REx HeLa cells were depleted of endogenous KNL1, rescued with the indicated GFP-KNL1 fragment upon doxycycline addition, and immunostained with Bub1 (B), or hBub1-mCherry was overexpressed (C). (B) Kinetochores fluorescence intensities were quantified. Error bars represent s.d. from independent experiments ($n=3$). For each experiment $n \geq 100$ kinetochores, $n \geq 10$ cells. $***p < 0.001$, NS= not statistically significantly different (Student's t-test). (C) Live-cell imaging in control and 300N KNL1 cells expressing Bub1-mCherry and treated with nocodazole. Time is indicated in minutes. Upon KNL1 depletion 90% of cells had no detectable Bub1, while 10% of cells showed high levels of Bub1, presumably due to incomplete knockdown. Scale bars, 5 μm .

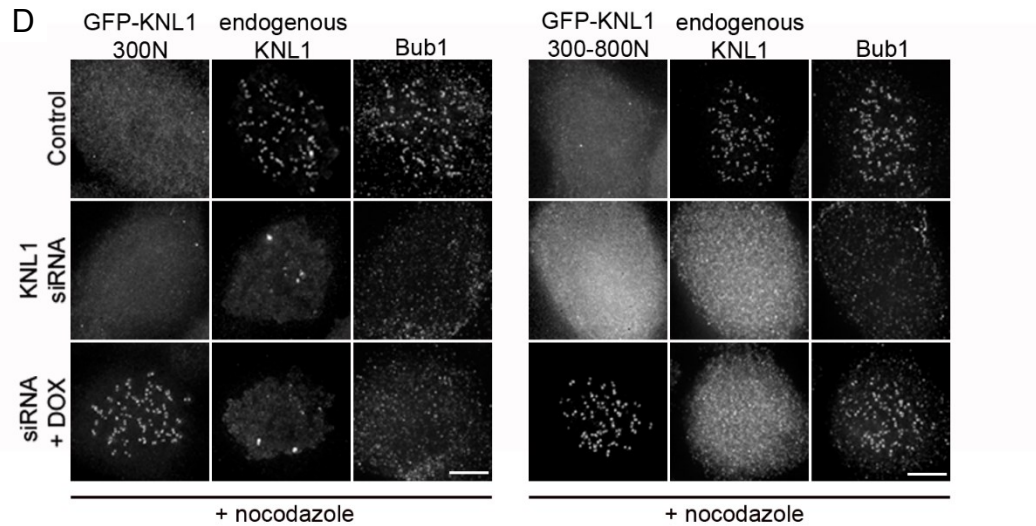


Figure 2.11. KNL1 mediates Aurora B activity in a Bub1-accumulation independent manner. (D) HeLa FlpIn KNL1 300N and 300-800N stable cell lines were depleted of KNL1 and rescued upon doxycycline addition. Cells were synchronized via a double-thymidine block and treated with 30 μ M nocodazole for 3 hours. Cells were subsequently fixed and immunostained with KNL1 and Bub1 antibodies. Scale bars, 5 μ m.

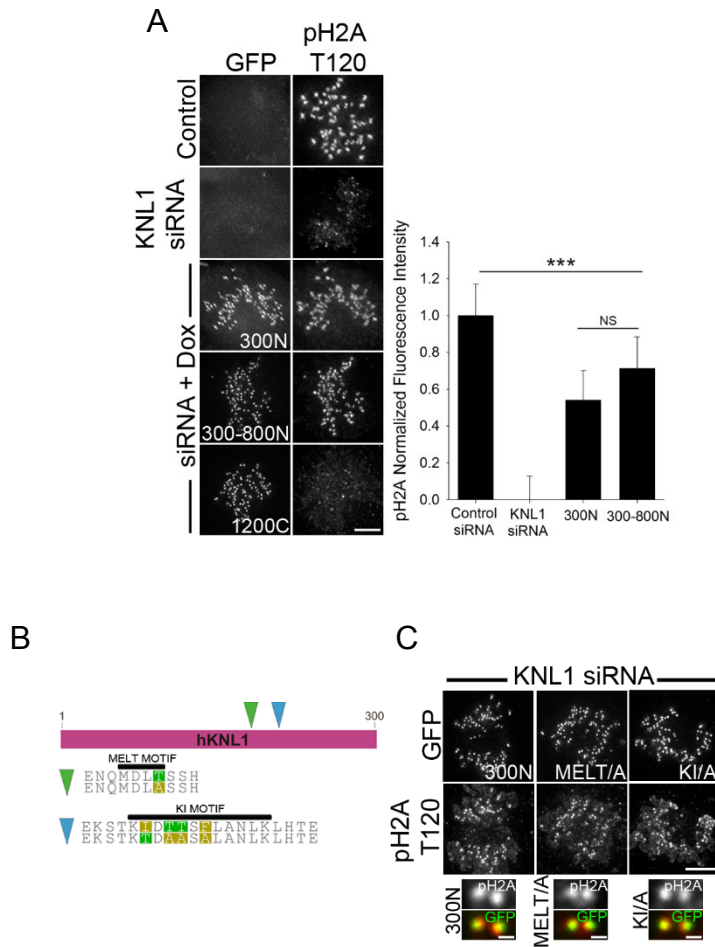


Figure 2.12. KNL1 N-terminus is required for Bub1 kinase activity at the kinetochore. (A) Flp-In T-REx HeLa cells were depleted of endogenous KNL1, rescued with the indicated GFP-KNL1 fragment upon doxycycline addition, and immunostained with histone H2A pT120. Kinetochore fluorescence intensities were quantified. Error bars represent s.d. from independent experiments ($n=2$). For each experiment $n \geq 50$ kinetochores, $n \geq 5$ cells in. $***p < 0.001$, NS= not statistically significantly different (Student's t-test). (B) Schematic of GFP-KNL1 300N fragments containing mutations in the MELT or KI motifs. The wild-type (top) and mutated (bottom) sequences are shown. (C) HeLa cells depleted of endogenous KNL1 were rescued with N-terminal GFP-tagged 300N, 300N-KI (300N-KI/A) or 300N-MELT (300N-MELT/A) mutants and immunostained for histone H2A pT120. Scale bars, 5 μm (cell panels) or 0.5 μm (kinetochore pair insets).

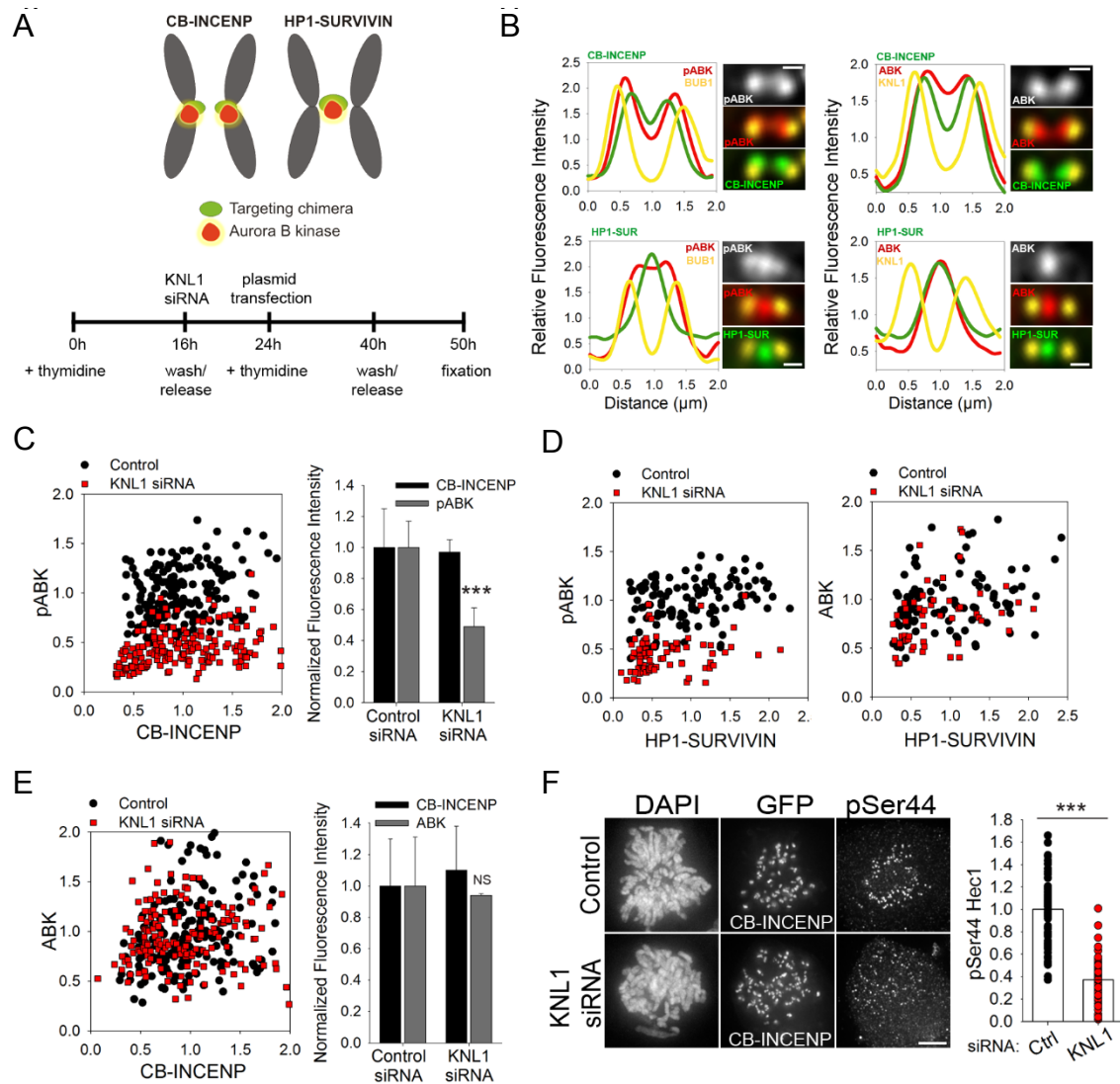


Figure 2.13. Aurora B accumulation is not sufficient for wild-type levels of Aurora B activity in KNL1-depleted cells. (A) Schematic of the localization of CB-INCENP and HP1-Survivin chimera (top) and schematized experimental procedure (bottom). (B) Line-scans of sister kinetochore pairs from HeLa cells expressing CB-INCENP or HP1-Survivin and immunostained with the indicated antibodies. Line scans show the fluorescence intensity across sister kinetochores for a pan-antibody to Aurora B (AIM1) or Aurora B pT232 antibody and the kinetochore markers Bub1 or KNL1. Line-scans represent the average position of at least 30 kinetochores per condition. Scale bars, 0.5 μm . (C-E) Normalized kinetochore fluorescence intensities of control and KNL1-depleted HeLa cells expressing either CB-INCENP or HP1-Survivin and immunostained with antibodies to Aurora B pT232 (C, D) or Aurora B (AIM1) (D, E). Scatter plots show intensities at individual kinetochores for Aurora B pT232 or Aurora B (AIM1) versus GFP intensities of the indicated chimera. (C) shows $n \geq 180$ kinetochores from at least 10 cells and 3 independent experiments; (D) shows $n \geq 50$ kinetochores from at least 8 cells; (E) shows $n \geq 180$ kinetochores from at least 8 cells and 2 independent experiments. Graphs in (C, E) right) represent the mean and s.d from independent experiments. *** $p < 0.001$, NS= not statistically significantly different (Mann-Whitney rank sum test). (F) Control and KNL1-depleted HeLa cells expressing CB-INCENP and immunostained with a Hec1 phospho-specific antibody to Ser44. Fluorescence intensity quantification is shown on the right. *** $p < 0.001$ (t- test). Scale bars, 5 μm .

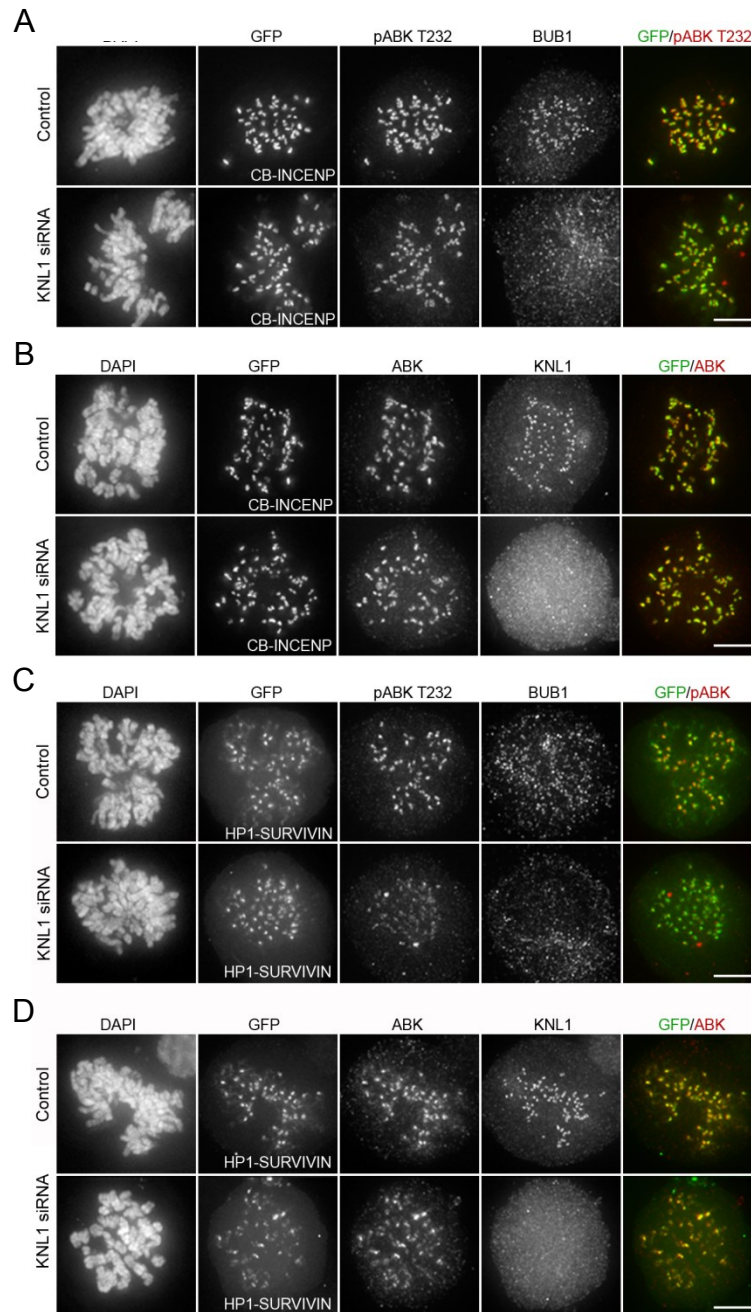


Figure 2.14. Aurora B recruitment is not sufficient to restore full Aurora B activity in KNL1-depleted cells. (A-D) Control and KNL1-depleted HeLa cells expressing either CB-INCENP or HP1-Survivin and immunostained with antibodies to Aurora B pT232 (A, C) or pan Aurora B (AIM1) (B, D). Scale bars, 5 μ m.

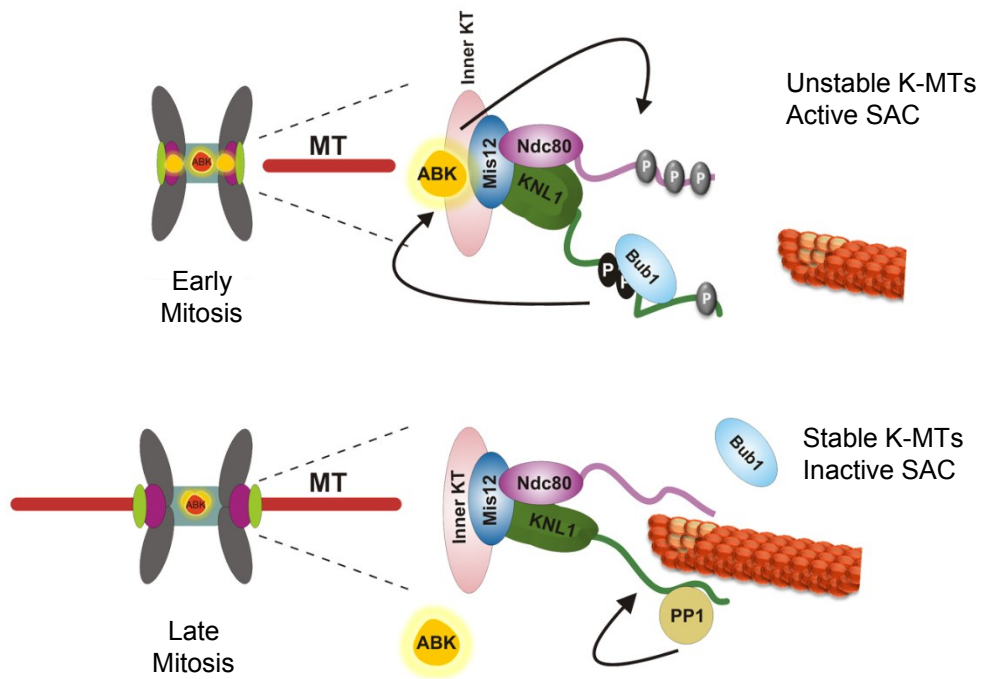


Figure 2.15. Model for KNL1-Mediated Aurora B activation. In early mitosis, phosphorylation of outer kinetochore substrates relies on Aurora B kinase activity, which is dependent on the N-terminus of KNL1. KNL1-mediated Bub1 kinase activity enhances Aurora B activation at both the inner centromere and the kinetochore. Upon generation of stable kinetochore-MT attachments and sister kinetochore bi-orientation, KNL1 is no longer able to mediate Bub1 kinase activity and Bub1 accumulation, resulting in decreased levels of active Aurora B. During metaphase, reduced levels of active Aurora B at the kinetochore region [73] lead to further stabilization of kinetochore-MT attachments and checkpoint silencing (mediated in part through PP1 binding) [63, 65].

CHAPTER 3

KNL1 AS A TOOL TO INVESTIGATE KINETOCHORE ARCHITECTURE AND KINETOCHORE PROTEIN DEPENDENCIES

3.1 Introduction

The kinetochore is a network of proteins assembled during mitosis on the centromeric region of DNA that functions as the physical link between chromosomes and microtubules (MTs). Such physical connection between chromosomes and MTs is an absolute requirement for correct chromosome congression to the equator of the cell and final separation of the sister chromatids. Therefore, a functional kinetochore is necessary for mitosis fitness. The kinetochore protein KNL1 facilitates the localization of several proteins implicated in a wide range of kinetochore functions, including checkpoint activation, checkpoint silencing, kinetochore-MT attachment stabilization, and kinetochore-MT attachment destabilization. Not surprisingly, loss of KNL1 function leads to i) abrogation of kinetochore localization of multiple mitotic proteins and ii) perturbation of a variety of mitotic processes, resulting in defective mitotic progression and chromosome missegregation.

The work presented here has not been published, but is intended to be used as part of a future publication (suggested reference below). The section named future experiments, at the end of this chapter, describes the experiments in progress and/or the experiments required for publication.

J.G.D and I conceived the paper. T.L and I performed the research. I analyzed the data. D.V. provided reagents. T.L and I will perform the additional research and corresponding data analysis required for publication of this work. I will write the manuscript with input from J.G.D.

Caldas, G. V., Lynch, T., Varma, D., DeLuca, J.G. (2014) KNL1 As a Tool to Investigate Kinetochore Architecture and Kinetochore Protein Dependencies. Manuscript in preparation.

Although there is limited structural information for human KNL1, its predicted lack of structure (more than half of the protein) and its multiple binding partners, agree with the notion that KNL1 behaves as a scaffold protein [95]. Scaffold proteins generally contain modular regions that allow for conformational flexibility and for the establishment of large protein networks [96]. Thus, despite their lack of enzymatic activity, these subcellular organizers can influence and even regulate signaling pathways, not only by serving as a site where signaling takes place, but also by modulating activities of other molecules upon binding and/or by temporally regulating the binding of specific proteins. In this regard, KNL1 was recently shown to be required for the activities of two important mitotic kinases, Aurora B and Bub1 [44], raising the possibility that KNL1 directly influences mitotic regulatory pathways. Requirement of KNL1 for the activities of Aurora B, involved in the regulation of kinetochore-MT attachment, and Bub1, involved in checkpoint signaling, is an example of how KNL1 may integrate different signaling pathways at the kinetochore.

Despite a central role for KNL1 in defining kinetochore structure and function [95], the specific regions of KNL1 that mediate kinetochore localization of many kinetochore proteins have not been investigated. Here, we use a set of KNL1 fragments [44] to determine the regions of KNL1 involved in the recruitment of a suite of checkpoint-related proteins by immunofluorescence. We additionally investigate by proteomics analysis the binding profile of KNL1 fragments from human cells. Our results reveal that checkpoint activating and checkpoint silencing proteins are recruited to the N-terminal region of KNL1 and demonstrate KNL1 as a practical tool to dissect the organization of kinetochore components, and the extent of protein dependencies for kinetochore localization. This systematic approach has led to a comprehensive

analysis of how KNL1 influences individual signaling pathways during mitosis and will contribute to our overall understanding of the complex kinetochore regulatory network.

3.2 Results

KNL1 KI motifs are sufficient for kinetochore localization of the checkpoint protein BubR1

Within its N-terminal region, KNL1 contains two KI motifs KI1 and KI2, that directly interact with the TPR domains of the checkpoint proteins Bub1 and BubR1, respectively [12, 13, 21, 22] (Figure 3.1A). In addition, the central and N-terminal regions of KNL1 contain several MELT motifs that upon Mps1 phosphorylation directly bind to a Bub3/Bub1 complex [24-26] (Figure 3.1B). The KI1/TPR interaction between KNL1 and Bub1 is not sufficient for Bub1 accumulation at kinetochores [22,44]. Instead, the phosphorylated MELT motifs on KNL1 act as individual binding units that promote and enhance the recruitment of Bub1 [97, 98]. While the Bub1 recruitment pathway is now well established, the requirements of KI and/or MELT repeats on KNL1 for kinetochore recruitment of BubR1 is not clear, and a flurry of recent papers offers no consensus on how BubR1 is recruited to kinetochores [97, 98, 99]. Zhang et al. found that MELT repeats are sufficient to mediated BubR1 kinetochore accumulation [98], and an engineered KNL1 construct lacking the KI motifs, but containing modules of MELT repeats and a kinetochore localization domain was able to mediate BubR1 kinetochore accumulation [97]. On the other hand, Vleugel et al. found that LacI-arrays of a fragment of KNL1 containing both KI motifs and one MELT repeat (KNL1 250N), was able to mediate accumulation of BubR1 at the LacI-LacO site, and mutations of any of these three motifs abolished BubR1 recruitment [98]. In agreement with this result, Krenn et al. showed that purified BubR1 binds to KNL1 250N specifically with intact KI motifs, and that KNL1 250C co-immunoprecipitates with

BubR1 from cells [99]. In contrast, however, Vleugel et al. reported that KNL1 250N was not able to mediate recruitment of BubR1 at kinetochores [98]. Therefore, the significance of the KI motifs for BubR1 localization needs to be confirmed in a consistent kinetochore background. For this purpose, we tested which of our HeLa cell lines stably expressing KNL1 fragments [44], that differ in the presence and number of KI and MELT motifs, were able to mediate BubR1 kinetochore recruitment (Figure 3.1A).

In agreement with two of the three recent studies [97, 98], we detected BubR1 at kinetochores in cells depleted of endogenous KNL1 and expressing 300-800N KNL1, which contains several MELT repeats, but is missing the KI motifs. Furthermore, we did not detect BubR1 in cells expressing KNL1 C-terminal fragments (1200C), which only contains one MELT repeat (Figure 3.2A). Therefore, as concluded by Zhang et al. and Vleugel et al., modules of MELT repeats, which enhance accumulation of Bub1 (and Bub3) at kinetochores, are sufficient to mediate BubR1 kinetochore recruitment [97, 98]. Contrary to the Vleugel et al. study [98], however, we were able to detect BubR1 in cells depleted of endogenous KNL1 and expressing 300N KNL1, which, similar to 250N KNL1 [97, 99], contain both KI motifs and two MELT repeats (Figure 3.2B). BubR1 was detected in 300N KNL1 cells by both immunofluorescence (data not shown) and by expression of a BubR1-mCherry construct (Figure 3.2B). When compared to 300-800N KNL1, 300N KNL1 expressing cells exhibit BubR1 localization, albeit at low levels (data not shown). It is possible that the two MELT repeats contained in 300N KNL1 mediates low levels of BubR1 localization. However, based on previous evidence demonstrating the relevance of the KI motifs for BubR1 binding to KNL1 250C, our results indicate that both the KI motifs and MELT repeats are sufficient, individually, to mediate BubR1 accumulation, although at different levels.

Kinetochores localization of the checkpoint proteins Mad1 and Mad2 is MELT-dependent

The current model for checkpoint activation during mitosis suggests that kinetochore accumulation of Mad1 and Mad2 is a required step for the amplification of the inhibitory signal that prevents anaphase onset and mitotic exit [9]. Mad1 allows for Mad2 kinetochore recruitment by direct binding [6, 8, 9, 56], and recently, it was demonstrated that Bub1/Bub3 are the main receptors for Mad1/Mad2 at yeast kinetochores [100]. Previous studies in mammalian cells have also implicated Bub1 as an essential factor for Mad1/Mad2 accumulation, along with the Ndc80 complex, and the RZZ complex [7-9, 27]. We asked whether the dependence of Mad1/Mad2 on KNL1 for kinetochore localization followed a similar localization pattern to that of Bub1 in human cells. We generated Mad1 and Mad2 constructs tagged with mCherry at their N-terminus and overexpressed them in HeLa cell lines depleted of endogenous KNL1 and expressing different GFP-tagged KNL1 fragments. In agreement with the localization pattern observed for Bub1 [44], Mad1 and Mad2 accumulated in control cells and also in cells expressing KNL1 fragments that contained multiple MELT repeats (300-800N, 1500C) but did not accumulate in cells expressing KNL1 fragments lacking MELT repeats (800C) or containing only 1-2 MELT repeats (300N, 1200C) (Figure 3.3A and 3.3B). Our results demonstrate that Mad1/Mad2 accumulation at human kinetochores requires the presence of MELT-repeats modules and follows Bub1 localization.

The checkpoint-related RZZ components localize to KNL1 N-terminus

The RZZ complex, formed by Zwilch, Zw10, and Rod, functions as a receptor for the protein Spindly, which directly recruits the dynein-dynactin complex to kinetochores [52, 54]. The motor protein dynein is responsible for stripping of Mad1/Mad2 from kinetochores after MT

attachment and subsequent silencing of the checkpoint [101, 102]. Interestingly, components of the RZZ complex have also been implicated in kinetochore recruitment of Mad1 and Mad2 [103, 104]. As for Mad1 and Mad2, kinetochore localization of the RZZ components depends on KNL1 [42]. Despite these dependencies, there is no evidence for direct interaction between RZZ components and Mad1/Mad2, Bub1, BubR1, or KNL1. It is known, however, that the RZZ component Zw10 directly interacts with Zwint1, a protein that directly binds to the C-terminal region of KNL1 and exhibits interdependency with KNL1 for kinetochore localization [42, 52, 105] (Figure 3.1A). Because Zwint1 directly interacts with Zw10, and its depletion causes a significant reduction of RZZ components, it has been assumed that Zwint1 is the primary kinetochore receptor for the RZZ complex [104], and that the Zwint1/RZZ pathway is directly involved in Mad1/Mad2 recruitment. Recent data from yeast, however, demonstrates that Bub1/Bub3 directly interact with Mad1, and Bub1/Bub3 localization is a required step for Mad1/Mad2 kinetochore accumulation [100]. In addition, a recent study in human cells showed that Zwint1 depletion partially reduces KNL1 and RZZ components at kinetochores to similar levels (~60%), while KNL1 depletion completely abolishes both Zwint1 and RZZ kinetochore localization [42]. These results suggest that RZZ components may rely on a Zwint1-independent, KNL1-mediated pathway for kinetochore localization. To determine the region of KNL1 sufficient to recruit RZZ components to kinetochores and to assess whether localization of RZZ correlates with Zwint1, we analyzed the kinetochore recruitment of both Zwint1 and RZZ components in our FlpIn HeLa stable cell lines. As shown in Figure 3.4A, only cells expressing the C-terminal KNL1 fragments 1500C, 1200C and 800C, which contain the Zwint1 binding region (aa 1834-2107), were able to mediate Zwint1 recruitment. As expected, the minimal KNL1 C-terminal region (2056-2316) required for KNL1 kinetochore localization and contained

in 300N and 300-800N KNL1, was not able to mediate Zwint1 recruitment (Figure 3.4B). In contrast, KNL1 300N, 300-800N, and 1500C, were sufficient to drive kinetochore accumulation of the RZZ components (Figure 3.5A and 3.5B). Surprisingly, these results show that the RZZ complex does not follow the localization pattern of Zwint1, but instead, it follows a similar localization pattern as BubR1, in which MELT enrichment is sufficient but not necessary for localization. It is possible that, at wild-type kinetochores, the RZZ complex localizing proximal to Bub1/Bub3, helps in the recruitment of Mad1/Mad2. Whether direct interaction between Zw10 and Zwint1, either at the kinetochore or in the cytoplasm, is required for RZZ localization to the KNL1 N-terminus remains to be tested. Regardless, these data demonstrate that Zwint1 kinetochore localization is not sufficient or necessary for RZZ recruitment.

Proteomics analysis of KNL1 fragments reveals positioning of known kinetochore proteins and uncharacterized kinetochore proteins

KNL1 functions as a spatial coordinator of multiple kinetochore protein complexes that direct the signaling events required for correct segregation of chromosomes during mitosis. Identifying the repertoire of KNL1 binding partners, and the regions of KNL1 involved in such interactions, are key for the understanding of kinetochore architecture and its activities. Aiming for a comprehensive view of the kinetochore network, with KNL1 as a central player, we generated inducible 293T cells stably expressing Flag-tagged KNL1 fragments for proteomics analysis (Figure 3.6A and 3.6B). Specifically, we immunoprecipitated Flag-tagged 300N, 300-800N and 1500C KNL1 after synchronization, nocodazole treatment, and doxycycline induction, and performed LC-MS/MS analysis to determine the binding profiles of the different KNL1 regions (see Methods for details). We used FlpIn 293T host cells lysates as control. As expected,

the KNL1 peptides identified by LC-MS/MS on each sample or cell line corresponded to the region of the protein expressed by each cell line (Figure 3.7A). We used the normalized spectral abundance factor (NSAF) as an estimate reference of the relative abundance of KNL1 in each sample, and we found highly similar values between them, indicating that we immunoprecipitated the KNL1 fragments (300N, 300-800N, 1500C) at similar levels, and therefore, differences in protein binding profiles between them are likely independent of KNL1 abundance (Figure 3.6B). Importantly, the NSAF values used here are only an approximation of relative abundance and precise quantitative values need to be determined by comparing samples across multiple experiments.

Although only 12 known kinetochore proteins were identified in all samples, several of them corresponded to the cell lines expressing the regions of KNL1 known to mediate their localization (Figure 3.7A and 3.7B). For instance, components of the Ndc80 were identified in all samples (the three KNL1 fragments contain a short C-terminal region for kinetochore binding; see Figure 3.1A). Similarly, the phosphatase PP1, known to interact with the SILK and RVSF motifs in the far N-terminal region of KNL1 [20], was only identified in 300N KNL1 (Figure 3.8A). Furthermore, although tubulin was detected in all samples, including the control, a 3-fold higher NSAF value was found for 300N KNL1, the fragment that contains the KNL1 MT binding domain (data not shown) [28, 29].

In addition to previously mapped kinetochore proteins, we identified some centromere and kinetochore proteins whose precise kinetochore localization mechanism is unknown, such as Aurora B kinase, INCENP and dynein (Figure 3.8A and 3.8B) (see discussion below). Moreover, previously unidentified proteins were differentially found across KNL1 fragments (Table 3.1 and 3.2). From this list of “new” kinetochore proteins, Poly (ADP-ribose) polymerase-1 (PARP-1),

comes to our attention. PARP1 catalyzes polyADP-ribosylation of proteins, and is involved in the DNA damage response [106]. Interestingly, however, a previous report demonstrated that PARP1 co-immunoprecipitates with its functional homolog PARP2 and with the kinetochore proteins CenpA, CenpB and Bub3, suggesting a possible role for PARP1 during mitosis [107]. It will be interesting to confirm whether PARP1 is observed at kinetochores, and to determine its localization pattern on KNL1 by other means.

Together, our results establish proteomics analysis of different KNL1 mutants as a practical approach to evaluate kinetochore architecture in cells.

3.3 Discussion

Unraveling the composition and organization of the kinetochore is an essential task to understand how kinetochore proteins coordinate mitotic processes. As a central kinetochore scaffold, KNL1 functions as an integrator of kinetochore activities, and exploring the details regarding KNL1 interactions will provide much-needed insights into the regulatory processes occurring at the kinetochore. Here, we mapped the kinetochore localization of six known checkpoint-related proteins and the kinetochore protein Zwint1, using a HeLa cells stably expressing a suite of KNL1 fragments. While Zwint1 localized to the C-terminal region of KNL1, all checkpoint-related proteins localized to the N-terminus of KNL1.

Since the discovery of MELT repeats at the N-terminal and central regions of KNL1, Bub1 and Bub3 have been the only proteins shown to have physical association with these regions of KNL1 [24, 26]. In addition, it has been clearly demonstrated that MELT-rich regions enhance the accumulation of Bub1 (and presumably Bub3) at kinetochores, and they are mutually dependent for this interaction [24, 26, 44, 97, 98]. In contrast, the KI motifs on KNL1

are not sufficient for Bub1 kinetochore accumulation [44]. Bub1 was recently demonstrated to be a kinetochore receptor for Mad1 and Mad2 in yeast [100]. In agreement with this, we find that Mad1/Mad2 localization perfectly matches with Bub1 localization in human cells. Bub1 has also been shown to be required for BubR1 kinetochore localization [43], however, direct interaction between Bub1 and BubR1 has not been reported. Instead, Bub1 and BubR1 directly bind to the checkpoint protein Bub3, and in both cases, it is proposed that binding to Bub3 is required for their kinetochore localization [48]. From our KNL1 mapping analysis, we find that BubR1 accumulates at kinetochores in cells expressing both MELT-rich KNL1 fragments and KI-containing KNL1 fragments (300N). We previously reported that 300N KNL1 is not able to mediate Bub1 kinetochore accumulation [44]. A more recent study, however, reports that a similar KNL1 construct (250N KNL1) immunoprecipitates Bub1 and Bub3, and mediates low levels of Bub1 recruitment at kinetochores, suggesting that although not accumulated at high levels, Bub1 interacts with the far N-terminal region of KNL1 in the absence of multiple MELT repeat modules [99]. Together, these data suggest that BubR1 accumulation depends on the Bub1/Bub3/KNL1 interaction. Specifically, MELT-rich KNL1 fragments mediate BubR1 recruitment in absence of KI motifs due to their ability to accumulate Bub1/Bub3 at high levels. On the other hand, transient interactions between Bub1/Bub3 and 300N KNL1 (Bub1 interacting through the KI1 motif and Bub3 interacting through two MELT repeats), likely stabilizes the BubR1/KNL1 interaction (Figure 3.9). However, since Bub1/Bub3 do not highly accumulate at kinetochores in the absence of MELT repeats, low levels of BubR1 are also observed at kinetochores in cells expressing 300N KNL1. Based on the fact that Bub1 does not bind BubR1, but both proteins directly interact with Bub3, and Bub1/Bub3 are mutually dependent for interaction with the MELT repeats on KNL1, we propose a model in which BubR1 kinetochore

localization depends directly on Bub3 and indirectly on Bub1 accumulation (Figure 3.9). Further experiments are needed to corroborate this model. It remains to be tested whether a 300N KNL1 fragment containing mutations in the KI2, and/or the MELT motifs, abolish BubR1 kinetochore recruitment. Also, the use of a Bub3 mutant unable to bind the phosphorylated MELT repeats will disrupt Bub1 enrichment at kinetochores, and it will allow us to test whether Bub1/Bub3 recruitment is a requirement for BubR1 kinetochore localization (see Future Experiments).

Similar to the pattern observed for BubR1, the RZZ components Rod, Zwilch and Zw10 (data not shown), showed localization to both MELT-rich regions and KI-containing regions of KNL1. Although it is not clear what drives the accumulation of the RZZ components Zwilch, Rod and Zw10 to these regions of KNL1, the fact that both the MELT-rich regions and the KI-containing regions are sufficient for RZZ complex kinetochore accumulation, raises the possibility that the Bub1/Bub3/BubR1 complex may serve as the kinetochore receptor for RZZ (see Future Experiments) (Figure 3.9). *In vitro* binding assays and structural studies will be determinant in unraveling how the N-terminal region of KNL1 modulates interactions with checkpoint activating proteins such as Mad1, Mad2, Bub3 and BubR1 and also with proteins implicated in checkpoint silencing such as the RZZ complex and the phosphatase PP1.

Results from proteomics analysis with our different KNL1 mutants support the notion that expression of KNL1 modules in cells can provide us relevant information about kinetochore architecture. In addition, the identification of kinetochore-localized proteins previously unconsidered will undoubtedly provide a broader view of the kinetochore network. We identified several kinetochore proteins expected to immunoprecipitate with specific KNL1 regions. For instance, we found the phosphatase PP1 only in samples from cells expressing the 300N region of KNL1, where the PP1 binding motifs are contained [20], and Zwint1, in cells expressing

1500C KNL1, the only fragment that contained an intact Zwint1 binding domain (Figure 3.8A). Similarly, components of the Mis12 and Ndc80 complexes, known to reside at the C-terminal region of KNL1, were found in all our KNL1 mutants. These results demonstrate that proteomics analysis serves as a precise and complimentary tool to map kinetochore proteins.

An interesting finding from our proteomics data is the identification of Aurora B kinase and INCENP in cells expressing 300-800N KNL1 (Figure 3.8A). We recently demonstrated that the KNL1 N-terminus is required for Aurora B kinase activity at kinetochores. In the model that we envision, KNL1 and Bub1 directly influence the activation of Aurora B, independent of Aurora B accumulation at the inner centromere [44]. In such a model, however, it is not clear how activation occurs. A reasonable hypothesis is that Aurora B is recruited to the kinetochore region where the KNL1 N-terminus directly promotes its activation. We previously tested this through binding assays using purified components (data not shown), however, we did not find a direct interaction between the KNL1 N-terminus and Aurora B kinase. Our proteomics results raise the possibility that the KNL1 N-terminus indirectly mediates the localization of Aurora B and its primary activator, INCENP, to the kinetochore region (possibly via Bub1). Further analyses are necessary to determine how these interactions may be occurring. Also, optimization of KNL1 immunoprecipitations for use in proteomics experiments will be required to identify a larger number of kinetochore proteins and to provide a detailed map of the kinetochore network. In summary, our data show that mapping of kinetochore proteins from cells expressing different KNL1 modules, by complementary tools like immunofluorescence and proteomics, provides a foundation to define kinetochore organization and regulation.

3.4 Methods

Cell culture and transfection

HeLa (ATCC) and FlpIn T-REx HeLa cell lines were cultured in DMEM (Invitrogen), supplemented with 10% FBS and 1% penicillin/streptomycin at 37°C in 5% CO₂. For silence and rescue experiments, stable cell lines were doubly blocked with thymidine, depleted of endogenous KNL1 using the corresponding siRNAs (described in Caldas et al. 2013 [44]), and induced with doxycycline for overexpression. Briefly, cells were transfected with siRNA, 8h later treated with 2.5 mM thymidine for 16 h, washed with PBS, replaced with fresh medium, transfected with siRNA, and incubated for 8 h. Cells were treated with doxycycline (1 µg/ml) for induction, and for the second block, 2.5 mM thymidine was added for 16 h. Cells were then washed with PBS, replaced with fresh medium containing doxycycline (1 µg/ml), and fixed after 10 h for immunostaining. For all experiments, cells were plated to be 60% confluent at the time of transfection on acid-washed glass coverslips. siRNA transfections were performed using Oligofectamine (Invitrogen), according to the manufacturer's instructions. DNA transfections were performed using Effectene (Qiagen), using 0.3 µg of plasmid and according to manufacturer's instructions. DNA transfections were performed 6-7h after the first siRNA transfection and prior the first thymidine block.

The FlpIn T-REx 293T host cell line was a gift from T. Yao (Colorado State University, Fort Collins, Colorado, USA). To generate FlpIn T-REx 293T cells containing KNL1 fragments fused to HA-Flag-Flag at the N-terminus, Flp-In T-REx 293T host cells were co-transfected with a ratio of 9:1 (wt/wt) pOG44:pcDNA5/FRT/TO expression plasmid using Fugene HD (Promega). 48 h after transfection, cell lines were placed under selection with 100 µg/ml hygromycin (EMD Millipore) for 2 wk. Hygromycin-resistant foci were chosen, expanded, and

tested for expression by western blot with anti-Flag antibodies. Gene expression was induced with 1 µg/ml doxycycline (Sigma-Aldrich) for 24 h. For immunoprecipitation, Host 293T cells and each stable cell line were grown on six 150mm tissue culture dishes, doubly blocked with thymidine and induced with doxycycline for 24h.

Plasmids

Mad1, Mad2, and BubR1 were cloned into a pmCherry-C1 plasmid to generate Cherry-Mad1, Cherry-Mad2, and Cherry-BubR1. All plasmid DNAs were purified using an Endo-free Maxi kit (QIAGEN) before transfection. HA-flag-flag 1–300 (300N), 300–818 (300–800N), and 819–2316 (1500C) KNL1 were generated by PCR using KNL1 wild-type as the template [74] and cloned into the pcDNA5/FRT/TO vector using In-Fusion cloning (Clontech).

Immunofluorescence

Fixation and immunostaining of HeLa cells were performed as described previously [44]. In brief, cells were rinsed in 37°C PHEM buffer (60 mM Pipes, 25 mM Hepes, 10 mM EGTA, and 4 mM MgSO₄, pH 6.9), fixed in 4% paraformaldehyde for 20 min, and extracted in PHEM buffer + 0.5% Triton X-100 for 5 min. Immunostaining was performed using the following antibodies: rabbit polyclonal anti-Zwint1 (Gene Tex) was used at 1:200; rabbit polyclonal anti-Zwilch, provided by D. Varma but originally obtained from A. Musacchio (Max Planck Institute of Molecular Physiology, Dortmund, Germany) was used at 1:200; rabbit polyclonal anti-Zw10, provided by D. Varma but originally obtained from R. Vallee (Columbia University, New York, NY), was used at 1:200; rabbit polyclonal anti-Rod, provided by D. Varma but originally obtained from G. Chan (University of Alberta, Edmonton, Alberta,

Canada), was used at 1:200; human anti-centromere antibody (ACA; Antibodies, Inc.) was used at 1:500; and mouse anti-BubR1 (EMD Millipore) was used at 1:500. Secondary antibodies conjugated to either Alexa 647, or Rhodamine Red-X (Jackson ImmunoResearch Laboratories, Inc.) were used at 1:300.

Image acquisition and analysis

Image acquisition was performed on an imaging system (DeltaVision Personal DV; Applied Precision) equipped with a camera (CoolSNAP HQ2; Photometrics/Roper Scientific), a 60×/1.42 NA PlanApochromat objective (Olympus), and SoftWoRx acquisition software (Applied Precision). Images were acquired at room temperature as Z-stacks at 0.2- μ m intervals.

Immunoprecipitation and Proteomics analysis.

Cells were carefully washed with PBS twice, scraped from dishes with PBS and centrifuged at 1000rpm for 4min. Pellets were frozen at -80^oC until needed. For immunoprecipitation, cells were lysed in lysis buffer (75 mM Hepes, pH 7.5, 150 mM KCl, 1.5 mM EGTA, 1.5 mM MgCl₂, 0.1% NP-40, Complete protease inhibitor cocktail [Roche], and PhosSTOP phosphatase inhibitors [Roche]), passed through a 25 gauge needle several times and incubated on ice for 30 minutes. Lysates were clarified by centrifugation at 14000rpm for 10 min and total protein concentration was measured by BCA assay. Lysates were normalized and 2mg of total protein for each sample was used for immunoprecipitation. Normalized lysates were incubated with anti-Flag M2 magnetic beads (Sigma) for 2 h at 4°C. The unbound fraction was recovered and beads were washed with lysis buffer (3X). Interacting proteins were eluted by competition with 3XFlag peptide twice for 30min at 4°C.

Following acetone precipitation, the protein pellet was incubated with 15ul of 8M Urea and bath sonicated for 5min for denaturation. Then, 20 ul of 0.2% ProteaseMAX Surfactant (Promega) was added and the solution was mixed by shaking for 5min. 50mM Ammonium bicarbonate was added, followed by 1 ml of 0.5M DTT and incubated at 50°C for 20min. Proteins were alkylated with 2.5 ml of 0.55M Iodoacetamide and incubated in the dark for 15 min at room temperature. Finally, proteins were digested by adding 1 ul of 1% ProteaseMax and 18 ul of 0.1 ug /ul trypsin and incubating for 3hr at 37°C. The reaction was stopped with TFA to a final concentration of 0.5%. Peptides were desalted and concentrated using C18 Spin Columns (Thermo Scientific 5um, 100 um ID x 2cm C18 column) and then resuspended in Buffer A (3% ACN, 0.1% TFA) at a concentration of 1 ug/ul (45 mM) for analysis via LC-MS/MS. Chromatographic separation was performed on a reverse phase nanospray column (Thermo Scientific EASYnano-LC, 3um, 75 um ID x 100mm C18 column) using a 90 minute linear gradient from 10%-30% buffer B (100% ACN, 0.1% formic acid) at a flow rate of 400 nanoliters/min. Peptides were eluted directly into the mass spectrometer (Thermo Scientific Orbitrap Velos) and spectra were collected over a m/z range of 400-2000 Da using a dynamic exclusion limit of 2 MS/MS spectra of a given peptide mass for 90 s. Compound lists of the resulting spectra were generated using Xcalibur 2.2 software (Thermo Scientific) with a S/N threshold of 1.5 and 1 scan/group.

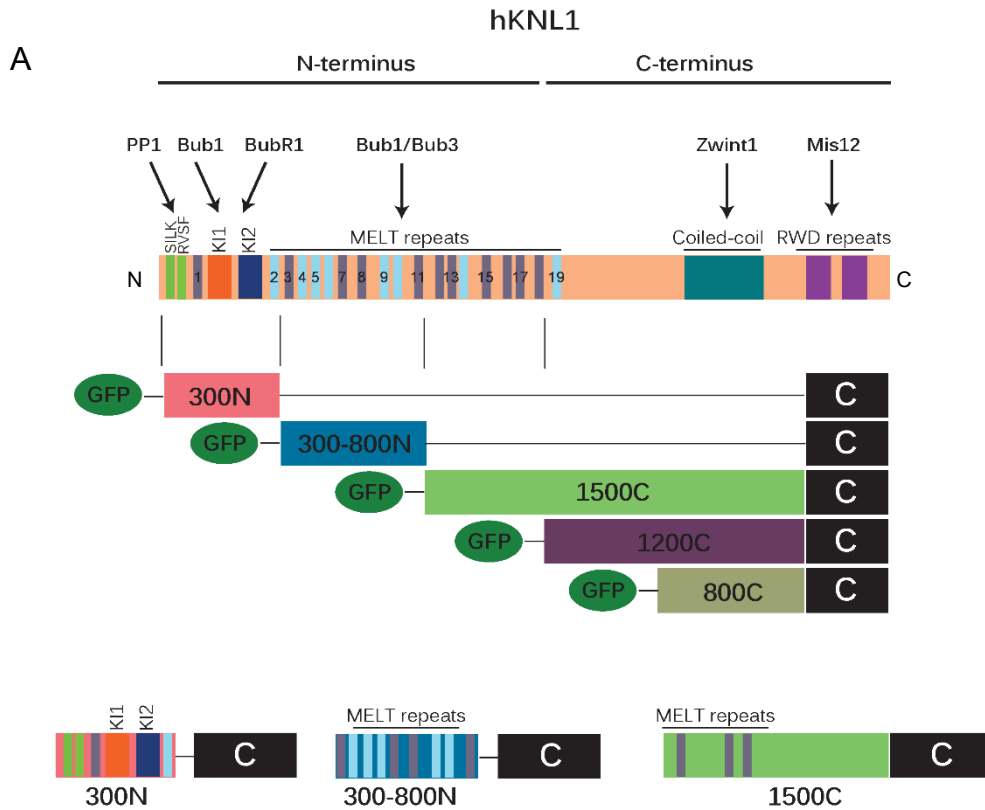
All MS/MS samples were searched against the uniprot_hum_rev_102513 database (176756 entries) using Mascot (Matrix Science, London, UK; version 2.3.02). The search was carried out with a fragment ion mass tolerance of 0.80 Da and a parent ion tolerance of 20 PPM. Carbamidomethyl of cysteine was specified as a fixed modification and oxidation of methionine was specified as a variable modification. Protein identification results were compiled and

validated using Scaffold v.4.3.2 (version Scaffold_4.3.2, Proteome Software Inc., Portland, OR). Peptide identifications were accepted if they could be established as greater than 95.0% probability by the Scaffold Local FDR algorithm. Protein identifications were accepted if they could be established at greater than 99.9% probability and contained at least 2 identified peptides.

3.5 Future Experiments and Experiments in Progress:

- We generated a Bub3-mCherry construct to map the localization of Bub3 in the KNL1 mutants set and we are generating an Mps1-mCherry construct for similar purposes. With these two proteins we will have the reagents to map the KNL1-dependent kinetochore recruitment of all of the essential checkpoint proteins.
- We are generating 300N KNL1 constructs containing mutations in the KI2 motif, the MELT motif (already completed), and both, to determine whether localization of BubR1 in 300N KNL1 is MELT and/or KI2 dependent. Additionally, we are designing Bub3 constructs containing mutations that disrupt Bub3-pMELT interaction (Bub3 disrupted MELT binding domain or Bub3-dMELTBD). Using this mutant, we aim to test whether BubR1 localization depends on Bub3/KNL1 interaction.
- In order to have a better understanding of the RZZ, Mad1/Mad2 and Bub1/Bub3/BubR1 dependencies, we are planning to carry out the following experiments:
 - Depletion of endogenous KNL1 and BubR1 followed by induction of 300-800N KNL1 expression, to assess whether the RZZ complex localizes to this region of KNL1 in the absence of BubR1. We will repeat the same experiment in 300N KNL1 expressing cells.

- Depletion of endogenous KNL1 and RZZ components (Zw10 and Zwilch independently) or Zwint1, followed by induction of 300-800N KNL1 expression, to assess whether Mad1/Mad2 localizes to this region of KNL1 in the absence of the RZZ or in the absence of Zwint1.
- Using our KNL1 mutant cell lines, we have generated a partial KNL1 dependency map for the proteins CenpE and CenpF, and we aim to complete these experiments and include them in the final manuscript.
- We will repeat the proteomics experiments using the 293T FlpIn cells expressing the KNL1 mutants.



B

MELT1	NDQ T V I F-----SDENQ (151)	MDL T S H T V M I T K L L D N P I S
MELT2	-N I T R L F -----REKDDG (281)	MN F T Q C H T A N I Q T L I P T S S E T
MELT3	GND I T I Y -----GND F (319)	MDL T F N H T L Q I L P A T G N F S E I
MELT4	--- T G N F -----SEIENQTQNA (347)	MD V T T G Y G T K A S G N K T V F K S K
MELT5	GN K T V F K S K Q N T A F Q D L S I N S A D K (383)	I H I T R S H I M G A E T H I V S Q T C N
MELT6	G C K T V F Y S S C N D A----- (437)	M E M T K C L S N M R E E K N L L K H D S
MELT7	L T E K T I Y S G E E N ----- (484)	MD I T K S H T V A I D N Q I F K Q D Q S
MELT8	---LSN P L S I S L T D R K T E L L S G E N (572)	MD L T S H T S N L G S Q V P L A A Y N
MELT9	V L K I L P Y ----L D K D S P Q S A D C N Q (664)	E I A T S H N I V Y C G G V L D K Q I T N
MELT10	S T T K P L F -----S S G Q F S M K N H (714)	D T A I S H T V K S V L G Q N S K L A E
MELT11	H D K M I I C -----S E E E Q N (762)	MD L T K S H T V I G F G P S E L Q E L
MELT12	I D K T I V F -----S E D D K N D (872)	MD I T K S Y T I E I N H R P L L E K R D
MELT13	T S E T I L Y -----T C R Q D D (914)	M E I T R S H T A L E C K T V S P D E I
MELT14	M D K T V V F -----V D N H V E (952)	L E M T S H T V I D Y Q E K E R T D R
MELT15	N R G P V E V -----A D N (1034)	M E L S K S A T V K N I K D V Q S P G F L
MELT16	N D K T I V F -----S E N H K N D (1086)	MD I T Q S C M V E I D N E S A L E D K E
MELT17	A S K T I L Y -----S C G Q D D (1126)	M E I T R S H T A L E C K T L L P N E I
MELT18	K D K T V L F -----T D N Y S D (1164)	L E V T D S H T V I D C Q A T E K I L E
MELT19	Q V E S C Q L -----N N R D R R N (1284)	V D F T S H A T A I C G S S D N Y S L

Figure 3.1. KNL1 domain architecture. (A) (upper) Representation of human KNL1 and all regions known to mediate protein interactions. MELT repeats initially identified by Yamagishi et al. 2012 [26] are shown in gray (MELT repeats reported in Caldas et al. 2013 [44]), and MELT repeats recently identified by Krenn et al. 2014 [99] and Vleugel et al. 2013 [97] are shown in light blue. (lower) Schematic of GFP-KNL1 constructs stably incorporated into Flp-In T-REx HeLa cell lines (Caldas et al. 2013 [44]); the amino acids of KNL1 constructs shown are as follows: amino acids 1-300 (300N), 300-818 (300-800N), 1174-2316 (1200C) 1519-2316 (800C), 819-2316 (1500C), 2056-2316 (C). (B) Alignment of MELT repeats in human KNL1, adapted from Krenn et al. 2014 [99]. The new consensus sequence for MELT repeats is [M/I/L/V]-[E/D]-[M/I/L/V]-T [99]. The yellow box indicates the MELT repeats not included in our KNL1 1500C construct (aa 910–1120 are not contained in the wild-type KNL1 from Liu et al. 2010 [20], from which the fragments were cloned).

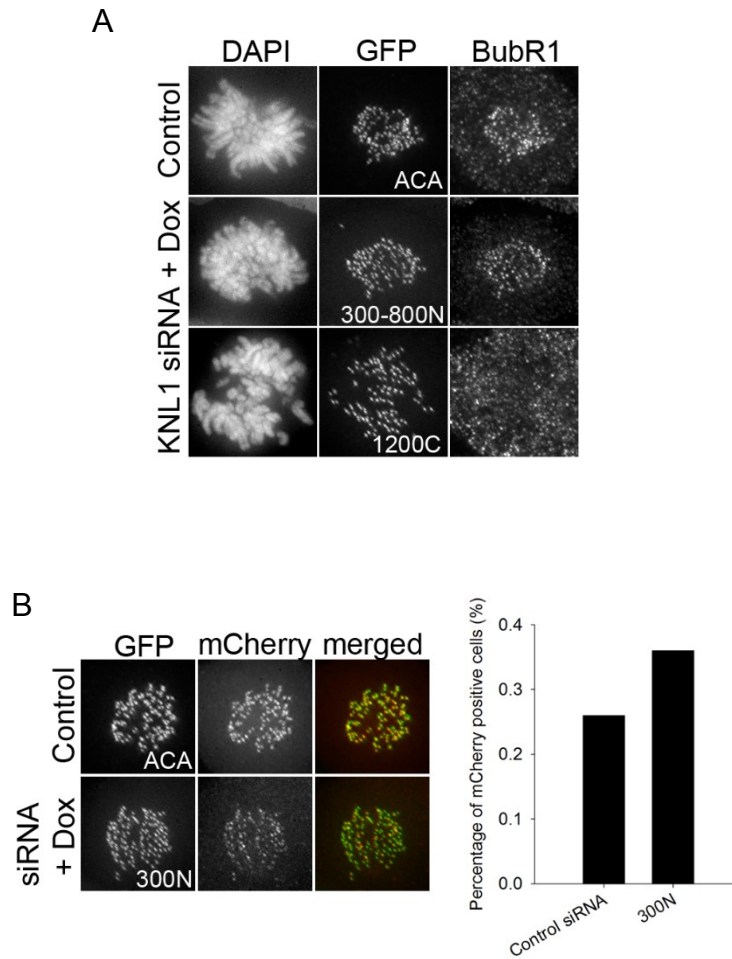


Figure 3.2. KNL1-mediated localization pattern of BubR1. (A-B) Flp-In T-REx HeLa cells were depleted of endogenous KNL1, rescued with the indicated GFP-KNL1 fragment upon doxycycline addition and immunostained with an antibody against BubR1 (A), or overexpression of a BubR1-mcherry construct was carried out (B). (A) Representative cells are shown, $n \geq 15$ cells for each condition (B) Percentage of cells with detectable levels of fluorescent BubR1-mcherry were scored as positive; $n \geq 50$ cells.

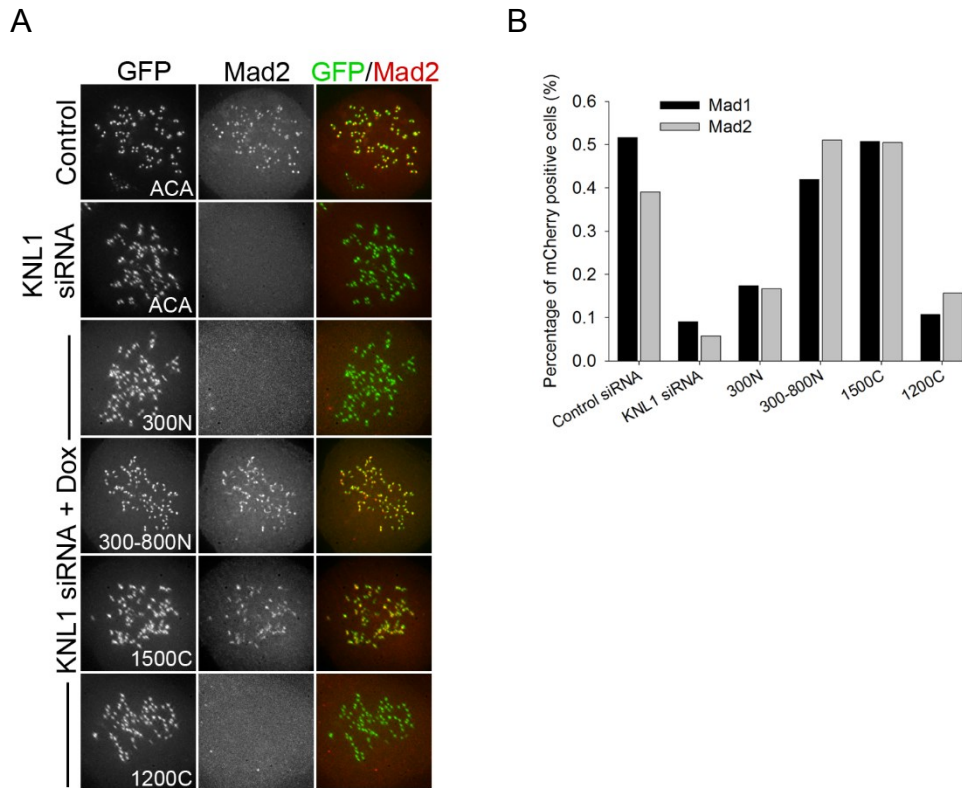


Figure 3.3. KNL1-mediated localization pattern of Mad1 and Mad2. (A-B) Flp-In T-REx HeLa cells were depleted of endogenous KNL1, rescued with the indicated GFP-KNL1 fragment upon doxycycline addition and overexpression of a Mad1-mcherry or Mad2-mcherry construct was carried out. (B) Percentage of cells with detectable levels of fluorescent Mad1-mcherry or Mad2-mcherry were scored as positive; $n \geq 50$ for each construct or condition evaluated.

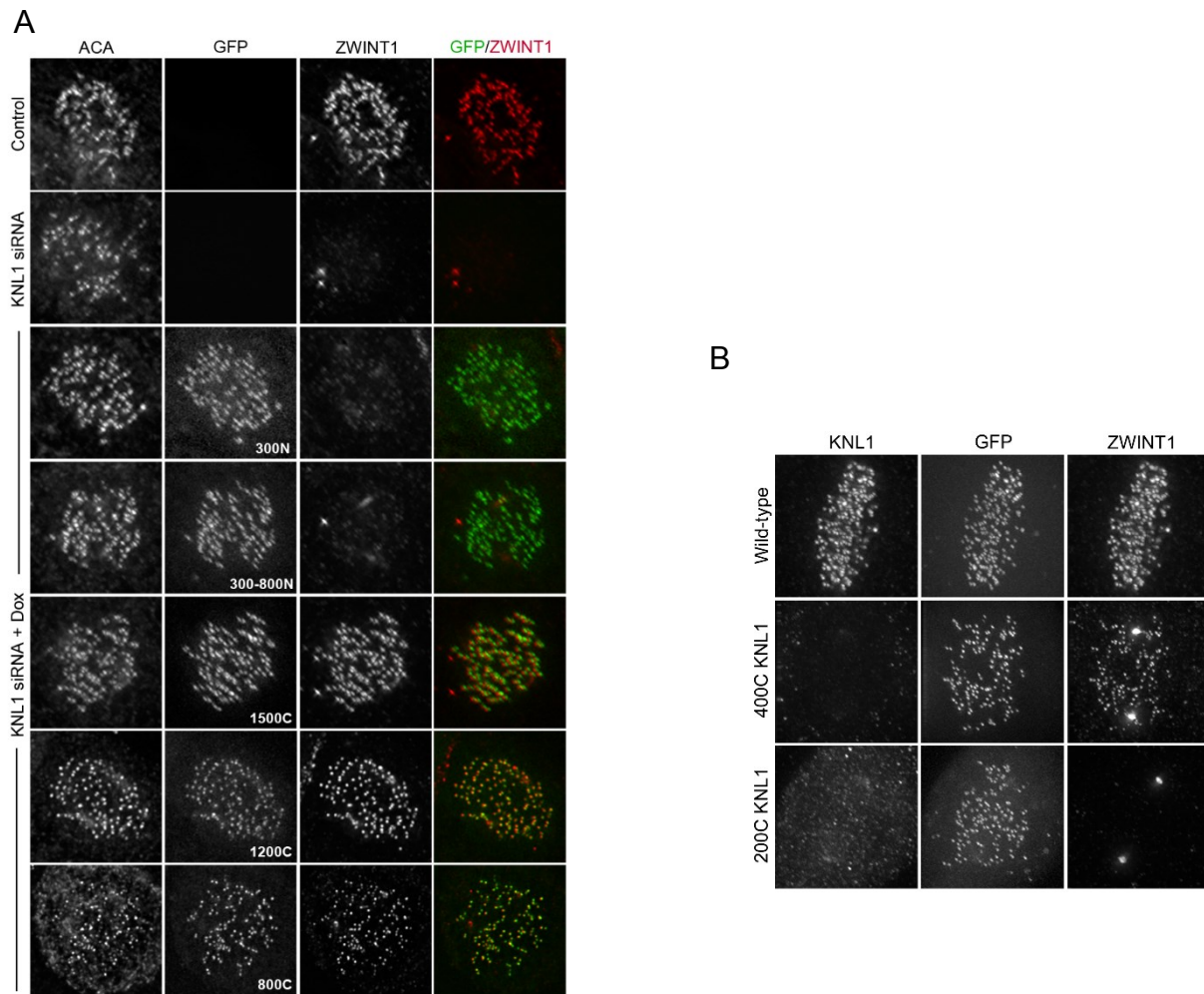


Figure 3.4. KNL1-mediated localization pattern of Zwint1. (A-B) Flp-In T-REx HeLa cells were depleted of endogenous KNL1, rescued with the indicated GFP-KNL1 fragment upon doxycycline (A), or by transient overexpression (B) and immunostained with an antibody against Zwint1. (B) 400C indicates amino acids 1834-2316 of hKNL1; 200C indicates amino acids 2016-2316 of hKNL1. (A,B) Representative cells are shown, $n \geq 15$ cells for each condition

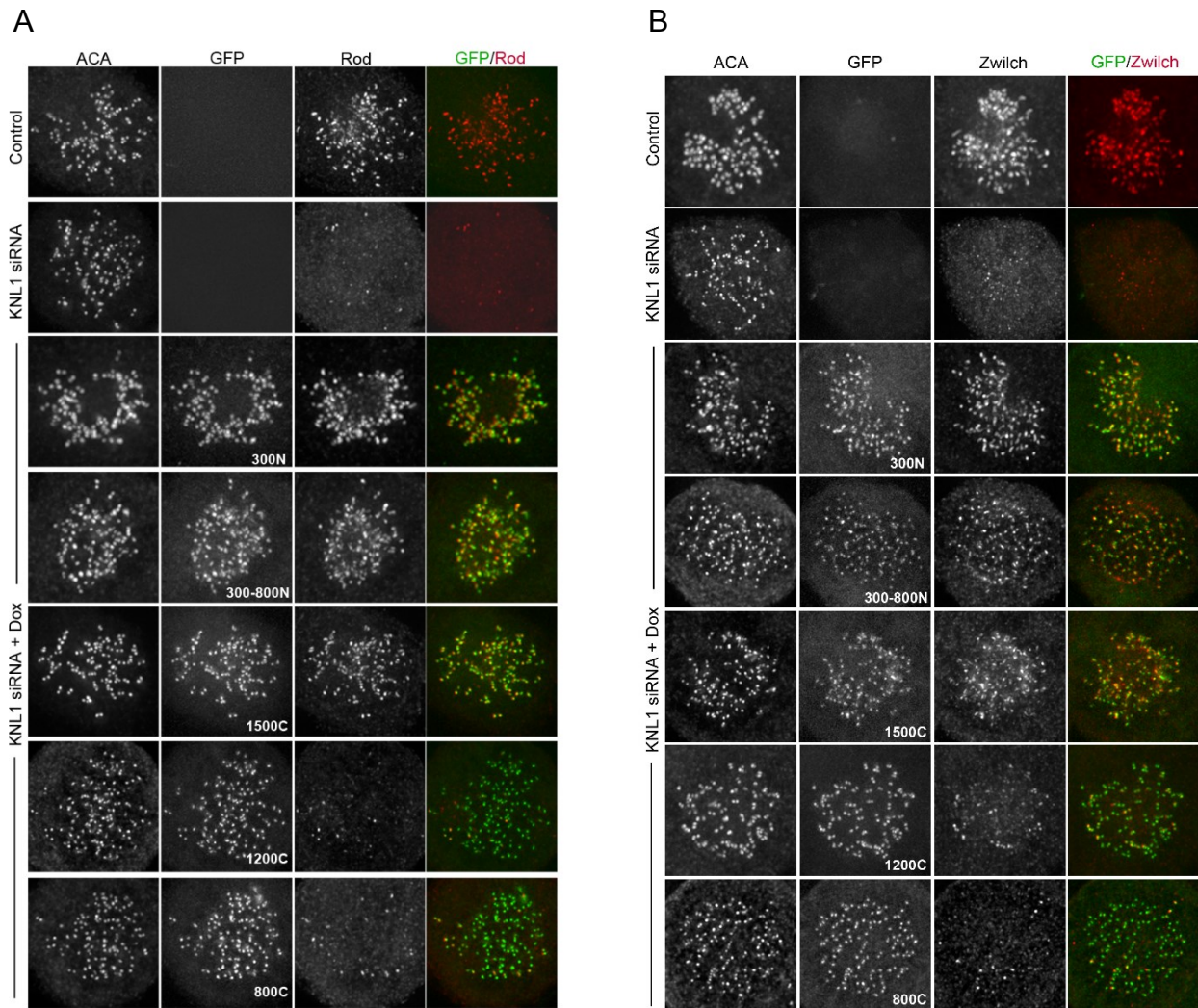


Figure 3.5. KNL1-mediated localization pattern of RZZ components. (A-B) Flp-In T-REx HeLa cells were depleted of endogenous KNL1, rescued with the indicated GFP-KNL1 fragment upon doxycycline addition and immunostained with the indicated antibody; Rod (A); Zwilch (B). (A,B) Representative cells are shown, $n \geq 15$ cells for each condition

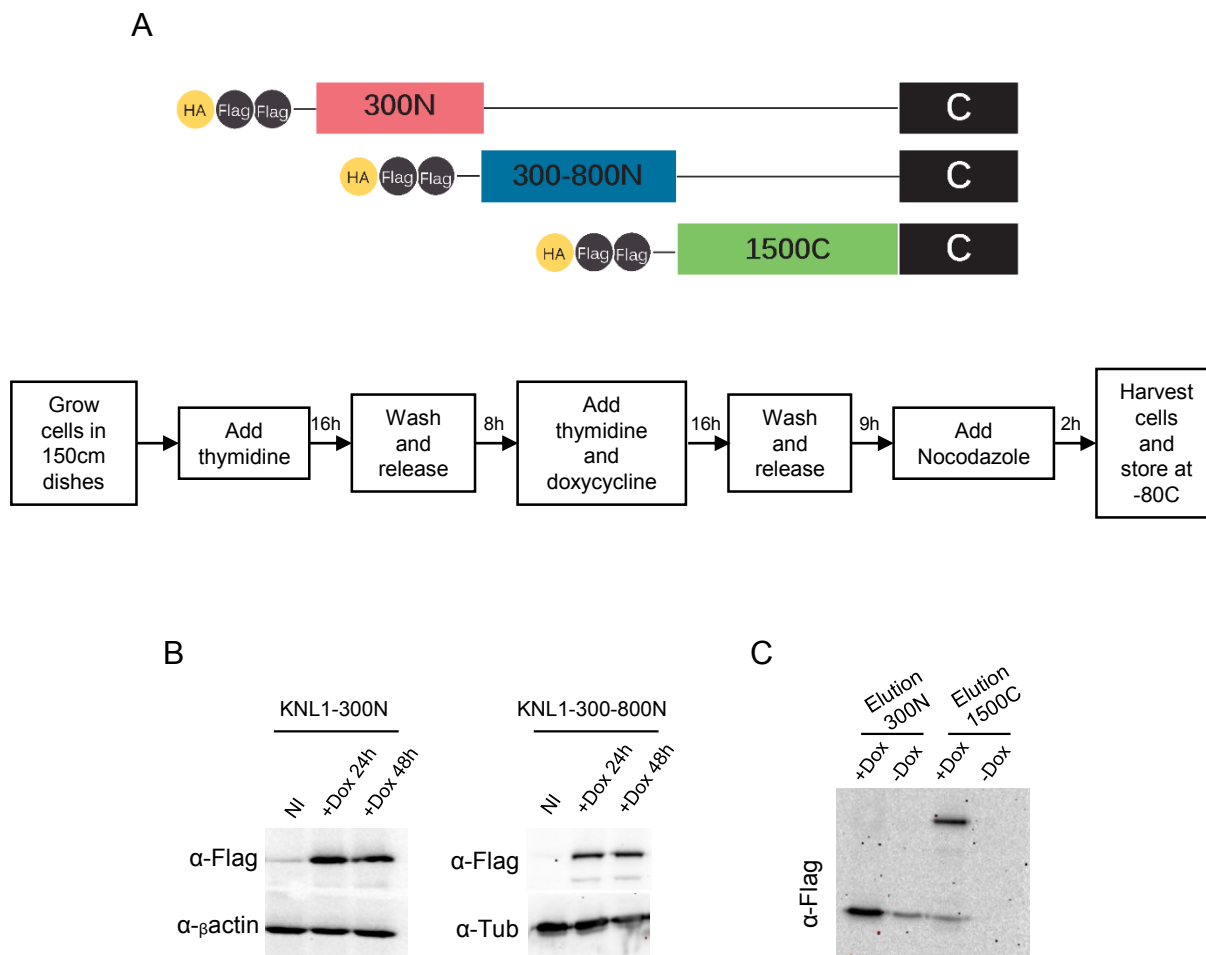


Figure 3.6. Flag-tagged KNL1 fragments used for proteomics analysis. (A) (upper) Schematic of the Flp-In T-REx 293T stable cell lines used for proteomics; (lower) protocol followed for collection of cell pellets for proteomics. (B) KNL1 expression of Flp-In T-REx 293T cells stably expressing Flag-tagged KNL1 fragments were analyzed by Western blotting; cells were not induced (NI), induced with doxyxyxline and analyzed after 24h, or after 48h. Tubulin and actin are shown as loading controls. (C) Eluted samples after small scale immunoprecipitations of not induced (-Dox) or induced (+Dox) Flag-tagged KNL1 fragments were analyzed by Western blot.

A

300N KNL1

Peptides between aminoacids 58-246:

```

MDGVSSSEANE ENDNIERPVR RRHSSILKPP RSPLQDLRGG NERVQESNAL RNKKNRS RVS
FADTIKVFQT ESHMKIVRKS EMEETETGEN LLLIQNKKLE DNYCEITGMN TLLSAPIHTQ
MQQKEFSIIE HTRERKHAND QTVIFSDENQ MDLTSSHTVM ITKGLLDNPI SEKSTKIDTT
SFLANLKLLHT EDSSRMKKEVN FSVDQNTSSE NKIDFNDFIK RLKKTGKCSAF PDVDPKENFE
IPIYSKEPNS ASSTHQMHVS LKEDENNSNI TRLFREKDDG MNFTQCHTAN IQTLIPT SSE
TNSRESKGN D ITIYGND FMD LTFNHTLQIL PATGNFSEIE NQTQNAMDV T TGYGTKASGN

```

300-800N KNL1

Peptides between aminoacids 366-799:

```

IPIYSKEPNS ASSTHQMHVS LKEDENNSNI TRLFREKDDG MNFTQCHTAN IQTLIPT SSE
TNSRESKGN D ITIYGND FMD LTFNHTLQIL PATGNFSEIE NQTQNAMDV T TGYGTKASGN
KT VFKSKQNT AFQDLSINSA DKIHITRSHI MGAETHIVSQ TCNODARILA MTPESIYSNP
SIOGCKTVFY SSSNDAMEMT KCLSNMREEK NLLKHDSNYA KMYCNPDAMS SLTEKTIYSG
EENMDITKSH TVAIDNQIFK QDQSNVQIAA APTPEKEMML QNLMTTSE DG KMNVN CN SVP
HVSKEIQQS LSNPLSISLT DRKTELLSGE NMDLTESHTS NLGSQVPLAA YNLAPES TSE
SHS QSKSSSD ECEEITKSRN EPFQRSDIIA KNSLTD TWNK DKDWV LKILP YLDKDS PQA
DCNQEIATSH NIVYCGGVLD KQITNNTVS WEQSLFSTTK PLFSSGQFSM KNHDTAISSH
TVKSVLGGNS KLAEP L R KSL SNPTPDYCHD KMIICSEEEQ NMDLTKSHTV VIGFGPSELQ
ELGKTNLEHT TGQLTTMNRQ IAVKVEKCGK SPIEKSGVLK SNCIMDVLED ESVQKPKFK
EKQNVKIWGR KSVGGPKIDK TIVFSEDDKN DMDITKSYTI EINHRPLLEK RDCHLVPLAG

```

1500C KNL1

Peptides between aminoacids 1432-2090:

```

LLCDKDEEKA NYCPVQNDLA YANDFASEYY LESEGGQPLSA PCPLLEKEEV IQTSTKGQLD
CVITLHKDQD LIKDPRNLLA NQTLVYSSDL GEMTKLNSKR VSFKLPK DQM KVYVDDIYVI
PQPHFSTDQP PLPKKGQSSI NKEEVILSKA GNKSLNIIEN SSAPICENKP KILNSEWFA
AACKKELKEN IQTNTYNTAL DFHSNSDVTK QVIQTHVNAG EAPDPVITSN VPCFHSIKPN
LNNLNGKTGE FLAFQTVHLP PLPEQLLELG NKAHNDMHI V QATEIHNINI ISSNAKDSRD
EENKKS HNGA ETTSLPPKTV FKDKVRRCSL GIFLPRLPNK RNC SVTGIDD LEQIPADTTO
INHLETQPV S SKDSGIGSVA GKLNLSPSQY INEENLPVYP DEINSSDSIN IETE EKALIE
TYQKEI SPYE NKMGKTCNSQ KRTWVQEEED IHKEKKIRKN EIKFSDTTQD REIFDHHTEE
DIDKSANSVL IKNLSRTPSS C S S S L D S I K A DGTSLDFSTY RSSQMESQFL RDTICEESLR
EKLQDGRITI REFFILLQVH ILIQKPRQSN L PGNFTVNTPT PEDLMLSQ YVYRPKIQIY
REDCEARRQK IEELKLSASN QDKLLVDINK NLWEKMRHCS DKELKAFGIY LNKI KSCFTK
MTKVFTTHQ GK VALY GKLVQS AQNEREKLOI KIDEMDKILK KIDNCLTEME TETKNLEDEE
KNNPVEEWD S EMRAAEKLE QLKTEEEELQ RNLLELEVQK EQLAQIDFM QKQRNRTEEL
LDQLSLSEWD VVEVSDDQAV FTFVYDTIQ L TITFEESVVG FPF LDKRYRK IVDVNFQSL L

```

B

	Host	300N	300-800N	1500C
KNL1 (NSAF)	0	0.0115	0.0111	0.0091

Figure 3.7. KNL1 peptides identified by mass spectrometry. (A) the KNL1 peptides identified in each 293T cell line stably expressing KNL1 fragments are shown. (B) Normalized Spectral Abundance Factor (NSAF) for KNL1 in each 293T cell line analyzed is shown.

A

	Host	300N	300-800N	1500C
Hec1	-	+	+	-
Nuf2	-	+	+	-
Spc24	-	+	+	+
Spc25	-	+	+	+
Nsl1	-	+	+	+
Mis12	-	+	+	-
Dsn1	-	+	+	-
PP1	-	+	-	-
Dynein	-	+	+	+
Aurora B	-	-	+	-
INCENP	-	-	+	-
Zwint1	-	-	-	+

B

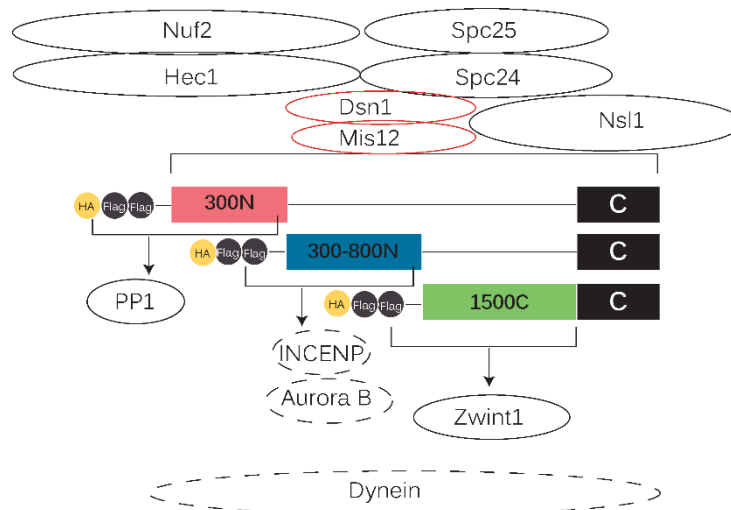


Figure 3.8. Known kinetochore proteins identified by proteomics. (A) Table showing the set of kinetochore and centromeric proteins identified by mass spectrometry on each KNL1 fragment. (B) Schematic showing the KNL1 fragments analyzed by mass spectrometry and the location of the proteins identified.

Table 3.1. New kinetochore proteins identified by proteomics analysis. Table showing the proteins identified by proteomics analysis, not previously reported to be at the kinetochore region or known to be dependent on KNL1 for kinetochore localization.

PROTEIN ID	HOST	300N	300-800N	1500C
Isoform 2 of DnaJ homolog subfamily A member 1 OS=Homo sapiens GN=DNAJA1	-	+	-	-
Isoform 2 of Mitochondrial import inner membrane translocase subunit TIM50 OS=Homo sapiens GN=TIMM50	-	+	-	-
26S proteasome non-ATPase regulatory subunit 2 OS=Homo sapiens GN=PSMD2 PE=2 SV=1	-	+	-	-
Isoform 2 of ATP-dependent RNA helicase DDX3X OS=Homo sapiens GN=DDX3X	-	+	-	-
Insulin receptor substrate 4 OS=Homo sapiens GN=IRS4 PE=1 SV=1	-	+	-	-
Importin subunit beta-1 OS=Homo sapiens GN=KPNB1 PE=1 SV=2	-	+	+	-
Poly [ADP-ribose] polymerase 1 OS=Homo sapiens GN=PARP1 PE=1 SV=4	-	+	+	-
THO complex subunit 4 OS=Homo sapiens GN=ALYREF PE=2 SV=1	-	-	+	-
Proteasome subunit beta type-3 OS=Homo sapiens GN=PSMB3 PE=1 SV=2	-	-	+	-
Isoform 2 of Polyamine-modulated factor 1 OS=Homo sapiens GN=PMF1	-	-	+	-
Isoform A2 of Heterogeneous nuclear ribonucleoproteins A2/B1 OS=Homo sapiens GN=HNRNPA2B1	-	-	+	-
Activated RNA polymerase II transcriptional coactivator p15 OS=Homo sapiens GN=SUB1 PE=1 SV=3	-	-	+	-
ELKS/Rab6-interacting/CAST family member 1 OS=Homo sapiens GN=ERC1 PE=2 SV=1	-	-	-	+

Table 3.2. Unique peptides and sequence coverage of newly identified kinetochore protein. Table showing the number of unique peptides and sequence coverage for proteins identified by proteomics analysis, not previously reported to be at the kinetochore region or known to be dependent on KNL1 for kinetochore localization.

PROTEIN ID	Unique Peptides(Sequence coverage)			
	HOST	300N	300-800N	1500C
Isoform 2 of DnaJ homolog subfamily A member 1 OS=Homo sapiens GN=DNAJA1	-	2(13%)	-	-
Isoform 2 of Mitochondrial import inner membrane translocase subunit TIM50 OS=Homo sapiens GN=TIMM50	-	3(9%)	-	-
26S proteasome non-ATPase regulatory subunit 2 OS=Homo sapiens GN=PSMD2 PE=2 SV=1	-	2(5%)	-	-
Isoform 2 of ATP-dependent RNA helicase DDX3X OS=Homo sapiens GN=DDX3X	-	2(5%)	-	-
Insulin receptor substrate 4 OS=Homo sapiens GN=IRS4 PE=1 SV=1	-	11(14%)	-	-
Importin subunit beta-1 OS=Homo sapiens GN=KPNB1 PE=1 SV=2	-	2(4%)	2(3%)	-
Poly [ADP-ribose] polymerase 1 OS=Homo sapiens GN=PARP1 PE=1 SV=4	-	-	13(20%)	-
THO complex subunit 4 OS=Homo sapiens GN=ALYREF PE=2 SV=1	-	-	3(27%)	-
Proteasome subunit beta type-3 OS=Homo sapiens GN=PSMB3 PE=1 SV=2	-	-	2(17%)	-
Isoform 2 of Polyamine-modulated factor 1 OS=Homo sapiens GN=PMF1	-	-	4(34%)	-
Isoform A2 of Heterogeneous nuclear ribonucleoproteins A2/B1 OS=Homo sapiens GN=HNRNPA2B1	-	-	2(9%)	-
Activated RNA polymerase II transcriptional coactivator p15 OS=Homo sapiens GN=SUB1 PE=1 SV=3	-	-	2(19%)	-
ELKS/Rab6-interacting/CAST family member 1 OS=Homo sapiens GN=ERC1 PE=2 SV=1	-	-	-	21(20%)

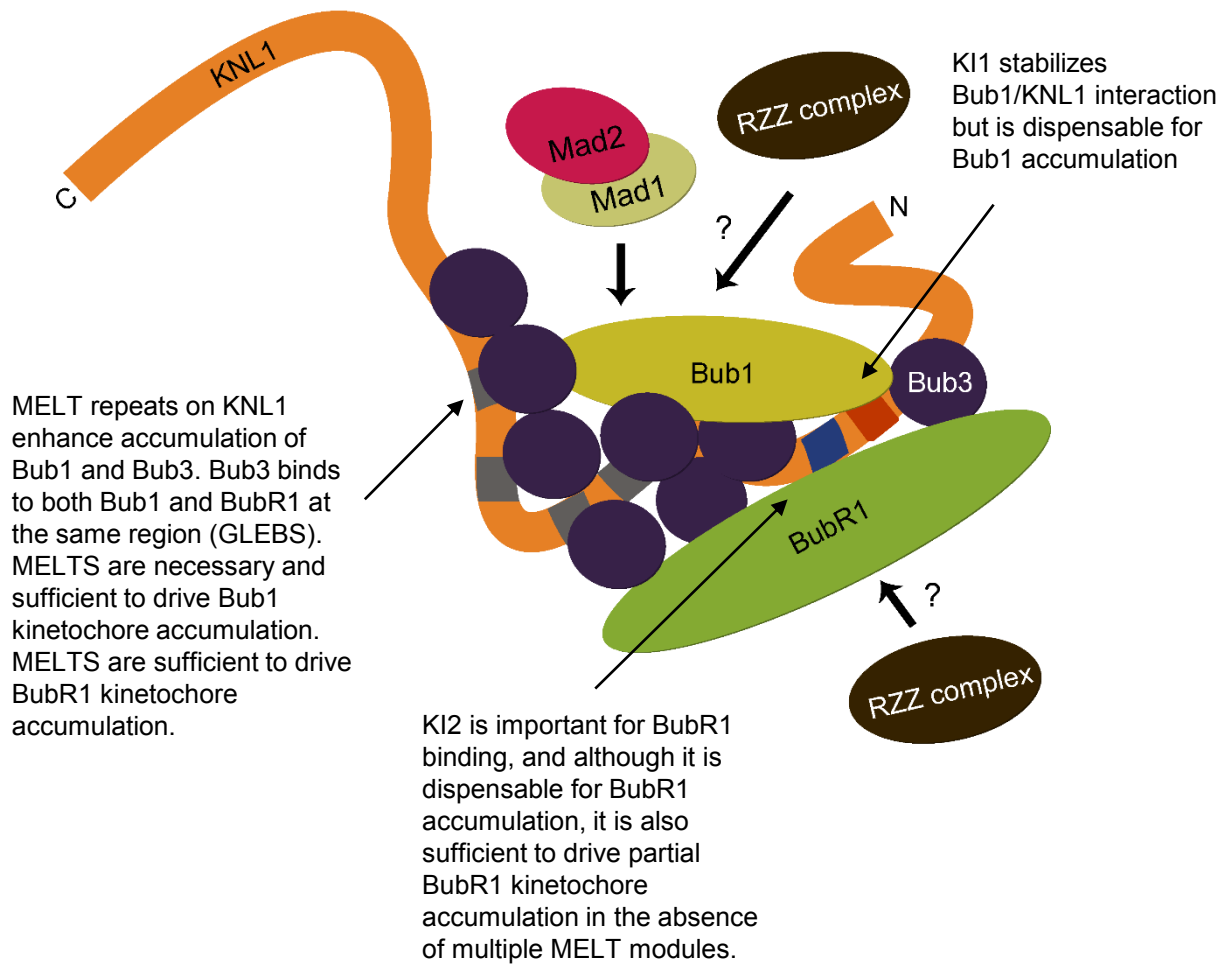


Figure 3.9. Model of KNL1 binding profile at its N-terminal region. Representation of human KNL1 and its known motifs residing at the N-terminus of the protein. KI1 motif, shown in red, interacts with Bub1. KI2 motif, shown in blue, interacts with BubR1. MELT motifs, shown in gray, interact with Bub3/Bub1. Stoichiometry of proteins is not considered in this cartoon for simplicity.

REFERENCES

1. Hori T, Fukagawa T (2012) Establishment of the vertebrate kinetochores. *Chromosome Res* 20:547-61.
2. Przewloka MR, Glover DM (2009) The kinetochore and the centromere: a working long distance relationship. *Annu Rev Genet* 43:439-65.
3. Santaguida S, Musacchio A (2009) The life and miracles of kinetochores. *EMBO J* 28:2511-31.
4. Kops GJ, Saurin AT, Meraldi P (2010) Finding the middle ground: how kinetochores power chromosome congression. *Cell Mol Life Sci* 67:2145-61.
5. McIntosh JR, Molodtsov MI, Ataullakhanov FI (2012) Biophysics of mitosis. *Q Rev Biophys* 45:147-207.
6. Walczak CE, Heald R (2008) Mechanisms of mitotic spindle assembly and function. *Int Rev Cytol* 265:111-58.
7. Jia L, Kim S, Yu H (2013) Tracking spindle checkpoint signals from kinetochores to APC/C. *Trends Biochem. Sci.* 38:302–311.
8. Lara-Gonzalez P, Westhorpe FG, Taylor SS (2012) The spindle assembly checkpoint. *Curr Biol* 22:R966-80.
9. Musacchio A (2012) Spindle assembly checkpoint: the third decade. *Philos Trans R Soc Lond B Biol Sci* 366:3595-604.
10. Cheeseman IM, Niessen S, Anderson S, Hyndman F, Yates JR 3rd, Oegema K, Desai A (2004) A conserved protein network controls assembly of the outer kinetochore and its ability to sustain tension. *Genes Dev* 18:2255–2268.
11. Cheeseman IM, Hori T, Fukagawa T, Desai A (2008) KNL1 and the CENP-H/I/K complex coordinately direct kinetochore assembly in vertebrates. *Mol Biol Cell* 19:587–594.
12. Kiyomitsu T, Obuse C, Yanagida M (2007) Human Blinkin/AF15q14 is required for chromosome alignment and the mitotic checkpoint through direct interaction with Bub1 and BubR1. *Dev Cell* 13:663–676.
13. Kiyomitsu T, Murakami H, Yanagida M (2011) Protein interaction domain mapping of human kinetochore protein Blinkin reveals a consensus motif for binding of spindle assembly checkpoint proteins Bub1 and BubR1. *Mol Cell Biol* 31:998–1011.
14. Kerres A, Vietmeier-Decker C, Ortiz J, Karig I, Beuter C, Hegemann J, Lechner J, Fleig U (2004) The fission yeast kinetochore component Spc7 associates with the EB1 family member Mal3 and is required for kinetochore-spindle association. *Mol Biol Cell.* 15:5255-67.
15. Nekrasov VS, Smith MA, Peak-Chew S, Kilmartin JV (2003) Interactions between centromere complexes in *Saccharomyces cerevisiae*. *Mol Biol Cell.* 14:4931-46.
16. Przewloka MR, Zhang W, Costa P, Archambault V, D'Avino PP, Lilley KS, Laue ED, McAinsh AD, Glover DM (2007) Molecular Analysis of Core Kinetochore Composition and Assembly in *Drosophila melanogaster*. *PLoS ONE* 2:e478.
17. Schittenhelm RB, Chaleckis R, Lehner CF (2009) Intrakinetochore localization and essential functional domains of *Drosophila* Spc105. *EMBO J* 28:2374-86.

18. Petrovic A, Mosalaganti S, Keller J, Mattiuzzo M, Overlack K, Krenn V, De Antoni A, Wohlgemuth S, Cecatiello V, Pasqualato S, Raunser S, Musacchio A. (2014) Modular Assembly of RWD Domains on the Mis12 Complex Underlies Outer Kinetochore Organization. *Mol Cell* 53:591-605.
19. Petrovic A, Pasqualato S, Dube P, Krenn V, Santaguida S, Cittaro D, Monzani S, Massimiliano L, Keller J, Tarricone A, Maiolica A, Stark H, Musacchio A (2010) The MIS12 complex is a protein interaction hub for outer kinetochore assembly. *J Cell Biol* 190:835–852.
20. Liu D, Vleugel M, Backer CB, Hori T, Fukagawa T, Cheeseman IM, Lampson MA (2010) Regulated targeting of protein phosphatase 1 to the outer kinetochore by KNL1 opposes Aurora B kinase. *J Cell Biol* 188:809–820.
21. Bolanos-Garcia VM, Lischetti T, Matak-Vinković D, Cota E, Simpson PJ, Chirgadze DY, Spring DR, Robinson CV, Nilsson J, Blundell TL (2011) Structure of a Blinkin-BUBR1 complex reveals an interaction crucial for kinetochore-mitotic checkpoint regulation via an unanticipated binding Site. *Structure* 19:1691-700.
22. Krenn V, Wehenkel A, Li X, Santaguida S, Musacchio A (2012) Structural analysis reveals features of the spindle checkpoint kinase Bub1-kinetochore subunit Knl1 interaction. *J Cell Biol* 196:451–467.
23. London N, Ceto S, Ranish JA, Biggins S (2012) Phosphoregulation of Spc105 by Mps1 and PP1 regulates Bub1 localization to kinetochores. *Curr Biol* 22:900–906.
24. Primorac I, Weir JR, Chiroli E, Gross F, Hoffmann I, van Gerwen S, Ciliberto A, Musacchio A (2013) Bub3 reads phosphorylated MELT repeats to promote spindle assembly checkpoint signaling. *Elife* 2:e01030.
25. Shepperd LA, Meadows JC, Sochaj AM, Lancaster TC, Zou J, Buttrick GJ, Rappsilber J, Hardwick KG, Millar JBA (2012) Phosphodependent recruitment of Bub1 and Bub3 to Spc7/KNL1 by Mph1 kinase maintains the spindle checkpoint. *Curr Biol* 22:891–899.
26. Yamagishi Y, Yang CH, Tanno Y, Watanabe Y (2012) MPS1/Mph1 phosphorylates the kinetochore protein KNL1/Spc7 to recruit SAC components. *Nat Cell Biol* 14:746-52.
27. Vleugel M, Hoogendoorn E, Snel B, Kops GJ (2012) Evolution and function of the mitotic checkpoint. *Dev Cell* 23:239-50.
28. Cheeseman IM, Chappie JS, DAWilson-Kubalek EM (2006) The conserved KMN network constitutes the core microtubule binding site of the kinetochore. *Cell* 127:983–997.
29. Espeut J, Cheerambathur DK, Krenning L, Oegema K, Desai A (2012) Microtubule binding by KNL-1 contributes to spindle checkpoint silencing at the kinetochore. *J Cell Biol* 196:469-82.
30. DeLuca JG, Musacchio A (2012) Structural organization of the kinetochore-microtubule interface. *Curr Opin Cell Biol* 24:48-56.
31. Tooley J, Stukenberg PT (2011) The Ndc80 complex: integrating the kinetochore's many movements. *Chromosome Res* 19:377-91.
32. Varma D, Salmon ED (2012) The KMN protein network--chief conductors of the kinetochore orchestra. *J Cell Sci* 125:5927-36.
33. McAinsh AD, Meraldi P (2011) The CCAN complex: Linking centromere specification to control of kinetochore–microtubule dynamics. *Semin Cell Dev Biol*. 22:946-52.
34. Alushin GM, Ramey VH, Pasqualato S, Ball DA, Grigorieff N, Musacchio A, Nogales E (2010) The Ndc80 kinetochore complex forms oligomeric arrays along microtubules. *Nature* 467:805-10.

35. Ciferri C, Pasqualato S, Screpanti E, Varetto G, Santaguida S, Dos Reis G, Maiolica A, Polka J, De Luca JG, De Wulf P, Salek M, Rappsilber J, Moores CA, Salmon ED, Musacchio A (2008) Implications for kinetochore-microtubule attachment from the structure of an engineered Ndc80 complex. *Cell* 133:427-39.
36. DeLuca J, Gall W, Ciferri C, Cimini D, Musacchio A, Salmon E (2006) Kinetochore microtubule dynamics and attachment stability are regulated by Hec1. *Cell* 127:969–982.
37. Powers AF, Franck AD, Gestaut DR, Cooper J, Graczyk B, Wei RR, Wordeman L, Davis TN, Asbury CL (2009) The Ndc80 kinetochore complex forms load-bearing attachments to dynamic microtubule tips via biased diffusion. *Cell* 136:865-75.
38. Kline SL, Cheeseman IM, Hori T, Fukagawa T, Desai A (2006) The human Mis12 complex is required for kinetochore assembly and proper chromosome segregation. *J Cell Biol* 173:9-17.
39. Pagliuca C, Draviam VM, Marco E, Sorger PK, De Wulf P (2009) Roles for the Conserved Spc105p/Kre28p Complex in Kinetochore-Microtubule Binding and the Spindle Assembly Checkpoint. *PLoS ONE* 4:e7640.
40. Desai A, Rybina S, Müller-Reichert T, Shevchenko A, Shevchenko A, Hyman A, Oegema K (2003) KNL-1 directs assembly of the microtubule-binding interface of the kinetochore in *C. elegans*. *Genes Dev* 17:2421-35.
41. Gassmann R, Holland AJ, Varma D, Wan X, Civril F, Cleveland DW, Oegema K, Salmon ED, Desai A (2010) Removal of Spindly from microtubule-attached kinetochores controls spindle checkpoint silencing in human cells. *Genes Dev* 24:957–971.
42. Varma D, Wan X, Cheerambathur D, Gassmann R, Suzuki A, Lawrimore J, Desai A, Salmon ED (2013) Spindle assembly checkpoint proteins are positioned close to core microtubule attachment sites at kinetochores. *J Cell Biol* 202:735-46.
43. Johnson VL, Scott MIF, Holt SV, Hussein D, Taylor SS (2004) Bub1 is required for kinetochore localization of BubR1, Cenp-E, Cenp-F and Mad2, and chromosome congression. *J Cell Sci* 117:1577–1589.
44. Caldas, GV, DeLuca, KF, DeLuca, JG (2013) KNL1 facilitates phosphorylation of outer kinetochore proteins by promoting aurora b kinase activity. *J Cell Biol* 203:957-969
45. Gascoigne KE, Takeuchi K, Suzuki A, Hori T, Fukagawa T, Cheeseman IM (2011) Induced ectopic kinetochore assembly bypasses the requirement for CENP-A nucleosomes. *Cell* 145:410-22.
46. Kerres A, Jakopec V, Fleig U (2007) The conserved Spc7 protein is required for spindle integrity and links kinetochore complexes in fission yeast. *Mol. Biol. Cell.* 18:2441–2454.
47. Musacchio A, Salmon ED (2007) The spindle-assembly checkpoint in space and time. *Nat Rev Mol Cell Biol* 8:379–393.
48. Taylor SS, Ha E, McKeon F (1998) The human homologue of Bub3 is required for kinetochore localization of Bub1 and a Mad3/Bub1-related protein kinase. *J Cell Biol* 142:1–11.
49. Klebig C, Korinth D, Meraldi P (2009) Bub1 regulates chromosome segregation in a kinetochore-independent manner. *J Cell Biol* 185:841–858.
50. Rischitor PE, May KM, Hardwick KG (2007) Bub1 is a fission yeast kinetochore scaffold protein, and is sufficient to recruit other spindle checkpoint proteins to ectopic sites on chromosomes. *PLoS One.* 2:e1342.
51. Sharp-Baker H, Chen RH (2001) Spindle checkpoint protein Bub1 is required for kinetochore localization of Mad1, Mad2, Bub3, and CENP-E, independently of its kinase activity. *J Cell Biol.* 153:1239-50.

52. Karess R (2005) Rod-Zw10-Zwilch: a key player in the spindle checkpoint. *Trends Cell Biol.* 15:386-92.
53. Vanoosthuysse V, Valsdottir R, Javerzat JP, Hardwick KG (2004) Kinetochore targeting of fission yeast Mad and Bub proteins is essential for spindle checkpoint function but not for all chromosome segregation roles of Bub1p. *Mol Cell Biol* 24:9786-801.
54. Kops GJ, Shah JV (2012) Connecting up and clearing out: how kinetochore attachment silences the spindle assembly checkpoint. *Chromosoma* 121:509-25.
55. Chen RH, Waters JC, Salmon ED, Murray AW (1996) Association of spindle assembly checkpoint component X MAD2 with unattached kinetochores. *Science* 274:242–246.
56. De Antoni A, Pearson CG, Cimini D, Canman JC, Sala V, Nezi L, Mapelli M, Sironi L, Faretta M, Salmon ED, Musacchio A (2005) The Mad1/Mad2 complex as a template for Mad2 activation in the spindle assembly checkpoint. *Curr Biol* 15:214-25.
57. Kulukian A, Han J, Cleveland D (2009) Unattached kinetochores catalyze production of an anaphase inhibitor that requires a Mad2 template to prime Cdc20 for BubR1 binding. *Dev Cell* 16:105–117.
58. Luo X, Tang Z, Xia G, Wassmann K, Matsumoto T, Rizo J, Yu H (2004) The Mad2 spindle checkpoint protein has two distinct natively folded states. *Nat Struct Mol Biol* 11:338–345.
59. Nezi L, Rancati G, De Antoni A, Pasqualato S, Piatti S, Musacchio A. (2006) Accumulation of Mad2-Cdc20 complex during spindle checkpoint activation requires binding of open and closed conformers of Mad2 in *Saccharomyces cerevisiae*. *J Cell Biol* 174:39–51.
60. Lesage B, Qian J, Bollen M (2011) Spindle checkpoint silencing: PP1 tips the balance. *Curr Biol* 21:R898-903.
61. Foley EA, Maldonado M, Kapoor TM (2011) Formation of stable attachments between kinetochores and microtubules depends on the B56-PP2A phosphatase. *Nat Cell Biol* 13:1265–1271.
62. Suijkerbuijk SJ, Vleugel M, Teixeira A, Kops GJ (2012) Integration of kinase and phosphatase activities by BUBR1 ensures formation of stable kinetochore-microtubule attachments. *Dev Cell* 23:745-55.
63. Meadows JC, Shepperd LA, Vanoosthuysse V, Lancaster TC, Sochaj AM, Buttrick GJ, Hardwick KG, Millar JBA (2011) Spindle checkpoint silencing requires association of PP1 to both Spc7 and kinesin-8 motors. *Dev Cell* 20:739–750.
64. Pinsky BA, Nelson CR, Biggins S (2009) Protein phosphatase 1 regulates exit from the spindle checkpoint in budding yeast. *Curr Biol* 19:1182–1187.
65. Rosenberg JS, Cross FR, Funabiki H (2011) KNL1/Spc105 recruits PP1 to silence the spindle assembly checkpoint. *Curr Biol* 21:942–947.
66. Vanoosthuysse V, Hardwick KG (2009) A novel protein phosphatase 1-dependent spindle checkpoint silencing mechanism. *Curr Biol* 19:1176–1181.
67. Lodish H et al., (1995) *Molecular Cell Biology*, 3rd ed., copyright 1995, W.H. Freeman and Company, reprinted with permission. Figure 23-38, p. 1094.
68. Maiato, H, Deluca, J, Salmon, ED, Earnshaw, WC (2004) The dynamic kinetochore-microtubule interface. *Journal of Cell Science* 117:5461–5477.
69. Welburn JPI, Vleugel M, Liu D, Yates JR, Lampson MA, Fukagawa T, Cheeseman IM (2010) Aurora B phosphorylates spatially distinct targets to differentially regulate the kinetochore-microtubule interface. *Mol Cell* 38:383–392.

70. Biggins S, Severin FF, Bhalla N, Sassoon I, Hyman AA, Murray AW (1999) The conserved protein kinase Ipl1 regulates microtubule binding to kinetochores in budding yeast. *Genes Dev* 13:532–544.
71. Tanaka TU, Rachidi N, Janke C, Pereira G, Galova M, Schiebel E, Stark MJ, Nasmyth K (2002) Evidence that the Ipl1-Sli15 (Aurora kinase-INCENP) complex promotes chromosome bi-orientation by altering kinetochore-spindle pole connections. *Cell* 108:317–329.
72. Cimini D, Wan X, Hirel CB, Salmon ED (2006) Aurora kinase promotes turnover of kinetochore microtubules to reduce chromosome segregation errors. *Curr Biol* 16:1711-1718.
73. DeLuca KF, Lens SM, DeLuca JG (2011) Temporal changes in Hec1 phosphorylation control kinetochore-microtubule attachment stability during mitosis. *J Cell Sci* 124:622-634.
74. Liu D, Vader G, Vromans MJ, Lampson MA, Lens SM (2009) Sensing chromosome bi-orientation by spatial separation of aurora B kinase from kinetochore substrates. *Science* 323:1350–1353.
75. Wang E, Ballister ER, Lampson MA (2011) Aurora B dynamics at centromeres create a diffusion-based phosphorylation gradient. *J Cell Biol* 194:539–549.
76. Lipkow K, Odde DJ (2008). Model for Protein Concentration Gradients in the Cytoplasm. *Cell Mol Bioeng* 1:84-92.
77. Kruse T, Zhang G, Larsen MS, Lischetti T, Streicher W, Kragh NT, Bjørn SP, Nilsson J (2013) Direct binding between BubR1 and B56-PP2A phosphatase complexes regulate mitotic progression. *J Cell Sci* 1:1086-1092.
78. Lampson MA, Kapoor TM (2005) The human mitotic checkpoint protein BubR1 regulates chromosome-spindle attachments. *Nat Cell Biol* 7:93-98.
79. Posch M, Khoudoli GA, Swift S, King EM, DeLuca JG, Swedlow JR (2010) Sds22 regulates Aurora B activity and microtubule–kinetochore interactions at mitosis. *J Cell Biol* 191:61–74.
80. Yasui Y, Urano T, Kawajiri A, Nagata K, Tatsuka M, Saya H, Furukawa K, Takahashi T, Izawa I, Inagaki M (2004) Autophosphorylation of a newly identified site of Aurora-B is indispensable for cytokinesis. *J Biol Chem* 279:12997-13003.
81. Petsalaki E, Akoumianaki T, Black EJ, Gillespie DA, Zachos G (2011) Phosphorylation at serine 331 is required for Aurora B activation. *J Cell Biol* 195:449–466.
82. Crosio C, Fimia GM, Loury R, Kimura M, Okano Y, Zhou H, Sen S, Allis CD, Sassone-Corsi P (2002) Mitotic phosphorylation of histone H3: spatio-temporal regulation by mammalian Aurora kinases. *Mol Cell Biol* 22:874-885.
83. Rieder CL (1981). The structure of the cold-stable kinetochore fiber in metaphase PtK1 cells. *Chromosoma* 84:145-158.
84. Stevens D, Gassmann R, Oegema K, Desai A (2011) Uncoordinated Loss of Chromatid cohesion is a common outcome of extended metaphase arrest. *PLoS ONE* 6:e22969.
85. Ricke RM, Jeganathan KB, van Deursen JM (2011) Bub1 overexpression induces aneuploidy and tumor formation through Aurora B kinase hyperactivation. *J Cell Biol* 193: 1049–1064.
86. Ricke RM, Jeganathan KB, Malureanu L, Harrison AM, van Deursen JM (2012) Bub1 kinase activity drives error correction and mitotic checkpoint control but not tumor suppression. *J Cell Biol* 199:931-949.
87. Kawashima SA, Yamagishi Y, Honda T, Ishiguro K, Watanabe Y (2010) Phosphorylation of H2A by Bub1 prevents chromosomal instability through localizing shugoshin. *Science* 327:172-177.
88. Tsukahara T, Tanno Y, Watanabe Y (2010) Phosphorylation of the CPC by Cdk1 promotes chromosome bi-orientation. *Nature* 467:719-723.

89. Yamagishi Y, Honda T, Tanno Y, Watanabe TY (2010) Two histone marks establish the inner centromere and chromosome bi-orientation. *Science* 330:239–243.
90. Yue Z, Carvalho A, Xu Z, Yuan X, Cardinale S, Ribeiro S, Lai F, Ogawa H, Gudmundsdottir E, Gassmann R, Morrison CG, Ruchaud S, Earnshaw WC (2008) Deconstructing Survivin: comprehensive genetic analysis of Survivin function by conditional knockout in a vertebrate cell line. *J Cell Biol* 183:279–296.
91. Campbell CS, Desai A (2013) Tension sensing by Aurora B kinase is independent of survivin-based centromere localization. *Nature* 497:118-121.
92. Hoffman DB, Pearson CG, Yen TJ, Howell BJ, Salmon ED (2001) Microtubule-dependent changes in assembly of microtubule motor proteins and mitotic spindle checkpoint proteins at PtK1 kinetochores. *Mol Biol Cell* 12:1995–2009.
93. Stumpff J, von Dassow G, Wagenbach M, Asbury C, Wordeman L (2008) The kinesin-8 motor Kif18A suppresses kinetochore movements to control mitotic chromosome alignment. *Dev Cell* 14:252–262.
94. Honda RK, Nigg EA (2003) Exploring the functional interactions between B. Aurora, INCENP, and survivin in mitosis. *Mol Biol Cell* 14:3325-3341.
95. Caldas GV, DeLuca JG (2013) KNL1: Bringing order to the kinetochore. *Chromosoma*, Epub ahead of print.
96. Dyson HJ, Wright PE (2005) Intrinsically unstructured proteins and their functions. *Nat Rev Mol Cell Biol* 6:197-208.
97. Vleugel M, Tromer E, Omerzu M, Groenewold V, Nijenhuis W, Snel B, Kops GJ (2013) Arrayed BUB recruitment modules in the kinetochore scaffold KNL1 promote accurate chromosome segregation. *J Cell Biol* 203:943-55.
98. Zhang G, Lischetti T, Nilsson J (2014) A minimal number of MELT repeats supports all the functions of KNL1 in chromosome segregation. *J Cell Sci* 127:871-84.
99. Krenn V, Overlack K, Primorac I, van Gerwen S, Musacchio A (2014) KI motifs of human Knl1 enhance assembly of comprehensive spindle checkpoint complexes around MELT repeats. *Curr Biol* 24:29-39.
100. London N, Biggins S (2014) Mad1 kinetochore recruitment by Mps1-mediated phosphorylation of Bub1 signals the spindle checkpoint. *Genes Dev* 28:140-52
101. Howell BJ, McEwen BF, Canman JC, Hoffman DB, Farrar EM, Rieder CL, Salmon ED (2001) Cytoplasmic dynein/dynactin drives kinetochore protein transport to the spindle poles and has a role in mitotic spindle checkpoint inactivation. *J Cell Biol* 155:1159-72.
102. Basto R, Scaerou F, Mische S, Wojcik E, Lefebvre C, Gomes R, Hays T, Karess R (2004) In vivo dynamics of the rough deal checkpoint protein during *Drosophila* mitosis. *Curr Biol* 14:56-61.
103. Buffin E, Lefebvre C, Huang J, Gagou ME, Karess RE (2005) Recruitment of Mad2 to the kinetochore requires the Rod/Zw10 complex. *Curr Biol* 15:856-61.
104. Kops GJ, Kim Y, Weaver BA, Mao Y, McLeod I, Yates JR 3rd, Tagaya M, Cleveland DW (2005) ZW10 links mitotic checkpoint signaling to the structural kinetochore. *J Cell Biol* 169:49-60.
105. Wang H, Hu X, Ding X, Dou Z, Yang Z, Shaw AW, Teng M, Cleveland DW, Goldberg ML, Niu L, Yao X (2004) Human Zwint-1 specifies localization of Zeste White 10 to kinetochores and is essential for mitotic checkpoint signaling. *J Biol Chem* 279:54590-8.
106. Polo SE, Jackson SP (2001) Dynamics of DNA damage response proteins at DNA breaks: a focus on protein modifications. *Genes Dev* 25:409-33.

107. Saxena A, Wong LH, Kalitsis P, Earle E, Shaffer LG, Choo KH (2002) Poly(ADP-ribose) polymerase 2 localizes to mammalian active centromeres and interacts with PARP-1, Cenpa, Cenpb and Bub3, but not Cenpc. *Hum Mol Genet* 11:2319-29.
108. Sakuma T1, Woltjen K (2014) Nuclease-mediated genome editing: At the front-line of functional genomics technology. *Dev Growth Differ.* 56:2-13.
109. Pauwels, K, Podevin N, Breyer D, Carroll D, Herman P (2013) Engineering nucleases for gene targeting: safety and regulatory considerations. *N Biotechnol* 31:18-27.
110. Gaj T, Gersbach CA, Barbas CF 3rd (2013) ZFN, TALEN, and CRISPR/Cas-based methods for genome engineering. *Trends Biotechnol* 31:397-405.
111. Carroll D (2014) Genome Engineering with Targetable Nucleases. *Annu Rev Biochem* [Epub ahead of print].
112. Zhang F, Wen Y, Guo X (2014) CRISPR/Cas9 for genome editing: progress, implications and challenges. *Hum Mol Genet* [Epub ahead of print].
113. Mali P, Yang L, Esvelt KM, Aach J, Guell M, DiCarlo JE, Norville JE, Church GM (2013) RNA-guided human genome engineering via Cas9. *Science* 339:823-6.
114. Mali P, Aach J, Stranges PB, Esvelt KM, Moosburner M, Kosuri S, Yang L, Church GM (2013) CAS9 transcriptional activators for target specificity screening and paired nickases for cooperative genome engineering. *Nat Biotechnol* 31:833-8.
115. Rong Z, Zhu S, Xu Y, Fu X (2014) Homologous recombination in human embryonic stem cells using CRISPR/Cas9 nickase and a long DNA donor template. *Protein Cell* [Epub ahead of print].
116. Xue H, Wu J, Li S, Rao MS, Liu Y (2014) Genetic Modification in Human Pluripotent Stem Cells by Homologous Recombination and CRISPR/Cas9 System. *Methods Mol Biol* [Epub ahead of print].
117. Yang L, Mali P, Kim-Kiselak C, Church G (2014) CRISPR-Cas-Mediated Targeted Genome Editing in Human Cells. *Methods Mol Biol* 1114:245-67.
118. Jinek M, Chylinski K, Fonfara I, Hauer M, Doudna JA, Charpentier E (2012) A programmable dual-RNA-guided DNA endonuclease in adaptive bacterial immunity. *Science* 337:816-21.
119. Jinek M, Jiang F, Taylor DW, Sternberg SH, Kaya E, Ma E, Anders C, Hauer M, Zhou K, Lin S, Kaplan M, Iavarone AT, Charpentier E, Nogales E, Doudna JA (2014) Structures of Cas9 endonucleases reveal RNA-mediated conformational activation. *Science* 343:1247997.
120. Shaner NC, Lambert GG, Chammas A, Ni Y, Cranfill PJ, Baird MA, Sell BR, Allen JR, Day RN, Israelsson M, Davidson MW, Wang J (2013) A bright monomeric green fluorescent protein derived from *Branchiostoma lanceolatum*. *Nat Methods* 10:407-9.
121. Cong L, Ran FA, Cox D, Lin S, Barretto R, Habib N, Hsu PD, Wu X, Jiang W, Marraffini LA, Zhang F (2013) Multiplex genome engineering using CRISPR/Cas systems. *Science* 339:819-23.
122. Mali P, Esvelt KM, Church GM (2013) Cas9 as a versatile tool for engineering biology. *Nat Methods* 10:957-63.

APPENDIX I

THE KNL1 N-TERMINUS DOES NOT RESCUE ALIGNMENT DEFECTS IN KNL1 DEPLETED CELLS

A1.1 Introduction

We recently demonstrated that the N-terminal region of KNL1 is necessary and sufficient for Aurora B-mediated regulation of kinetochore-MT attachments [44]. In addition, we and others confirm that the N-terminal half of KNL1, which contains the MELT and MELT-like repeats, is also sufficient for accumulation of the checkpoint-related proteins Bub1, BubR1, Mad1/Mad2 and RZZ components (see Chapter 3). Since the N-terminal region of KNL1 is able to both mediate activity of the principal error correction mechanism regulator (Aurora B) and mediate accumulation of critical checkpoint components, we asked whether the KNL1 N-terminus was sufficient for correct mitotic progression.

A1.2 Results and Discussion

Depletion of KNL1 causes chromosome misalignment and missegregation in several organisms [95]. We quantified the level of chromosome misalignment in metaphase in cells depleted of endogenous KNL1 and rescued with our set of KNL1 fragments. In agreement with Vleugel et al., depletion of KNL1 caused severe chromosome misalignment (quantified as cells with no discernable metaphase plate or cells with one or more chromosomes off of the metaphase plate), and the C-terminal KNL1 fragments (1200C) were not able to recover

alignment defects [97] (Figure A1.1A). In contrast, KNL1 fragments containing several MELT motifs (300-800N) partially restored alignment defects (Figure A1.1A). Also, in agreement with the results reported by Vleugel et al., the 300N fragment (similar to 250N in that study) did not restore alignment defects (Figure A1.1A and A1.1C) [97]. We also quantified alignment defects in cells treated with MG132, a proteasome inhibitor that arrests cells in metaphase. We found that cells expressing MELT-containing KNL1 fragments (300-800N and 1500C) behaved similarly with or without MG132 treatment (Figure A1.1A and A1.1B). However, cells expressing 300N KNL1 exhibited better alignment upon MG132 treatment (Figure A1.1B). A reasonable explanation for this result is that cells expressing 300N KNL1 have the same capacity to align chromosomes as cells expressing 300-800N or 1500C KNL1, but alignment to metaphase in 300N KNL1 cells takes longer. Importantly, our results indicate that despite its ability to recruit checkpoint proteins and mediate Aurora B phospho-regulation, the N-terminal region of KNL1 is not sufficient to fully restore the alignment defects observed upon KNL1 depletion.

We next analyzed timing through mitosis in cells expressing the KNL1 mutants. The time a cell spends in mitosis depends on the time it takes to completely align chromosomes, stabilize MT attachments, and also, on the ability of the checkpoint machinery to prevent mitotic exit while these processes are occurring. For instance, cells with a functional checkpoint machinery but with defective chromosome alignment exhibit a mitotic delay. Similar to the results reported by Vleugel et al. we find that 300N and 1200C cells exhibit a significant delay in mitosis, while 300-800N KNL1 expressing cells had a slight mitosis delay (Figure A1.1D) [97]. Cells expressing 300-800N KNL1 cells exhibit alignment defects, but are able to accumulate checkpoint proteins at high levels, therefore, a slight delay in mitotic progression is not

surprising. Counterintuitively, 300N KNL1 expressing cells, which do not accumulate high levels of checkpoint proteins, exhibit a longer delay in mitosis when compared to 300-800N KNL1 (Figure A1.1D). One possibility is that the checkpoint in these cells is as robust as in 300-800N KNL1 expressing cells, but because cells expressing 300N KNL1 take more time aligning chromosomes [97], the total time through mitosis is longer. Indeed, Vleugel et al. showed that 250N KNL1 supports a checkpoint as efficiently as wild-type KNL1 in the presence of nocodazole and reversine [97]. Interestingly, KNL1-depleted cells and 1200C expressing cells exhibit a significant mitotic delay despite their inability to accumulate checkpoint proteins (Figure A1.1D). Furthermore, KNL1 depleted cells can arrest in mitosis in the presence of different doses of nocodazole for at least 6 hours, indicative of a functioning checkpoint (data not shown) [98]. Only when the cells are challenged with nocodazole and small amounts of reversine, an Mps1 inhibitor, is the checkpoint abrogated in KNL1-depleted cells or cells expressing the KNL1 C-terminus [97]. How cells that are unable to recruit checkpoint proteins at kinetochores can mediate a mitotic arrest for a significant amount of time (~6h) in presence of microtubule poisons is an interesting question that demands further investigation. Perhaps there are alternative mechanisms that trigger a mitotic arrest in presence of disrupted spindles and a defective checkpoint.

A1.3 Methods

Cell culture and transfection

HeLa (ATCC) and FlpIn T-REx HeLa cell lines were cultured in DMEM (Invitrogen), supplemented with 10% FBS and 1% penicillin/streptomycin at 37°C in 5% CO₂. For silence and rescue experiments, stable cell lines were doubly blocked with thymidine, depleted of

endogenous KNL1 using the corresponding siRNAs (described in Caldas et al. 2013), and induced with doxycycline for overexpression (see methods in Chapter 2 and Chapter 3). siRNA transfections were performed using Oligofectamine (Invitrogen), according to the manufacturer's instructions. For chromosome alignment analysis, MG132 was used at 5 μ M for 45min before fixation.

Immunofluorescence and Live cell imaging

Fixation and immunostaining of HeLa cells were performed as described previously [44]. For live cell imaging, HeLa cells in 35-mm glass-bottomed dishes (MatTek Corporation) were transfected with KNL1 siRNA and induced with doxycycline as described above. Cells were imaged in Leibovitz's L-15 media (Invitrogen) supplemented with 10% FBS, 7 mM HEPES, pH 7.0, and 4.5 g/L glucose. Stage temperature was maintained at 37°C with an environmental chamber (Precision Control). Fluorescence images of GFP-KNL1 expressing cells were acquired every 5min for 8-9h.

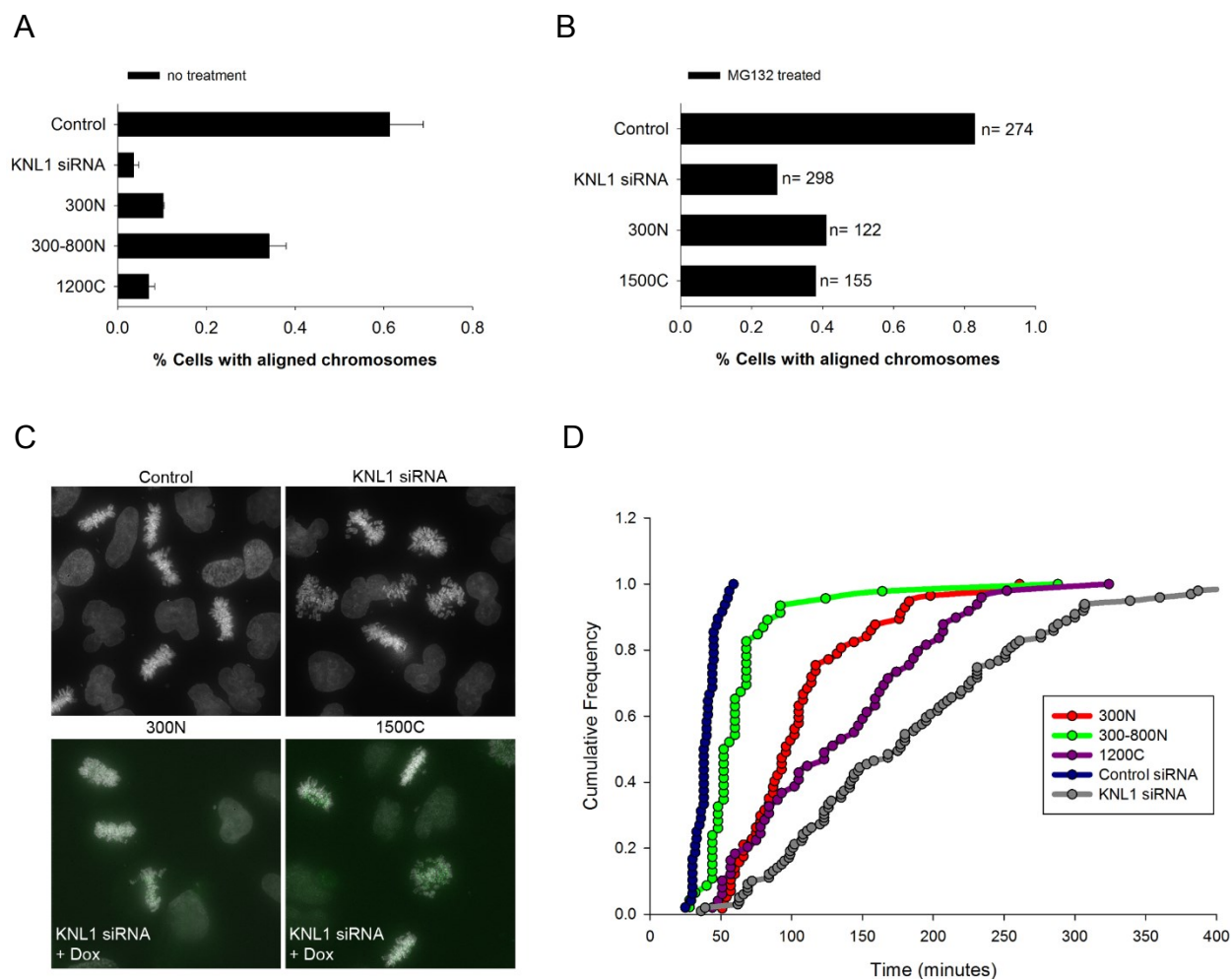


Figure A1.1. Phenotypic analysis of cells containing KNL1 fragments. (A-D) Flp-In T-REx HeLa cells were depleted of endogenous KNL1, rescued with the indicated GFP-KNL1 fragment upon doxycycline addition, and analyzed for chromosome alignment (A); chromosome alignment after MG132 treatment (B,C); or analyzed by live cell imaging (D). (A) Error bar represent standard deviation between experiments; n=3 independent experiments; n \geq 50 cells scored per experiment. (C) representative images of metaphase chromosomes in the indicated conditions. (D) Cumulative frequency of timing through mitosis.

APPENDIX II

IMPLEMENTATION OF THE CRISPR SYSTEM FOR EDITING ENDOGENOUS KINETOCHORE GENES

A2.1 Introduction

Understanding the function of a particular gene relies on the ability to manipulate it, silence it, or make changes to specific regions of the gene in order to investigate the defects that such changes may induce in the cell. For this purpose, genome editing tools are ideal, since they allow for penetrant modification of the gene of interest in a cell and its progeny.

Genome editing in mammalian cells was first established in mouse embryonic stem (ES) cells, for which, Capecchi, Evans, and Smithies received the Nobel Prize in 2007. Yet, this technology has been mainly applied to yeast, chicken DT40 cells, and mouse ES cells [108]. Modification of endogenous genes within differentiated human cell types is much less efficient than in the mentioned organisms, however, different technologies that allow higher efficiencies in genome alteration have arisen. For instance, genome editing using engineered nucleases has been demonstrated as a powerful technology that enables manipulation of targeted genes in several organisms as well as in highly proliferative human cell lines [107, 108].

Engineered nucleases permit random or designed genomic modification at precise loci through the stimulation of endogenous double-strand break (DSB) repair [107, 108]. Following targeted DNA DSB, cellular DNA repair mechanisms including non-homologous end-joining (NHEJ) and the homology-directed repair (HDR) are activated. NHEJ is an error-prone repair

mechanism that results in insertions and/or deletions (indels) at the target site [110]. HDR on the other hand, uses a homologous segment of DNA as a template to repair the damaged DNA and therefore, it is assumed to be error free [110]. Thus, when an engineered nuclease that creates a DSB in the gene of interest, and a donor DNA containing left and right homology arms flanking the breaking site, are introduced into the cell, homologous recombination-mediated modifications to the target gene can be achieved.

To date, there are three main types of customizable nuclease-based gene editing systems, zinc-finger nucleases (ZFNs), transcription activator-like effector nucleases (TALENs), and clustered regularly interspaced short palindromic repeats (CRISPR). They all differ in the machinery that guides the binding of the nuclease to a specific DNA sequence. ZFN and TALENs are composed of sequence-specific DNA binding domains fused to a nonspecific DNA cleavage module [108-110]. The nuclease used in the CRISPR system on the other hand, is guided by a molecule of RNA [110]. Compared with TALENs and ZFN, the CRISPR system offers a simpler means of achieving specificity (a guide RNA rather than a DNA-binding protein domain that requires complex engineering), but also demonstrates equal or greater cleavage efficiency [111].

The most widely used method for studying gene function to date is RNA interference (RNAi). RNAi functions by delivery of short RNA molecules complementary to the messenger RNA (mRNA) produced by the target gene, resulting in its destruction. Despite its remarkable utility, RNAi does not provide the means to obtain absolute silencing of a gene. Furthermore, when evaluation of mutations within a gene is the goal, RNAi must be combined with overexpression of DNA containing the desired mutations, which results in fluctuating expression conditions when compared with the endogenous gene. Newer genome editing methodologies are

allowing investigators to modify endogenous genes in a relatively easy manner. Clearly, these technologies will be the mainstay for evaluation of gene function in the near future. The CRISPR system in particular, is an efficient and reliable approach that at the same time offers ease of design and cheap costs [112]. Despite being a very recent technology, the CRISPR system has gained prominence during the last year [112]. More importantly, recent reports have demonstrated efficient editing of the human genome using CRISPR [113-117]. As an alternative approach to RNAi methodology, we decided to implement the use of CRISPR technology in the lab for analysis of genes involved in kinetochore function. As a proof of principle, I will fluorescently tag the endogenous kinetochore Hec1 gene in the non-cancer Retinal Pigment Epithelial cell line RPE1. Here, I describe the experimental design rationale and discuss the factors to be considered during the course of these experiments. The establishment of this technology in the lab will allow for knock-out and knock-in of genes in the cell lines commonly used for our analysis of kinetochore function.

A2.2 CRISPR: Overview

The Clustered Regularly Interspaced Short Palindromic Repeats (CRISPR) system was first discovered in bacteria as a defense mechanism against foreign DNA, either viral or plasmid [112]. So far, three distinct bacterial CRISPR systems have been identified, termed type I, II and III. The Type II system is the basis for the current genome engineering technology available and is often simply referred to as CRISPR.

The bacterial CRISPR locus contains the RNA-guided nuclease Cas9, Cas proteins involved in the generation of “spacer” sequences (fragments of the viral or invading DNA), a region of repeats and spacers from which a pre-crRNA is transcribed, and a tracrRNA important

for processing of the crRNA-Cas9 complex that directs the double strand break on the target DNA (Figure A2.1) [112, 113]. Upon invasion, the Cas complex cleaves the foreign DNA generating spacers that are integrated in the CRISPR locus. Each spacer is localized between repeats present in the CRISPR locus. This region (sequence of repeat/spacer/repeat) is then transcribed, generating a long pre-crRNA. The pre-crRNA is recognized by the tracrRNA, Cas9 and RNase III, resulting in cleavage within each spacer and generating mature crRNAs that remain associated with Cas9 and the tracrRNA. Since this crRNA-tracrRNA-Cas9 complex contains a portion of the foreign DNA or spacer, and Cas9 has nuclease activity, the complex is able to recognize a new molecule of the foreign DNA and induce cleavage in a selective manner (Figure A2.1) [112, 113]. Recently, it was demonstrated that a crRNA-tracrRNA fusion (gRNA) together with Cas9 are functional *in vivo* (Figure A2.2) [113, 118, 119]. Importantly, Cas9 only mediates cleavage of the target if a protospacer adjacent motif (PAM) is present in the immediate 3' region of the target (Figure A2.2). For the *S. thermophilus* system, Cas9 cuts 3bp upstream of the protospacer [113, 118]. By using this CRISPR minimal system, different labs have been able to modify the genome of several organisms with relatively high efficiency [112]. Specifically, the Cas9 protein together with the gRNA containing the target region (spacer in the bacterial system), are ectopically expressed in cells to generate a DSB in the desired region. If a donor plasmid is also provided, homologous recombination is induced. Below, I describe the detailed procedure for CRISPR-mediated tagging of endogenous Hec1 in RPE1 cells.

A2.3 Experimental Design

Here, I aim to introduce the codifying region of the fluorescent protein Neon green [120] at the C-terminus of the last exon of the Hec1 gene in the genome of the mammalian cell line

RPE-1. For this purpose I will introduce a DNA DSB in the last exon of Hec1 (the potential break site depends on the bioinformatics analysis for search of the guide RNA in this region). This break will be achieved by transfecting cells with a bicistronic vector that expresses codon-humanized Cas9 nuclease, together with a Hec1-specific crRNA-tracrRNA chimera (guideRNA) [121]. In parallel, I will introduce a donor plasmid to serve as a template to repair the induced DSB. I designed two different donor plasmids, one aimed to introduce Neon green (pNeon-Hec1), and another one aimed to introduce Neon green and a Puromycin cassette (pNeon-Hec1 Puro) containing flanking LoxP sites for removal after selection. Cells expressing Neon green upon transfection with pNeon-Hec1 will be selected by Fluorescence Activated Cell-Sorting (FACS), while cells expressing Neon green upon transfection with pNeon-Hec1 Puro will be selected by their resistance to treatment with Puromycin. Recent studies have demonstrated that a version of the dimeric nuclease Cas9, in which one of its nuclease domains is mutated and rendered inactive, is able to produce a single-strand DNA break (nick) [114, 122]. This nickase Cas9 has been reported as an alternative for genome editing with less off-target effects than a wild-type Cas9 [114, 122]. Thus, I will use both wild-type Cas9 and nickase Cas9, in parallel experiments, to compare efficiency and resulting phenotypes possibly caused by off-target effects. Table A.2.1 summarizes the four experiments described.

A2.4 Experimental procedure

1. Genomic sequence analysis:

1.1. Go to the webpage <http://genome.ucsc.edu/> and go to Genome Browser.

1.2. Type the name of your gene of interest. An assembly map will appear, containing the different transcript variants for this gene.

- 1.3. Click on the correct transcript variant for the gene. For example, make sure that the variant you choose contains the right number of exons and it gives the right size of the protein. A description for the gene and transcript variant will appear.
- 1.4. At the bottom of the description of the gene you will find a box with links to tools and databases. Click on the option “Genomic sequence”. A window called “Get Genomic Sequence Near Gene” will appear.
- 1.5. Choose to retrieve 1000 bp upstream and downstream, UTR in lower case, and the sequence in FASTA mode.
- 1.6. Paste the retrieved sequence in a DNA sequence analyzer. For all analysis shown in this document, I used Geneious v5.0.4.
- 1.7. In Genome browser, go back to the description page for the gene and copy the RefSeq summary number. This is the annotation number in GeneBank (NCBI).
- 1.8. Go to NCBI and search for the RefSeq number. You will have the mRNA sequence of your gene, with the annotations for all exons. Transfer this information to your sequence analyzer software. Alternatively, identify the exons and introns only in the region in which you want to modify your endogenous gene. For example, I want to introduce the fluorescence protein Neon Green at the C-terminus of the last Exon of Hec1, therefore, I need to be familiar with all the features around that region, introns, exons, 3’UTR, and polyadenylation region, if possible.
- 1.9. With both sequences, the one obtained from NCBI and the one from Genome Browser UCSC, you now have the sequence for your entire gene and 1000bp upstream and downstream of your gene. In addition, you know all the features of your gene required to

design your donor plasmid and your guide RNA plasmid. See Figure A2.3 as an example of the architecture of the CASC5 gene (KNL1 protein).

2. guideRNA design and cloning:

- 2.1. Go to the webpage <http://crispr.mit.edu/> and paste 250nt DNA sequence of the region of your gene in which you aim to induce the DSB or nick and submit your query.
- 2.2. In the results webpage, look for the guide RNA sequence with highest score (listed as guide RNA #1) and copy the information related to this guide RNA in an excel document. Make sure you save the list of potential off-target sites for this guide RNA for future reference.
- 2.3. Go to your sequence analyzer, find this sequence and make its annotation in your genomic sequence. Importantly, the guide RNA sequence found here contains the PAM sequence (last 3 nucleotides), but the PAM sequence is NOT cloned into the Cas9-gRNA chimera vector (Figure A2.4).
- 2.4. Design the oligos (primers) for cloning of the guide RNA (without PAM sequence) into the vectors pX330 and pX335 (Figure A2.4). Specifically, oligo 1: 5'-CAACG-(19-25N)-3' and oligo 2: 5'-AAAC-(19-25N)-C-3' (Figure A2.4). The guide RNA needs to initiate with a G (bold base in oligo sequence) in order to be transcribed by the U6 promoter. If your guide RNA does not start with a G, this G base can be added.
- 2.5. The cloning protocol for the guide RNA (gRNA) into pX330 and pX335 can found here: http://www.addgene.org/static/cms/files/CRISPR_cloning_protocol.pdf. Briefly:
 - a) Digest 1-2ug of pX330/pX335 with BbsI for 30min at 37C
 - b) Gel purify digested pX330/pX335
 - c) Phosphorylate and anneal oligos 1 and 2:

1uL oligo 1 (100uM)

1ul oligo 2 (100uM)

1ul 10X T4 ligation buffer (NEB)

6.5ul ddH₂O

0.5ul T4 PNK (NEB)

In a thermocycler: 37C for 30min/95C for 5min/down to 25C at 5C/min.

- d) Ligate phosphorylated and annealed oligo-duplex with pX330/pX335 using quick ligase (NEB). Use 1:250 dilutions of oligo-duplex.
- e) Treat ligation reaction with PlasmidSafe exonuclease.
- f) Transform ligation in *E coli*, miniprep and sequence.

3. Donor plasmid (homologous repair template) design and cloning

Cloning of the donor plasmid can be performed in several ways, including regular cloning. Based on information found on the Bob Goldstein lab webpage (<http://wormcas9hr.weebly.com/uploads/1/0/6/5/10652065/cloning.pdf>), Gibson assembly PCR is the easiest approach for cloning of these large constructs. The cloning protocol described here is based on the Gibson assembly system (New England Biolabs).

3.1. Design primers to amplify around 1500-2000bp downstream and upstream of the gRNA (Figure A2.5A).

3.2. Amplify the genomic fragment with primers designed in 3.1. Gel purify the amplified genomic PCR and use it as a template to amplify the different cassettes required for Gibson assembly (Figure A2.5B-D).

- a) In order to carry out the Gibson assembly approach, the primers need to be designed in a way that they overlap at least 30bp (Figure A2.6). In addition, I designed the forward primer amplifying the left homology arm and the reverse primer amplifying the right homology arm, containing “tails” for in-fusion cloning (Clontech), a ligation independent cloning system.
- 3.3. Carry out PCR to obtain the different fragments required for assembly (Figure A2.5D), gel purify them, and carry out Gibson Assembly. Specifically:
 - a) Mix ~200-300ng of each PCR product. If the fragment is <200bp use ~500ng.
 - b) Combine the PCR fragment mix with 2X Gibson assembly master mix and incubate at 50C for 60min in a thermocycler.
 - 3.4. Carry out the in-fusion reaction using the product of Gibson assembly reaction with the linearized vector backbone. I digested pEGFP-N1 (clontech) with NdeI and NotI, resulting in a linearized plasmid lacking the GFP coding region and a disrupted CMV promoter.
 - 3.5. Transform the in-fusion reaction in *E coli*, miniprep and sequence.
 - 3.6. Maps of both donor plasmids, pNeon-Hec1 and pNeon-Hec1 Puro are shown in Figures A2.7 and A2.8.

A2.5 Future Experiments

Transfection of RPE1 cells will be carried out using Fugene or nucleofection to compare transfection efficiencies. Also, different amounts and ratios of Hec1 gRNA and Hec1 donor plasmids will be examined. As controls, combinations of empty gRNAs (pX330 and pX335) with Hec1 donor plasmids and Hec1 gRNAs with empty donor plasmids (pNeon) will be used. Targeting efficiency will be evaluated by comparing the percentage of Neon green expressing

cells in experiments carried out with pNeon-Hec1 (without Puromycin selection), or, by the number of foci obtained after Puromycin selection in experiments carried out with pNeon-Hec1 Puro. Selection of individual cells will be carried out by FACS or by single-cell serial dilution.

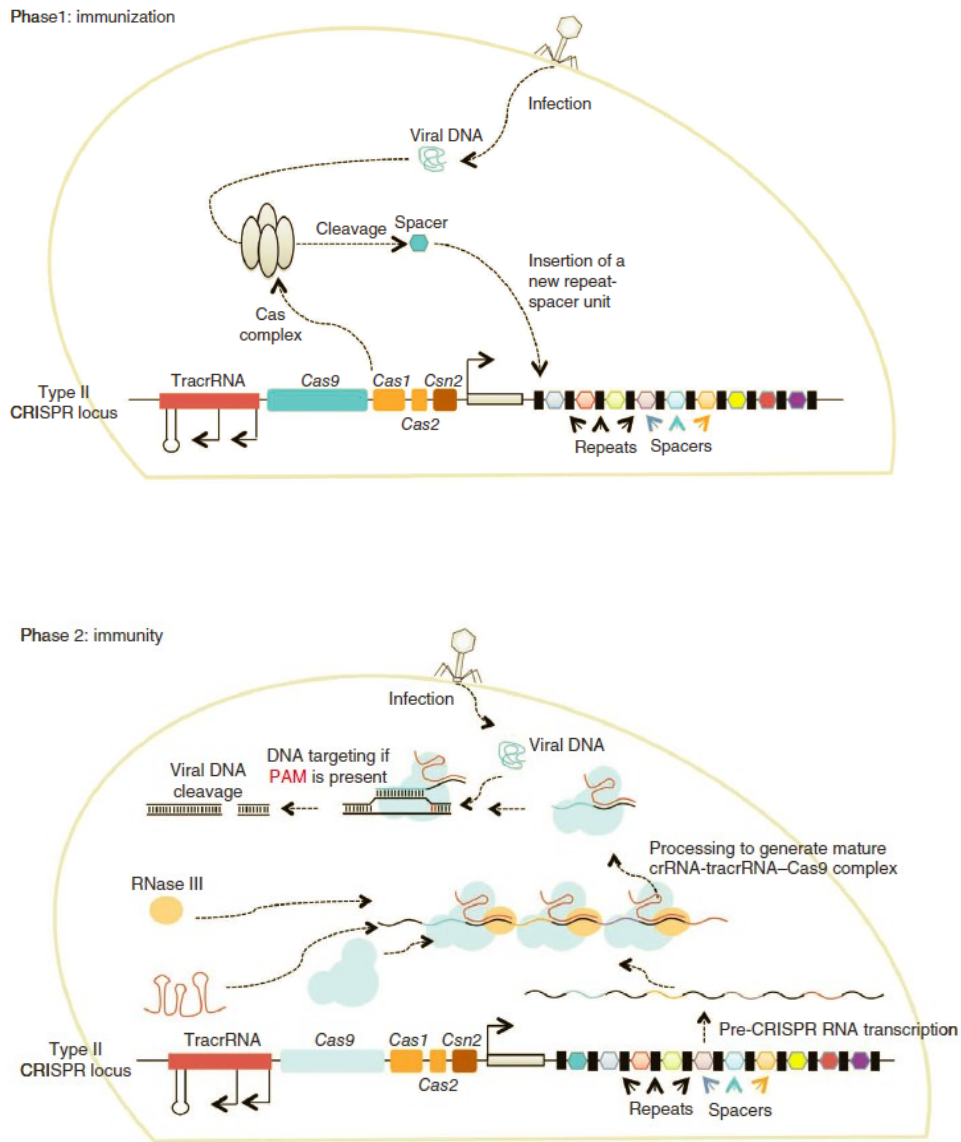


Figure A2.1. Representation of the molecular mechanism of CRISPR in bacterial cells. Adapted from Mali et al. 2013 [122].

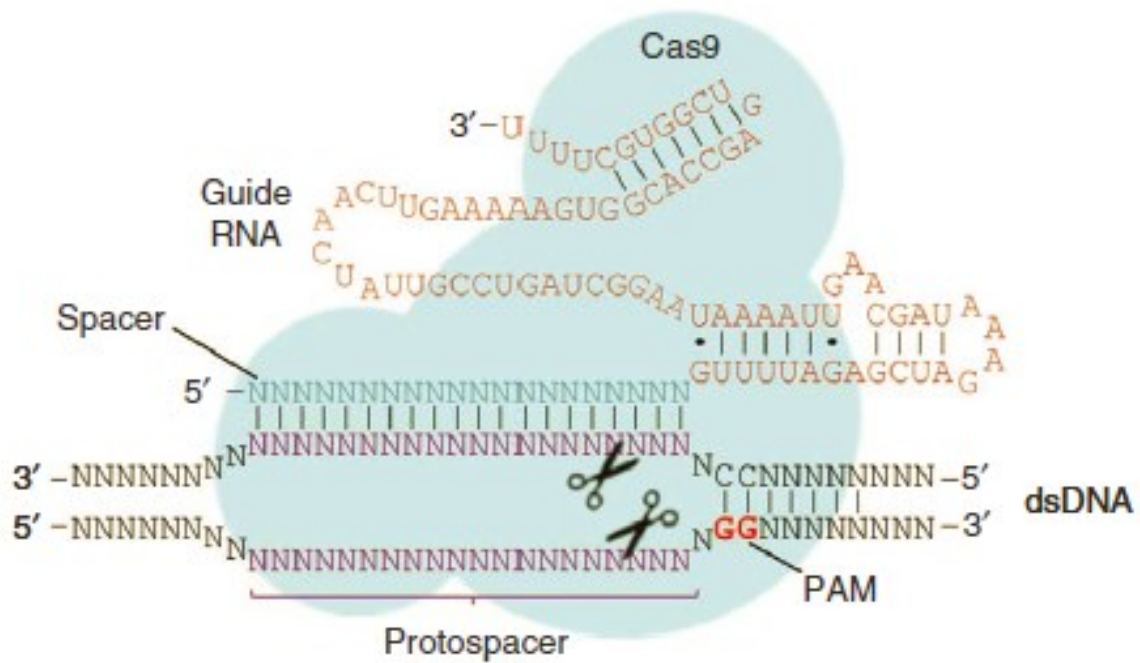


Figure A2.2. Representation of the complex formed between Cas9 nuclease and the chimera *tracRNA-crRNA* (guide RNA), recognizing the protospacer or endogenous DNA sequence and PAM sequence for subsequent cleavage. Adapted from Mali et al. 2013 [122].

Table A2.1. List of experiments designed for CRISPR-mediated fluorescent tagging of endogenous Hec1. The combination of donor plasmid and type of nuclease are indicated. pNeon-Hec1 Puro contains LoxP sites for removal after selection with Cre recombinase.

Donor Plasmid	Nuclease type	Purpose
pNeon-Hec1	Wild type	DSB in last exon of the Hec1 gene for insertion of Neon green fluorescent protein. Selection by FACS.
pNeon-Hec1	Nickase	Single strand break in last exon of the Hec1 gene for insertion of Neon green fluorescent protein. Selection by FACS.
pNeon-Hec1 Puro	Wild type	DSB in last exon of the Hec1 gene for insertion of Neon green fluorescent protein and a Puromycin cassette. Selection by resistance to Puromycin.
pNeon-Hec1 Puro	Nickase	Single strand break in last exon of the Hec1 gene for insertion of Neon green fluorescent protein and a Puromycin cassette. Selection by resistance to Puromycin.

KNL1 gene architecture

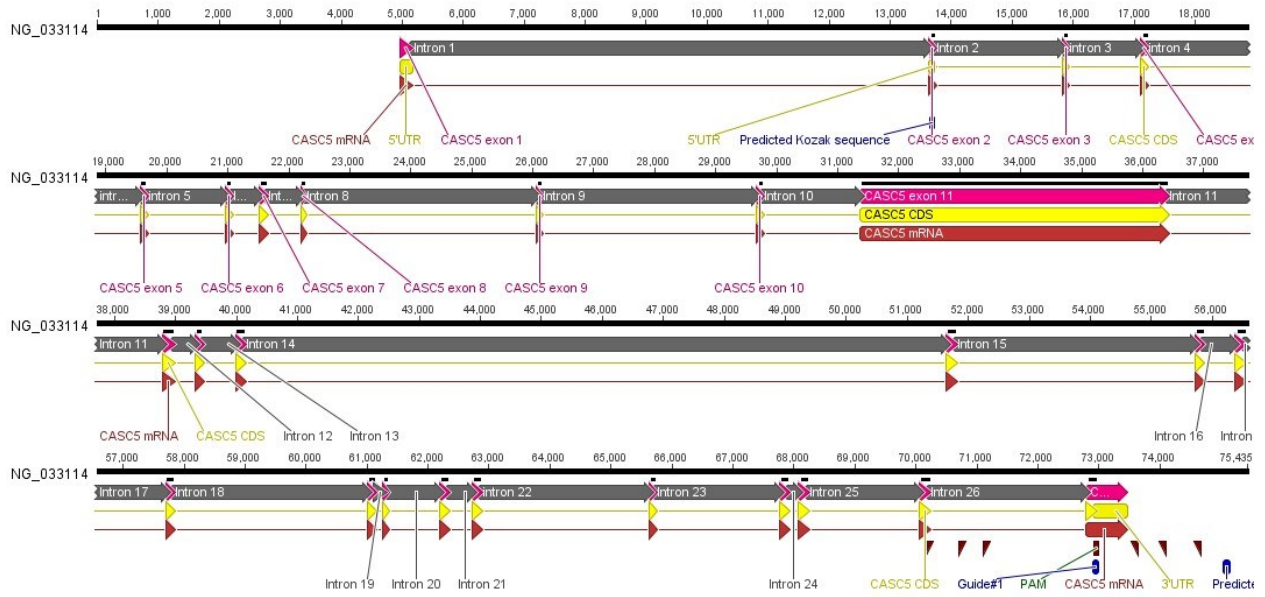


Figure A2.3. Architecture of the human KNL1 gene as an example of an annotated genomic sequence.

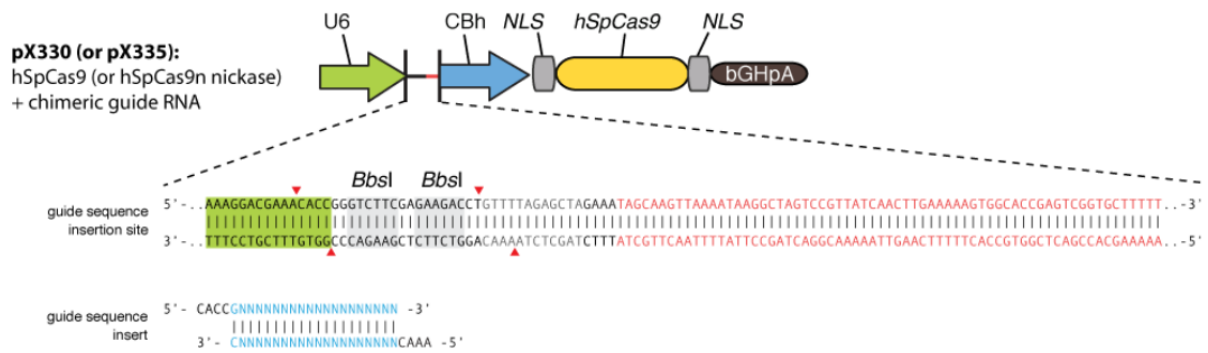


Figure A2.4. Plasmids pX330/pX335 for cloning of guide RNA. Adapted from (http://www.genome-engineering.org/crispr/?page_id=23).

A

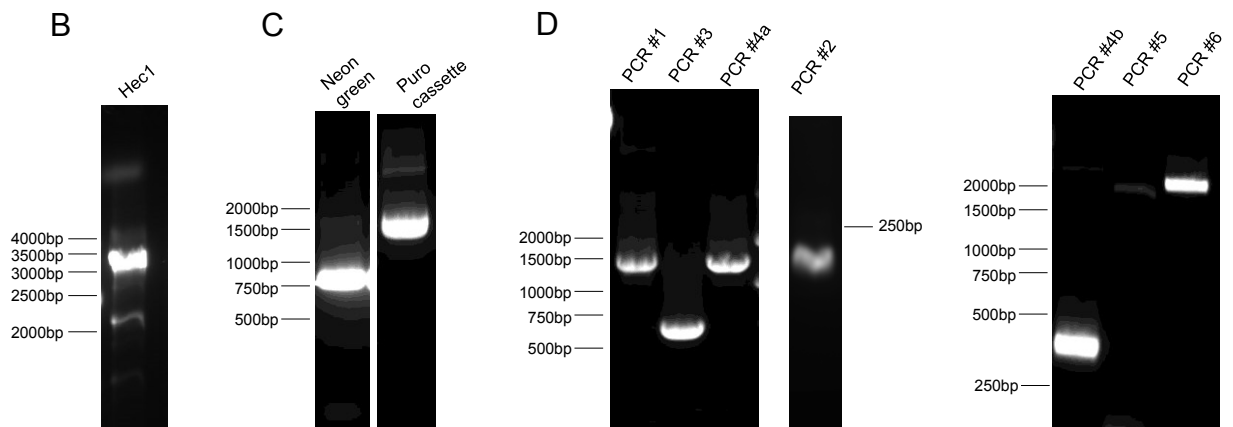
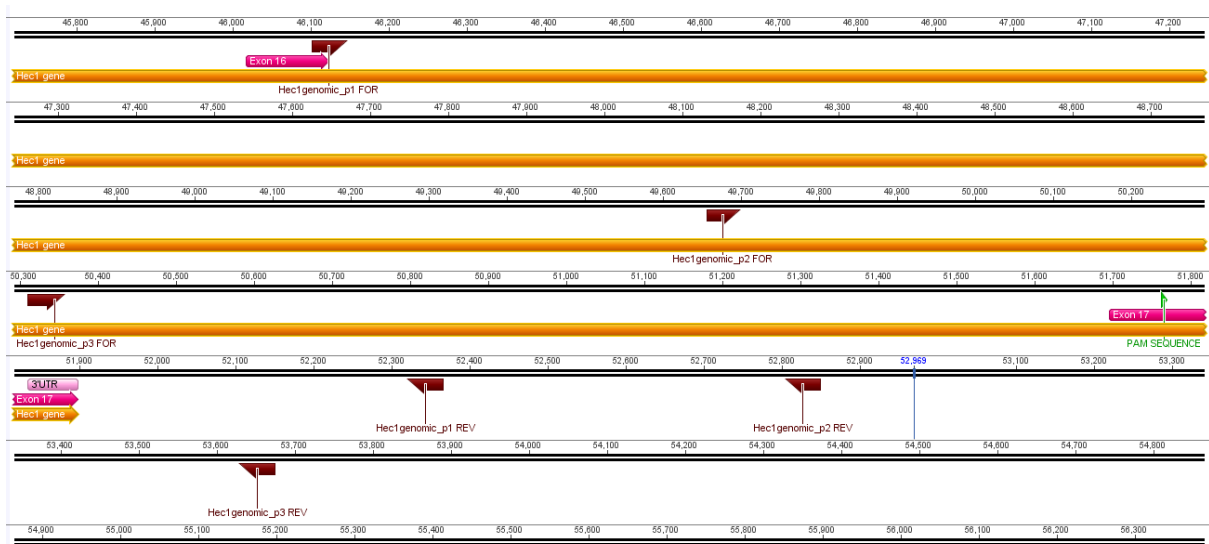


Figure A2.5. PCR fragments for Gibson Assembly cloning. (A) primer design for PCR of genomic Hec1 fragment from RPE-1 genomic DNA. (B) Amplification by PCR of a Hec1 genomic region using primers designed in (A). (C) Amplification by PCR of the Neon green coding region and the Puromycin cassette. (D) PCR fragments for Gibson assembly (see Figure A2.6). PCR fragments 1, 2, 3, and 4a were used for cloning of pNeon Hec1 donor plasmid; PCR fragments 1, 2, 3, 4b, 5, and 6 were used for cloning of pNeon Hec1 Puro.

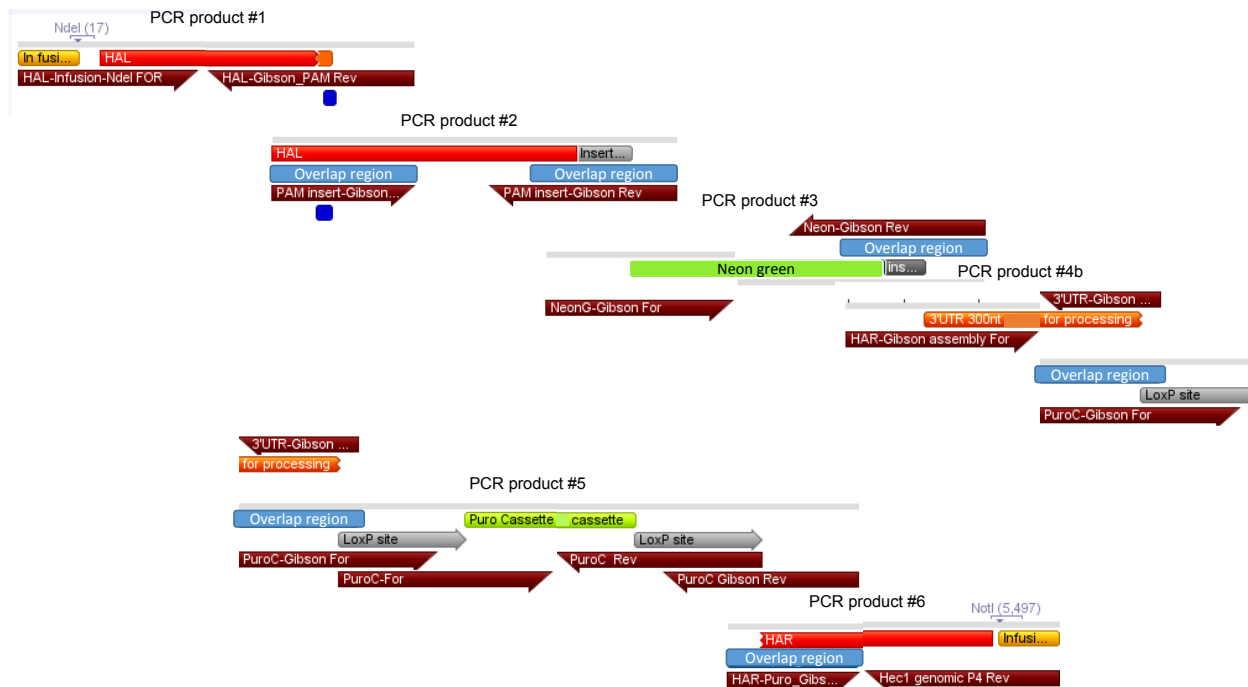


Figure A2.6. Primer design for Gibson Assembly. PCR fragments for cloning of pNeon-Hec1 Puro donor plasmid are indicated (see Figure A2.6). PCR product 1= left homology arm (HAL); PCR product 2= fragment of HAL containing the PAM sequence (the PAM sequence is mutated via primer design to avoid cleavage of the donor plasmid by the gRNA-chimera nuclease once transfected in cells); PCR product 3= Neon green coding region tagging inserted after and in-frame with last Hecl1 exon (stop codon is inserted after Neon green coding sequence); PCR product 4b= ~300nt of 3'UTR endogenous Hecl1 sequence inserted after Neon green coding region for mRNA processing of the Hecl1-Neon green transcript in cells; PCR product 5= Puromycin cassette containing a PGK promoter, the PURO coding sequence and a bGH polyadenylation site (pA) (LoxP sites are inserted before and after Puro cassette for removal of the cassette after Cre recombinase expression); PCR product 6= right homology arm (HAR). Overlapping regions between PCR fragments, required for Gibson Assembly cloning, are indicated in blue.

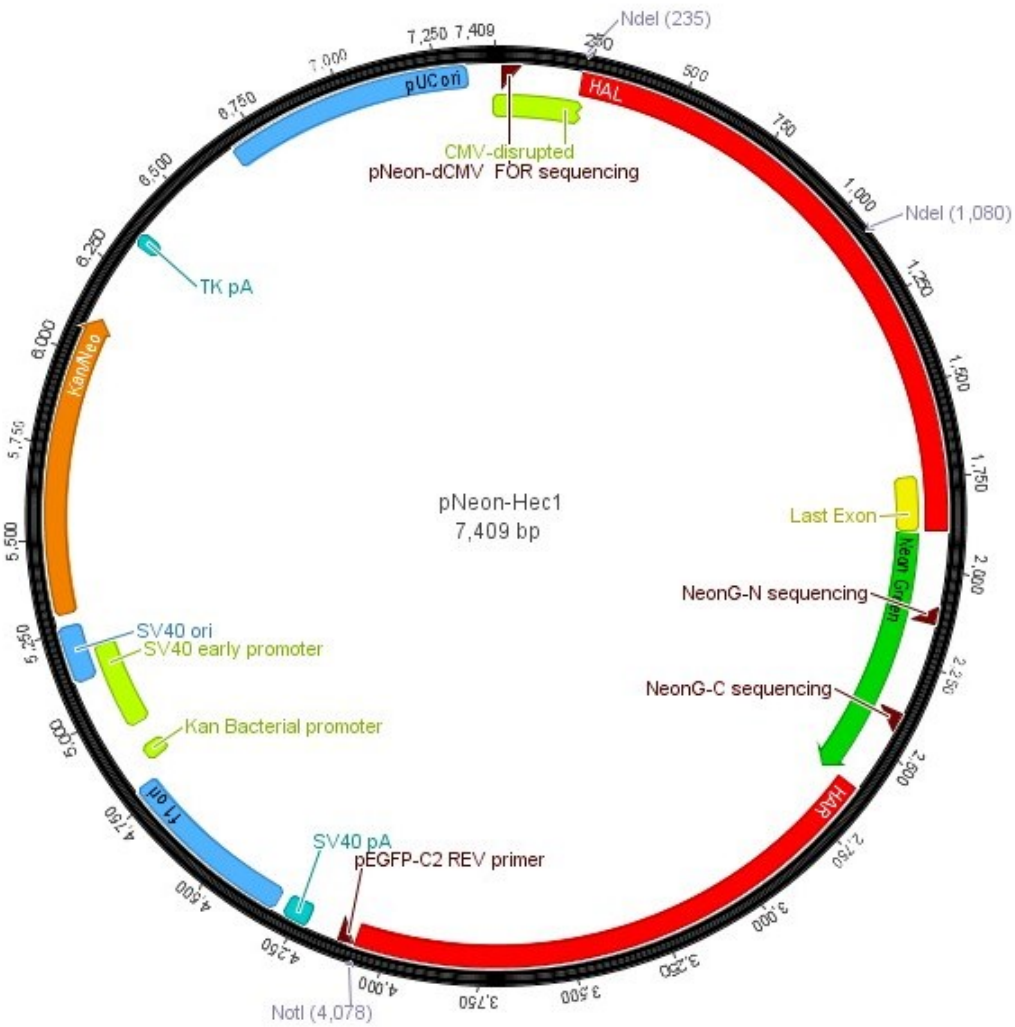


Figure A2.7. Map of Hec1 donor plasmid pNeon Hec1. HAL indicates left homology arm; HAR indicates right homology arm; NeonG-N and NeonG-C indicate the location of designed primers for sequencing upstream and downstream of the Neon Green coding region. pEGFP-C2 REV indicates location of designed primer for sequencing upstream NotI restriction site.

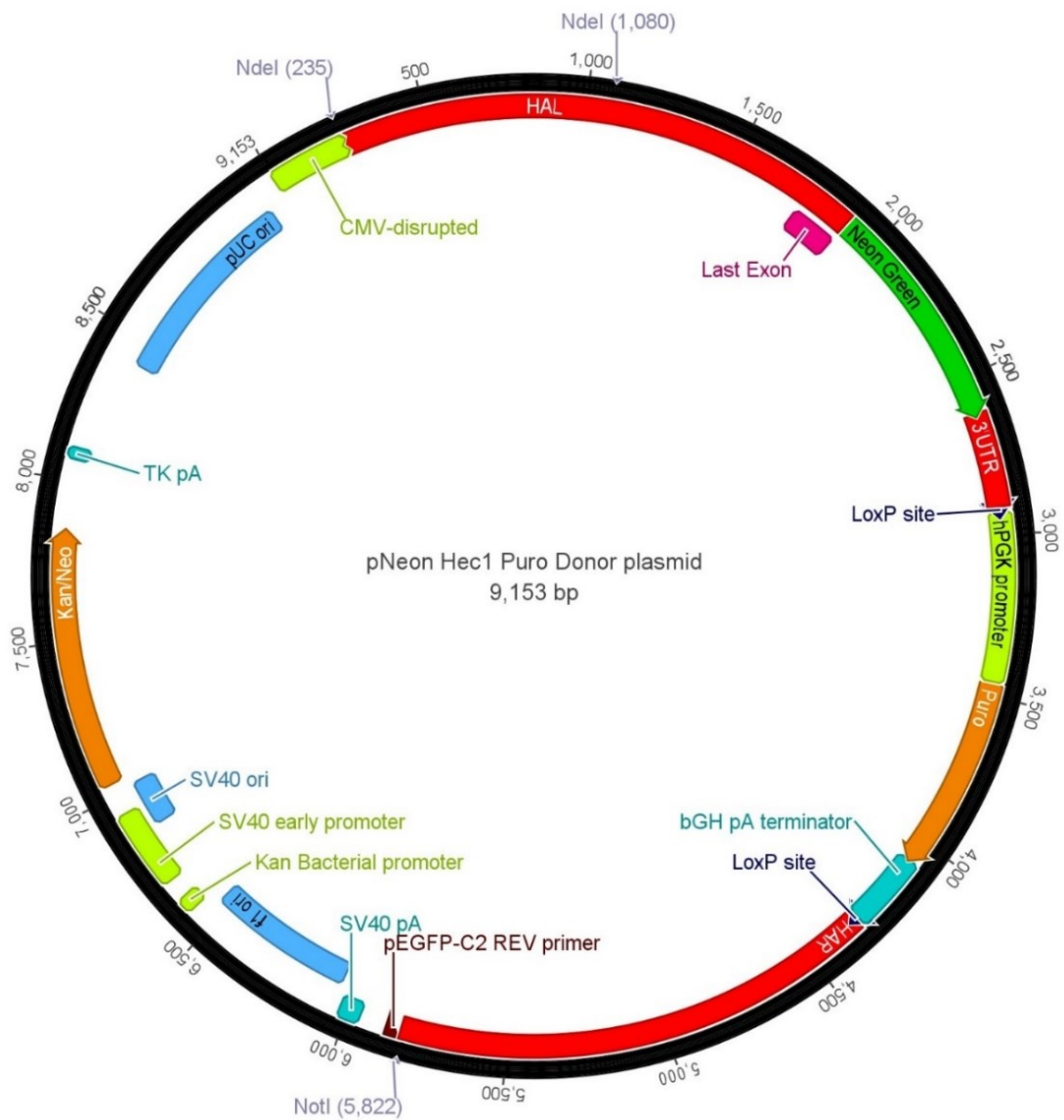


Figure A2.8. Map of Hec1 donor plasmid pNeon Hec1. HAL indicates left homology arm; 3'UTR indicates ~300nt of 3'UTR endogenous Hec1 sequence inserted after Neon green coding region and stop codon for mRNA processing; PGK promoter, PURO and bGH pA indicate the Puro cassette inserted for selection; HAR indicates right homology arm; LoxP sites are indicated; pEGFP-C2 REV indicates location of designed primer for sequencing upstream NotI restriction site.

LIST OF ABBREVIATIONS

ABK: Aurora B Kinase
APC/C: Anaphase Promoting Complex/Cyclosome
Bub1: Budding Uninhibited by Benzimidazoles 1
Bub3: Budding Uninhibited by Benzimidazoles 3
BubR1: Budding Uninhibited by Benzimidazoles 1 homolog Beta (Bub1B)
CASC5: Cancer Susceptibility Candidate 5
CCAN (Constitutive Centromere Associated Network)
Cdc20: Cell-division cycle protein 20
CMV: Cytomegalovirus
CPC: Chromosomal Passenger Complex
CRISPR: clustered regularly interspaced short palindromic repeats
DSB: Double Strand Break
FACS: Fluorescence-activated cell sorting
gRNA: guide RNA
H2A: Histone H2A
HDR: homology-directed repair
Hec1: Highly Express in Cancer
HP1: Heterochromatin Protein 1
INCENP: Inner Centromeric Protein
KMN: KNL1-Mis12-Ndc80
KNL1: Kinetochore Null 1
Mad1: Mitotic Arrest Deficient 1
Mad2: Mitotic Arrest Deficient 2
Mis12: Minichromosome Instability 12-like protein
Mps1: Monopolar Spindle 1
mRNA: messenger RNA
MS: Mass Spectrometry
MT: Microtubule
Ndc80: Non Disjunction of Chromosome 80

NHEJ: non-homologous end-joining
PAM: protospacer adjacent motif
PP1: Protein Phosphatase 1
PP2A: Protein Phosphatase 2A
RNAi: RNA interference
RZZ: Rod-Zw10-Zwilch
SAC: Spindle Assembly Checkpoint
TALENs: transcription activator-like effector nucleases
TPR: tetratricopeptide repeat
ZFN: Zinc Finger Nuclease
Zw10: Zeste white 10
Zwint1: Zw10 interacting protein 1